1995

Adaptive nonlinear attitude control of spacecraft

Cheng Tang
Iowa State University

Adaptive nonlinear attitude control of spacecraft

by

Cheng Tang

A Dissertation Submitted to the

Graduate Faculty in Partial Fulfillment of the

Requirements for the Degree of

DOCTOR OF PHILOSOPHY

Department: Aerospace Engineering and Engineering Mechanics
Major: Aerospace Engineering

Approved:

Signature was redacted for privacy.

In Charge of Major Work

Signature was redacted for privacy.

For the Major Department

Signature was redacted for privacy.

For the Graduate College

Members of the Committee:

Signature was redacted for privacy.

Signature was redacted for privacy.

Signature was redacted for privacy.

Signature was redacted for privacy.

Iowa State University
Ames, Iowa
1995

TABLE OF CONTENTS

LIST OF TABLES

LIST OF FIGURES

NOMENCLATURE

TEA	torque equilibrium attitude;
ACS	attitude control system;
CMG	control momentum gyro;
$LVLH$	local vertical local horizontal reference frame;
RBF	radial basis function neural network;
LS	least square method;
OLS	orthogonal least square algorithm;
θ	body Euler angles with respect to LVLH (roll, pitch, yaw);
ω	body axis components of absolute angular velocity ;
u	body axis components of CMG torque;
n	orbital angular velocity;
I_{11}, I_{22}, I_{33}	principle moments of inertia;
I_{12}, I_{23}, I_{13}	cross-product of inertia;
m_{gg}	Gravity gradient term;
τ	coordinated axis components of CMG torque;
$w(t)$	body axis components of the disturbance torque;
$d(t)$	coordinated axis components of disturbance torque;
$\bar{V}$	periodic signal vector;

M	number of RBF centroid;
N_c	number of RBF significant regressors;
Λ	weighting matrix for RBF network;
$\phi(\bullet)$	activation function;
τ_{ad}	coordinated axis components of neural network control torque;
$f(\bullet)$	radial basis function;

ACKNOWLEDGMENTS

I wish to thank my major professor: Dr. Ping Lu for his encouragement and guidance through this entire research. Valuable discussions and suggestions given by Dr. Bion L. Pierson and my classmates are greatly appreciated. Special thanks go to my family for their understanding and support.

CHAPTER 1. INTRODUCTION

Spacecraft Attitude Control

One of the most important problems in spacecraft design is that of attitude stabilization and control. Although the missions of space vehicles and their attitude requirements vary greatly, high pointing accuracy is an important part of the overall design problem for a spacecraft control system. Meeting the spacecraft attitude control system design requirements in a realistic environment where the knowledge about the system parameters may be incomplete and disturbances are present is a challenging task, since the traditional control techniques and even recent developments in feedback linearization methods have some difficulties in dealing with the attitude control problem with both uncertain system parameters and uncertain disturbances.

The conventional ACS method is to obtain a linear approximation to a nonlinear system model, then apply the linear control theory [1] to the linearized model. But the requirement to use control momentum gyros (CMGs) and the available gravity gradient torques as control actuators, and the highly varied modes of operation and configuration have highlighted the difficulties associated with using the conventional approaches. The Space Station system violates the assumptions used in linearizing the system such as: small TEAs and negligible cross-product of inertias. For most proposed configurations, these are not valid assumptions during nominal operation.

Therefore, stability and performance problems may occur when utilizing the linear ACS control method.

In recent years, the stability and performance problems have received considerable attention. Several nonlinear control approaches based on state transformation and nonlinear feedback have been developed to improve the system performance. This feedback linearization technique consists of a coordinate transformation which transforms the system to a nominal form and a nonlinear feedback control is employed to cancel the nonlinearility of the dynamic equations to result in an equivalent linear system. Then the well developed linear control theory can be applied. But it can only be applied to a certain class of nonlinear systems, and it requires exact knowledge about the nonlinear system model as well as the access to the full state.

For the ACS systems with external disturbances of some random form, or unknown parameters, it is difficult to apply the feedback linearization techniques. The aerodynamic disturbance torques acting on the Space Station are expected to have constant values and periodic components. As a result, attitude oscillation about torque equilibrium attitude will occur. The most common approach is called asymptotic disturbance rejection [2], which is based on the linearized model and it is necessary to know the frequencies of the periodic disturbances for the control design to minimize their effects. A neural network approach using Gaussian radial basis function networks for disturbance rejection which facilitates an adaptive regulation of spacecraft control systems is a very promising method. The radial basis function model can be regarded as a special two-layered network which is linear-in-the parameters and its weight training is fast and requires no system model assumptions.

The first objective of this research is to try to investigate adaptive nonlinear

techniques which avoid the need for a linearized model for a Space Station attitude control problem. This robustness of the system is required for imprecisely unknown moments of inertia and the unmodeled dynamics due to structural flexibility. The primary variation in moments of inertia come from changes during buildup sequence from its movable payloads, docking/undocking with the space shuttle, and the uncertainties in the moments of inertia of the station itself. These combined effects can be large. Another objective is to design a control law to stabilize the station against gravity gradient torques and to reject strong periodic disturbances caused by the rotation of solar panels and by variation in atmospheric density associated with the diurnal bulge. Finally, we try to apply the approximate linearization approaches to the attitude control and momentum management for the Space Station with unknown disturbances to achieve the system stability while the magnitude of the disturbances is large.

Literature Review

Linear Control Approach

Significant research effort has addressed the problem of stabilization and performance of the spacecraft attitude control systems. Most of the studies have been limited to a linearizable system. A certain class of solutions to the spacecraft attitude control problems employed the classical control approaches [3-8]. Linear quadratic regulator (LQR) synthesis technique has been exploited by many authors. Warren and Wie [2, 4] applied LQR approach to minimize the overall attitude and momentum oscillations caused by the cyclic aerodynamic disturbances. An indirect adaptive control of Space Station with the gain calculation which is based on LQR theory with

eigenvalue placement in a vertical strip is addressed by Bishop et al. [9]. Based on recent advanced robust control theory, many publications [10-16] have shown that the robust H^2, and H^∞ control design, μ-synthesis technique and game theory may be successfully applied to a Space Station with parameter uncertainty problems.

Feedback Linearization Control

With regard to the limitation of the imprecise knowledge of the actual model, Sheen [17] developed more promising approaches for a spacecraft attitude and/or momentum management based on the advanced theory of adaptive control of nonlinear systems by developing an update control law in order to enhance the robustness for the systems with uncertain parameters. Because the adaptive control techniques are based on obtaining the linear model and the condition for the feedback linearization is no longer satisfied when there are disturbances to the spacecraft, degradation in performance and stability may occur. Due to the restrictive condition for exact feedback linearization for many nonlinear systems, Krener [18] investigated the approximate full state linearization of nonlinear multi-output systems. Application of the approximate input-output linearization for ball and beam example which fails to have relative degree was studied by Hauser and Sastry [19].

Adaptive Nonlinear Control

For most situations, the assumptions needed for linear approximation for a Space Station is not valid. Therefore, feedback linearization techniques attract more attentions. Beginning with the work of Krener [18], many researchers have investigated the conditions under which nonlinear dynamical systems can be transformed into lin-

ear, controllable systems. Hunt, Su and Meyer [24-26] found a class of such systems using state dependent feedback, linear coordinate changes in the input, and nonlinear state coordinate changes. Detailed descriptions can be found in Sastry and Isidori [27, 28]. Its application to spacecraft attitude control can be seen in [29-33]. However, the requirement for exact cancelation of nonlinearities is the main limitation for a nonlinear system with parameter uncertainties and unknown disturbances.

To overcome the problem with parameter uncertainties, Sheen [17] has applied adaptive controller techniques for the Space Station because the inertia parameters are the major source of uncertainties.

Due to the similarities of the robotic control problem and the spacecraft attitude control, the well developed robotic control techniques can be applied to spacecraft attitude control. This has been indicated by Slotine and Li in [34, 35]. Sponge [36] also developed a similar algorithm to obtain a robust adaptive control law for n-link robot manipulators using the Lyapunov based theory of guaranteed stability of certain system. But comprehensive stability analysis of the nonlinear system with disturbance is very limited.

In handling periodic disturbance, Chen and Paden [37] developed an algorithm for a adaptive linearization of hybrid step motor problem that adaptively adds periodic signals to the input to reduce the output torque ripples.

Neural Network Control

In recent years, the blooming application of neural network control can be seen in many areas. Narendra [38] and Mills et al. [39] exploited the connection between neural network controllers and the adaptive controllers. One of the important roles of

neural networks is the function approximation. Many authors have proposed neural networks as feedforward inverse dynamic controllers. Sanner and Slotine [40] developed a direct adaptive tracking control using Gaussian radial basis function networks to adaptively compensate for system nonilinearities. Gomi and Kawato [41] have also proposed a similar scheme using neural networks. Calis et al. [42] employed a neural network in combination with nonlinear controllers to compensate for the inverse error present when feedback linearization methods are employed. A very effective learning algorithm (orthogonal least square) for radial basis function network is discussed by Chen et al. [43, 44]. This learning algorithm is used to select a suitable set of radial basis function centers in order to promote a more efficient training of neural networks.

A few papers have addressed flight control applications of neural networks [45-47]. But it appears to be a new approach to apply neural networks with radial basis function associated with nonlinear controllers for the spacecraft attitude control to adaptively cancel out the effect of the disturbances for better system performance.

Outline

The dissertation is organized as follows. In chapter 2, the coordinate systems are defined and the dynamic model of Space Station and its properties under several assumptions are summarized, following a description of the disturbance model. In order to compare the linear control approach as a tracking controller for a nonlinear Space Station model, a LQR controller is designed based on the linearized system and the simulation results for several tests are presented in chapter 3. These results reveal the inadequacy of the linear controller.

In chapter 4, based on two adaptive nonlinear control methods previously re-

peated in the literature for robot manipulators, Two controllers were developed to stabilize the space station with unknown inertia parameters and the periodic disturbances whose magnitudes and phase angles are assumed to be unknown. Better transient state response is achieved by the optimizing control parameters. Guaranteed global system stability and the convergence of the disturbance parameters are proved. The convergence analysis of the inertia parameters are provided. The performances of the adaptive controllers are evaluated using a number of test cases include the robustness test with unmodeled dynamics.

In chapter 5, a more effective direct adaptive neural network control with radial basis function networks associated with any of the above nonlinear controllers developed in chapter 4 is applied to the spacecraft attitude control problem. The performance tests including the extrapolation of the networks are provided. Compared to the nonlinear adaptive controllers in chapter 4, the required control torques to stabilize the Space Station are significantly smaller.

In chapter 6, a direct adaptive controller for both attitude control and momentum (CMGs) management for control momentum gyros with unknown disturbances is designed based on the approximate feedback linearization method by simply neglecting the small control terms which violate the exact feedback linearization condition. Simulation results prove that stabilization can be achieved with large disturbances.

Finally, conclusions and future research are included in chapter 7.

CHAPTER 2. MATHEMATICAL MODELS OF THE SPACE STATION

In this chapter, the Space Station is assumed to be a single rigid body. Several models are presented under certain assumptions for the controllers to be examined by simulation.

Coordinate System

The earth is considered inertially fixed so that all motion is relative to a geocentric point. The two coordinate systems of greatest interest are the local vertical and local horizontal and the body axes shown in Figure 2.1.

The Z_L axis originates at the center of mass of the Space Station and points through the center of the Earth. The Y_L points in the opposite direction of the instantaneous orbital angular momentum vector, and the X_L axis completes the right-handed coordinate system. The $X_L - Z_L$ plane is the instantaneous orbit plane. The rotating reference frame centered at the Space Station and oriented in these directions is referred to as Local Vertical and Local Horizontal (LVLH). This orientation facilitates the operation of antennas, star sensors, and other fixed experimental packages. However, the solar panels must be kept pointing towards the sun for maximal efficiency, so they are mounted on rotating joints to keep their attitude

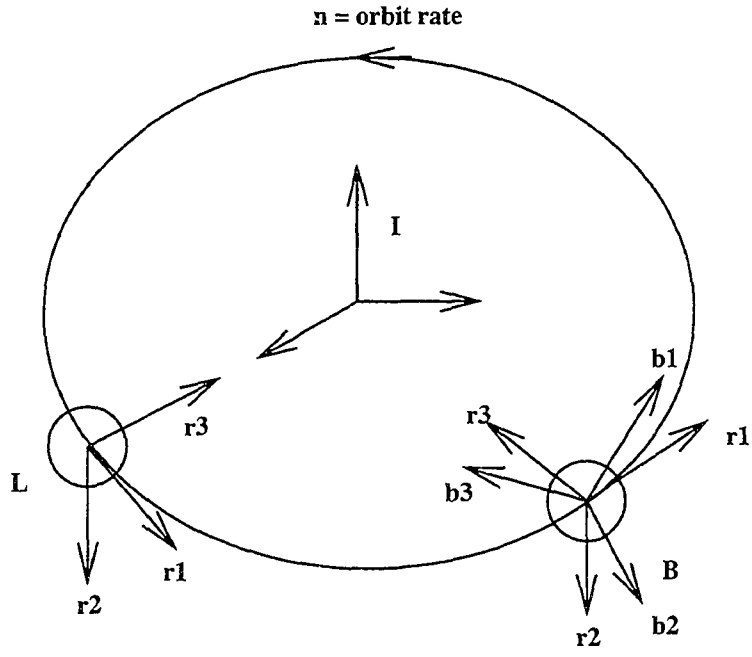

I = Inertial Reference Frame

L = LVLH Reference Frame

B = Body Fixed Reference Frame

Figure 2.1: Relationship between reference frames

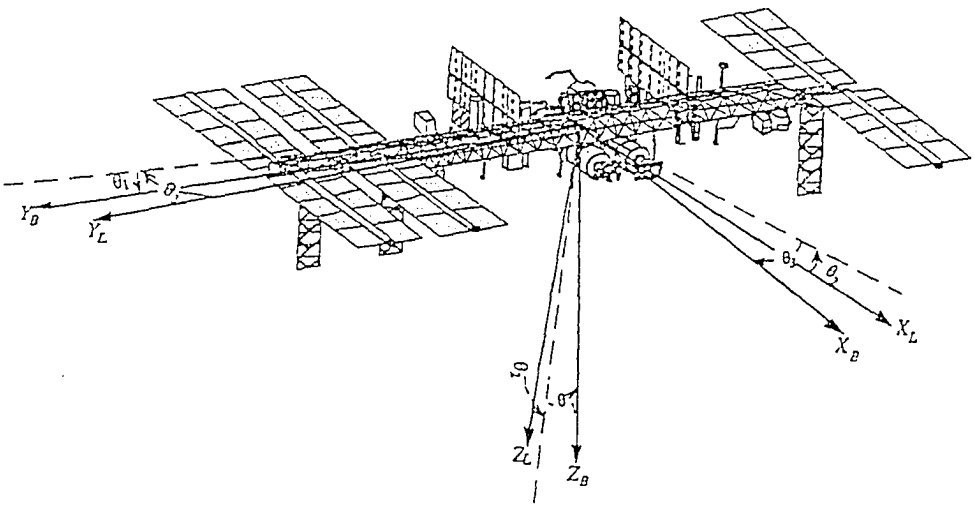

Figure 2.2: Spacecraft model

inertially fixed. Figure 2.2 shows the relationship between the LVLH and the body axes of a spacecraft model. Transformation between those two coordinate systems is stated in Appendix A. The sequence of the rotations is 2-3-1, which represents the Euler angle sequence pitch, yaw, and roll, respectively about Y_B, Z_B, and X_B. Details can be found in [54].

Nonlinear Model of Space Station

The Space Station is assumed to be in circular orbit about the Earth, and to maintain an LVLH during its operation. Since only the attitude of the Space Station is of interest in this work, rather than its orbital position, only the equations for the attitude dynamics are considered. The nonlinear equations of motion in terms of

components along the body-fixed control axes can be written as

$$\mathrm{I}\dot{\omega} + \omega \times \mathrm{I}\omega = \sum \mathrm{m}_{\mathrm{ext}} \tag{2.1}$$

where

$$I = \begin{bmatrix} I_{11} & I_{12} & I_{13} \\ I_{21} & I_{22} & I_{23} \\ I_{31} & I_{32} & I_{33} \end{bmatrix}$$

is the inertia matrix of the Space Station. (I_{11}, I_{22}, I_{33}) are the moments of inertia. $I_{ij}, j \neq i$ are the products of inertia.

The two major torques acting on the Space Station are the gravity gradient torque, and the control torque. Therefore, Eqn.(2.1) in a disturbance-free environment can be written

$$\mathrm{I}\dot{\omega} + \omega \times \mathrm{I}\omega = \mathrm{m}_{\mathrm{gg}} - \mathrm{u} \tag{2.2}$$

where m_{gg} is the gradient torque term, and $u = (u_1, u_2, u_3)^T$ are the components of control torque on the body-fixed axes. $\omega = (\omega_1, \omega_2, \omega_3)^T$ are the body-axis components of the absolute angular velocity of the station. The sign convention of u is chosen to be consistent with the baseline controller design. A disturbance torque, due to the principal environmental effects such as atmospheric drag, solar radiation pressure, is also acting on the Space Station. Other perturbing effects are associated with internal moving parts, thrust misalignment, thermal emissivity, electro-magnetic radiation, out-gassing, and propellant leakage. The disturbance model will be discussed later. In a (2-3-1) rotation sequence this gravity gradient torque can be described by

$$m_{gg} = 3n^2 c \times Ic \tag{2.3}$$

where

$$c = \begin{pmatrix} -\sin\theta_2 \cos\theta_3 \\ \cos\theta_1 \sin\theta_2 \sin\theta_3 + \sin\theta_1 \cos\theta_2 \\ -\sin\theta_1 \sin\theta_2 \sin\theta_3 + \cos\theta_1 \cos\theta_2 \end{pmatrix}$$

and where the $\theta_i's$ are the Euler angles of the body axes with respect to LVLH axes which rotate with the orbital angular velocity, and n is the Space Station orbital rate of 0.0011 rad/s.

$$\dot{\omega} = I^{-1}(-\omega \times I\omega + 3n^2 c \times Ic - u) \tag{2.4}$$

For a 2-3-1 body-axis rotation described in section 2.1, the attitude kinematics for the Space Station can be obtained in the following form

$$\dot{\theta} = D(\theta)\omega + \bar{n} \tag{2.5}$$

where

$$D(\theta) = \begin{bmatrix} 1 & -\cos\theta_1 \tan\theta_3 & \sin\theta_1 \tan\theta_3 \\ 0 & \cos\theta_1 \sec\theta_3 & -\sin\theta_1 \sec\theta_3 \\ 0 & \sin\theta_1 & \cos\theta_1 \end{bmatrix}$$

and $\bar{n} = (0\ n\ 0)^T$. Eqn.(2.5) relates the absolute angular velocity and the Euler rate. The Euler angles for LVLH position are (0, -$\pi/2$, $\pi/2$).

Linear Model with Small Attitude

For small attitude deviations from LVLH orientation, the linearized equations of motion can be written as

Space Station dynamics

$$\begin{bmatrix} I_{11} & I_{12} & I_{13} \\ I_{21} & I_{22} & I_{23} \\ I_{31} & I_{32} & I_{33} \end{bmatrix} \begin{bmatrix} \dot{\omega_1} \\ \dot{\omega_2} \\ \dot{\omega_3} \end{bmatrix} = n \begin{bmatrix} I_{31} & 2I_{32} & I_{33}-I_{22} \\ -I_{32} & 0 & I_{12} \\ I_{22}-I_{11} & -2I_{12} & -I_{13} \end{bmatrix} \begin{bmatrix} \omega_1 \\ \omega_2 \\ \omega_3 \end{bmatrix}$$
$$+3n^2 \begin{bmatrix} I_{33}-I_{22} & I_{21} & 0 \\ I_{12} & I_{33}-I_{11} & 0 \\ -I_{13} & -2I_{23} & 0 \end{bmatrix} \begin{bmatrix} \theta_1 \\ \theta_2 \\ \theta_3 \end{bmatrix} + n^2 \begin{bmatrix} -2I_{23} \\ I_{13} \\ -I_{12} \end{bmatrix} + \begin{bmatrix} -u_1 \\ -u_2 \\ -u_3 \end{bmatrix} \quad (2.6)$$

Attitude kinematics

$$\begin{aligned} \dot{\theta}_1 - n\theta_3 &= \omega_1 \\ \dot{\theta}_2 - n &= \omega_2 \\ \dot{\theta}_3 + n\theta_1 &= \omega_3 \end{aligned} \quad (2.7)$$

By eliminating $(\omega_1, \omega_2, \omega_3)$ in Eqn.(2.6) from Eqn.(2.7), the linearized second order attitude equations can also be written as

$$\begin{bmatrix} I_{11} & I_{12} & I_{13} \\ I_{21} & I_{22} & I_{23} \\ I_{31} & I_{32} & I_{33} \end{bmatrix} \begin{bmatrix} \ddot{\theta}_1 \\ \ddot{\theta}_2 \\ \ddot{\theta}_3 \end{bmatrix} = n \begin{bmatrix} 0 & 2I_{32} & I_{11}-I_{22}+I_{33} \\ -I_{32} & 0 & I_{12} \\ -I_{11}+I_{22}-I_{33} & -2I_{12} & 0 \end{bmatrix} \begin{bmatrix} \dot{\theta}_1 \\ \dot{\theta}_2 \\ \dot{\theta}_3 \end{bmatrix}$$
$$+n^2 \begin{bmatrix} 4(I_{33}-I_{22}) & 3I_{21} & 0 \\ 4I_{12} & 3(I_{33}-I_{11}) & I_{32} \\ -4I_{13} & -3I_{23} & I_{11}-I_{22} \end{bmatrix} \begin{bmatrix} \theta_1 \\ \theta_2 \\ \theta_3 \end{bmatrix} + n^2 \begin{bmatrix} -4I_{23} \\ 3I_{13} \\ I_{12} \end{bmatrix} + \begin{bmatrix} -u_1 \\ -u_2 \\ -u_3 \end{bmatrix} \quad (2.8)$$

Since the product of inertia causes three-axis coupling as well as a bias torque

term in each axis, the significant misalignment of the control axes with the principal axes will occur during the early flight configuration of assembly.

Small Attitude and Small Product of Inertia Model

In most of the cases, small products of inertia can also be assumed negligible for simplicity. The pitch motion will then be uncoupled from the roll/yaw axes which are still coupled to each other. For this case, the control axes are nearly aligned with the principal axes. Eqn.(2.8) becomes

$$I_{11}\dot{\omega}_1 + n(I_{22} - I_{33})\omega_3 + 3n^2(I_{22} - I_{33})\theta_1 = -u_1$$

$$I_{22}\dot{\omega}_2 + 3n^2(I_{11} - I_{33})\theta_2 = -u_2$$

$$I_{33}\dot{\omega}_3 - n(I_{22} - I_{11})\omega_1 = -u_3 \tag{2.9}$$

Finally, the linear equations for θ_1, θ_2,and θ_3 become:

$$I_{11}\ddot{\theta}_1 + 4n^2(I_{22} - I_{33})\theta_2 - n(I_{11} - I_{22} + I_{33})\dot{\theta}_3 = -u_1$$

$$I_{22}\ddot{\theta}_2 + 3n^2(I_{11} - I_{33})\theta_2 = -u_2$$

$$I_{33}\ddot{\theta}_3 + n^2(I_{22} - I_{11})\theta_3 + n(I_{11} - I_{22} + I_{33})\dot{\theta}_1 = -u_3 \tag{2.10}$$

Another special case for the study of passive or active gravity-gradient stabilization of earth-point satellites is while pitch motion TEA is large but the roll/yaw motion is small. The Eqn.(2.4) after eliminating ω from Eqn.(2.4) becomes

$$I_{11}\ddot{\theta}_1 + (1 + 3\cos^2\theta_2)n^2(I_{22} - I_{33})\theta_1 - n(I_{11} - I_{22} + I_{33})\dot{\theta}_3 +$$

$$+3(I_{22} - I_{33})n^2(\sin\theta_2\cos\theta_2)\theta_3 = -u_1$$

$$I_{22}\ddot{\theta}_2 + 3n^2(I_{11} - I_{33})\sin\theta_2\cos\theta_2 = -u_2$$
$$I_{33}\ddot{\theta}_3 + (1 + 3\sin^2\theta_2)n^2(I_{22} - I_{11})\theta_3 + n(I_{11} - I_{22} + I_{33})\dot{\theta}_1 +$$
$$+ 3(I_{22} - I_{11})n^2(\sin(\theta_2\cos\theta_2)\theta_1 = -u_3 \tag{2.11}$$

Configurations of the Space Station for Phase 3 and Phase 1 are given in Table 2.1 (see [7, 9]). In this case, we assume large pitch TEA because of the small gravity gradient torque available in the pitch axis.

Table 2.1: Space Station inertia configuration

Inertia $slug - ft^2$	Assembly flight3	Phase 1
I_{11}	23.22E6	50.28E6
I_{22}	1.30E6	10.80E6
I_{33}	23.23E6	58.57E6
I_{12}	-0.023E6	-0.39E6
I_{13}	0.477E6	0.16E6
I_{23}	-0.011E6	0.16E6

For the convenience of later applications, we replace θ_i by $\bar{\theta}_i$, where

$$\begin{aligned} \bar{\theta}_1 &= \theta_1 \\ \bar{\theta}_2 &= \theta_2 - nt \\ \bar{\theta}_3 &= \theta_3 \end{aligned} \tag{2.12}$$

Eqn.(2.5) will be rewritten as:

$$\dot{\bar{\theta}} = D(\bar{\theta})\omega \tag{2.13}$$

and $D(\bar{\theta})$ and c can also be written as function of $\bar{\theta}$.

$$D(\bar{\theta}) = \begin{bmatrix} 1 & -\cos\bar{\theta}_1\tan\bar{\theta}_3 & \sin\bar{\theta}_1\tan\bar{\theta}_3 \\ 0 & \cos\bar{\theta}_1\sec\bar{\theta}_3 & -\sin\bar{\theta}_1\sec\bar{\theta}_3 \\ 0 & \sin\bar{\theta}_1 & \cos\bar{\theta}_1 \end{bmatrix} \tag{2.14}$$

$$\bar{c} = \begin{pmatrix} -\sin(\bar{\theta}_2 + nt)\cos\bar{\theta}_3 \\ \cos\bar{\theta}_1 \sin(\bar{\theta}_2 + nt)\sin\bar{\theta}_3 + \sin\bar{\theta}_1 \cos(\bar{\theta}_2 + nt) \\ -\sin\bar{\theta}_1 \sin(\bar{\theta}_2 + nt)\sin\bar{\theta}_3 + \cos\bar{\theta}_1 \cos(\bar{\theta}_2 + nt) \end{pmatrix}$$

Differentiating Eqn.(2.13) and combining Eqn.(2.4) and Eqn.(2.13), we get

$$\mathrm{ID}^{-1}(\bar{\theta})\ddot{\bar{\theta}} - \mathrm{ID}^{-1}\dot{\mathrm{D}}\mathrm{D}^{-1}\dot{\bar{\theta}} - 3\mathrm{n}^2(\bar{\mathrm{c}} \times \mathrm{I}\bar{\mathrm{c}}) - \mathrm{D}^{-1}\dot{\bar{\theta}} \times \mathrm{ID}^{-1}\dot{\bar{\theta}} = -\mathrm{u} \qquad (2.15)$$

Let $u = -D^T\tau$, Eqn.(2.15) becomes

$$\mathrm{D}^{-\mathrm{T}}\mathrm{ID}^{-1}\ddot{\bar{\theta}} - \mathrm{D}^{-\mathrm{T}}\mathrm{ID}^{-1}\dot{\mathrm{D}}\mathrm{D}^{-1}\dot{\bar{\theta}} - 3\mathrm{n}^2\mathrm{D}^{-\mathrm{T}}(\bar{\mathrm{c}} \times \mathrm{I}\bar{\mathrm{c}}) - \mathrm{D}^{-\mathrm{T}}(\mathrm{D}^{-1}\dot{\bar{\theta}} \times \mathrm{ID}^{-1}\dot{\bar{\theta}}) = \tau \qquad (2.16)$$

Let

$$M(\bar{\theta}) = D^{-T}ID^{-1}$$

$$ID^{-1}\dot{\bar{\theta}} \times D^{-1}\dot{\bar{\theta}} = (p\times)D^{-1}\dot{\bar{\theta}}$$

where $(p\times)$ is a skew-symmetric matrix for vector $ID^{-1}\dot{\bar{\theta}}$, which for $p = (p_1, p_2, p_3)^T$ is defined as

$$(p\times) = \begin{pmatrix} 0 & -p_3 & p_2 \\ p_3 & 0 & -p_1 \\ -p_2 & p_1 & 0 \end{pmatrix}$$

$$C(\bar{\theta}, \dot{\bar{\theta}}) = -(D^{-T}ID^{-1}\dot{D}D^{-1} + D^{-T}(p\times)D^{-1})$$

$$\dot{D} = \begin{pmatrix} 0 & \dot{\bar{\theta}}_1 \sin\bar{\theta}_1 \tan\bar{\theta}_3 - \dot{\bar{\theta}}_3 \cos\bar{\theta}_1 \sec^2\bar{\theta}_3 & \dot{\bar{\theta}}_1 \cos\bar{\theta}_1 \tan\bar{\theta}_3 + \dot{\bar{\theta}}_3 \sin\bar{\theta}_1 \sec^2\bar{\theta}_3 \\ 0 & -\dot{\bar{\theta}}_1 sin\bar{\theta}_1 \sec\bar{\theta}_3 + \dot{\bar{\theta}}_3 \cos\bar{\theta}_1 \tan\bar{\theta}_3 \sec\bar{\theta}_3 & -\dot{\bar{\theta}}_1 \cos\bar{\theta}_1 \sec\bar{\theta}_3 - \dot{\bar{\theta}}_1 \tan\bar{\theta}_3 \sec\bar{\theta}_3 \\ 0 & \dot{\bar{\theta}}_1 \cos\bar{\theta}_1 & -\dot{\bar{\theta}}_1 \sin\bar{\theta}_1 \end{pmatrix}$$

$$g(\bar{\theta}) = -3n^2 D^{-T}\bar{c} \times I\bar{c}$$

The Eqn.(2.15) can be written in the form

$$M(\theta)\ddot{\theta} + C(\theta, \dot{\theta})\dot{\theta} + g(\theta) = \tau \tag{2.17}$$

For simplicity, we eliminate the bar sign over each variable.

Disturbance Model

The disturbance torque acting on each axis is obtained at the NASA Johnson Space Center by a nonlinear simulation program which simulated a translational and rotational motion about an oblate earth. It includes solar panels, time-varying surface areas, time-varying center-of-pressure location. The expected disturbances are modeled as a bias plus periodic terms in the three body-fixed control axes:

$$w_i(t) = b_i + A^i_{1n}\sin(nt+\phi^i_1) + A^i_{2n}\sin(2nt+\phi^i_2) + A^i_{3n}\sin(3nt+\phi^i_3) + A^i_{4n}\sin(4nt+\phi^i_4) \tag{2.18}$$

where $i = 1, 2, 3$, $A^i_{1n}, A^i_{2n}, A^i_{3n}, A^i_{4n}$ are the magnitudes of the periodic disturbances along the three body axes. And $\phi^i_1, \phi^i_2, \phi^i_3, \phi^i_4$ are the phase angles in the body axes. The dominant torque frequencies at n and $2n$ are caused by the Earth's diurnal bulge and solar panel rotation effects, respectively. Configuration of the torque disturbance on each axis for Phase 1 is taken from Table 2.2 (see [2]).

Actual magnitudes and phases of these disturbance torques are assumed to be unknown for control design. Therefore for each periodic term, there are two unknowns. Total unknowns in Eqn.(2.18) is nine which can then be rewritten as

$$w(t) = P\bar{V} \tag{2.19}$$

where

$$P = [b, \alpha_1, \beta_1, \alpha_2, \beta_2, \alpha_3, \beta_3, \alpha_4, \beta_4]$$

Table 2.2: Phase 1 disturbance model for Space Station, ft-lb

d_1	1+sin(nt)+0.5sin(2nt) +0.3sin(3nt)+0.5sin(4nt)
d_2	4+1.2sin(nt)+3.5sin(2nt)+ 0.3sin(3nt)+0.5sin(4nt)
d_3	1+sin(nt)+0.5sin(2nt)+ 0.3sin(3nt)+0.4sin(4nt)

$$b = (b_1, b_2, b_3)$$

$$\alpha_i = (\alpha_{i1}, \alpha_{i2}, \alpha_{i3})^T$$

$$\beta_i = (\beta_{i1}, \beta_{i2}, \beta_{i3})^T$$

$$\alpha_{i1} = A_{1n}^i \cos\phi_1^i, \beta_{i1} = A_{1n}^i \sin\phi_1^i$$

$$\tilde{V} = [1, \sin(nt), \cos(nt), \sin(2nt), \cos(2nt), \sin(3nt), \cos(3nt), \sin(4nt), \cos(4nt)]^T \tag{2.20}$$

CHAPTER 3. LINEAR QUADRATIC REGULATOR SYNTHESIS

In this chapter, a linear attitude control law through conventional LQR techniques with proposed pole assignment developed on the basis of a linearized Space Station model under the assumption of the small attitude errors is applied to the nonlinear system to evaluate the performance limit of the linear control approach when the Space Station undergoes initial errors and configuration changes of inertia as well as external disturbances.

Control Design

The attitude deviations from LVLH orientation of the Space Station is assumed to be small. Both the dynamic equation and the kinematic equation are shown in Eqns.(2.6) and (2.7). Defining the state vector $x(t)$ as

$$x(t) := (\theta_1, \omega_1, \theta_2, \omega_2, \theta_3, \omega_3)^T \tag{3.1}$$

the state space model is

$$\dot{x} = Ax + BU \tag{3.2}$$

where

$$A = \begin{pmatrix} 0 & 1 & 0 & 0 & n & 0 \\ a_{21} & a_{22} & a_{23} & a_{24} & a_{25} & a_{26} \\ 0 & 0 & 0 & 1 & 0 & 0 \\ a_{41} & a_{42} & a_{43} & a_{44} & a_{45} & a_{46} \\ n & 0 & 0 & 0 & 0 & 1 \\ a_{61} & a_{62} & a_{63} & a_{64} & a_{65} & a_{66} \end{pmatrix} \tag{3.3}$$

$$\begin{aligned}
a_{21} &= 3n^2((I_{33}-I_{22})(I_{22}I_{33}-I_{23}^2)-I_{12}(I_{12}I_{33}-I_{13}I_{23})-I_{13} \\
&\quad (I_{12}I_{23}-I_{13}I_{22}))/\Delta \\
a_{22} &= n(I_{13}(I_{22}I_{33}-I_{23}^2)+I_{23}(I_{12}I_{33}-I_{13}I_{23})+(I_{33}-I_{22}) \\
&\quad (I_{12}I_{23}-I_{13}I_{22}))/\Delta \\
a_{23} &= 3n^2(I_{12}(I_{22}I_{33}-I_{23}^2)-(I_{33}-I_{11})(I_{12}I_{33}-I_{13}I_{23})-2I_{23} \\
&\quad (I_{12}I_{23}-I_{13}I_{22}))/\Delta \\
a_{24} &= n(2I_{23}(I_{22}I_{33}-I_{23}^2)+2I_{12}(I_{12}I_{23}-I_{13}I_{22}))/\Delta \\
a_{25} &= 0 \\
a_{26} &= n((I_{33}-I_{22})(I_{22}I_{33}-I_{23}^2)-I_{12}(I_{12}I_{33}-I_{13}I_{23})-I_{13} \\
&\quad (I_{12}I_{23}-I_{13}I_{22}))/\Delta \\
a_{41} &= 3n^2((I_{33}-I_{22})(I_{12}I_{23}-I_{13}I_{22})+I_{12}(I_{11}I_{33}-I_{13}^2)+I_{13} \\
&\quad (I_{11}I_{23}-I_{12}I_{13}))/\Delta \\
a_{42} &= n(-I_{31}(I_{12}I_{23}-I_{13}I_{22})-I_{32}(I_{11}I_{33}-I_{13}^2)-(I_{33}-I_{22}) \\
&\quad (I_{11}I_{23}-I_{12}I_{13}))/\Delta \\
a_{43} &= 3n^2(-I_{12}(I_{12}I_{33}-I_{13}I_{23})+(I_{33}-I_{11})(I_{11}I_{33}-I_{13}^2)+2I_{23}
\end{aligned}$$

$$
\begin{aligned}
& (I_{11}I_{23} - I_{12}I_{13}))/\Delta \\
a_{44} &= n(2I_{23}(I_{12}I_{23} - I_{13}I_{22}) + 2I_{12}(I_{11}I_{23} - I_{12}I_{13}))/\Delta \\
a_{45} &= 0 \\
a_{46} &= n((I_{33} - I_{22})(I_{12}I_{23} - I_{13}I_{22}) - I_{12}(I_{11}I_{23} - I_{12}I_{13}) - I_{13} \\
& (I_{11}I_{22} - I_{12}^2))/\Delta \\
a_{61} &= 3n^2((I_{33} - I_{22})(I_{12}I_{23} - I_{13}I_{22}) - I_{12}(I_{11}I_{23} - I_{12}I_{13}) - I_{13} \\
& (I_{11}I_{22} - I_{12}^2))/\Delta \\
a_{62} &= n(I_{13}(I_{12}I_{23} - I_{13}I_{22}) + I_{23}(I_{11}I_{23} - I_{12}I_{13}) + (I_{33} - I_{22}) \\
& (I_{11}I_{22} - I_{12}^2))/\Delta \\
a_{63} &= 3n^2(I_{12}(I_{12}I_{23} - I_{13}I_{22}) - (I_{33} - I_{11})(I_{11}I_{23} - I_{12}I_{13}) - 2I_{23} \\
& (I_{11}I_{22} - I_{12}^2))/\Delta \\
a_{64} &= n(2I_{23}(I_{12}I_{23} - I_{13}I_{22}) - 2I_{12}(I_{11}I_{22} - I_{12}^2))\Delta \\
a_{65} &= 0 \\
a_{66} &= n((I_{33} - I_{22})(I_{12}I_{23} - I_{13}I_{22}) - I_{12}(I_{11}I_{23} - I_{12}I_{13}) - I_{13} \\
& (I_{11}I_{22} - I_{12}^2))/\Delta \\
\Delta &= I_{11}I_{22}I_{33} - I_{11}I_{23}^2 - I_{12}^2I_{33} + 2I_{12}I_{13}I_{23} - I_{13}^2I_{22}
\end{aligned}
$$

$$
B = \begin{pmatrix} 0 & b_{21} & 0 & b_{41} & 0 & b_{61} \\ 0 & b_{22} & 0 & b_{42} & 0 & b_{62} \\ 0 & b_{23} & 0 & b_{43} & 0 & b_{63} \end{pmatrix}^T \tag{3.4}
$$

$$
b_{21} = \frac{I_{22}I_{33} - I_{23}^2}{\Delta}
$$

$$
\begin{aligned}
b_{22} &= -\frac{I_{12}I_{33} - I_{13}I_{23}}{\Delta} \\
b_{23} &= \frac{I_{12}I_{23} - I_{13}I_{22}}{\Delta} \\
b_{41} &= -\frac{I_{12}I_{33} - I_{13}I_{23}}{\Delta} \\
b_{42} &= \frac{I_{11}I_{33} - I_{13}^2}{\Delta} \\
b_{43} &= -\frac{I_{11}I_{23} - I_{12}I_{13}}{\Delta} \\
b_{61} &= \frac{I_{12}I_{23} - I_{13}I_{22}}{\Delta} \\
b_{62} &= -\frac{I_{11}I_{23} - I_{12}I_{13}}{\Delta} \\
b_{63} &= \frac{I_{11}I_{22} - I_{12}^2}{\Delta}
\end{aligned}
$$

$$
U = \begin{pmatrix} -u_1 - 2I_{23} \\ -u_2 + I_{13} \\ -u_3 - I_{12} \end{pmatrix} \tag{3.5}
$$

The control design method is full state feedback with

$$
U = -Kx \tag{3.6}
$$

The approach is to find the control gain matrix K so that the eigenvalues of $A - BK$ are equal to the proposed pole assignments.

Simulation Results

We take the space station inertia matrix from Table 2.1. The proposed closed-loop poles are chosen to be $(-1.05 \pm 0.68i)n, (-1.5 \pm 1.5i)n$, and $(-1.42 \pm 1.38i)n$, where $n = 0.0011 rad/s$. The LQR synthesis can be accomplished quickly with MATLAB. The gain matrix K is calculated and shown in Table 3.1.

Table 3.1: Controller gain matrix for the phase 1 Space Station

1.361E+5	5.333E+4	-6.577E+1	-7.741E+1	8.208E+3	5.553E+4
-1.238E+2	3.625E+0	6.666E+3	4.620E+3	-1.197E+2	-1.189E+2
-7.109E+3	-5.607E+4	-2.453E+1	-6.899E+0	1.235E+5	7.307E+4

The Space Station state is first initialized at $\theta = [5^o, 10^o, 5^o]deg$, and $\omega = [0.2n, -n, 0]rad/s$. The simulation results for applying this control to both the linearized model and the complete nonlinear model are shown from Figure 3.1 - Figure 3.9. The results show that the LQR control scheme performs quite well in stabilizing the station for small initial errors in both the linearized model and the complete nonlinear model especially for pitch angle and pitch rate control. But the peak value of the control required for the yaw axis is close to 20 times in the nonlinear case as in the linearized system. This is shown in Figure 3.9. When the configuration changes from phase 1 to 3 and the inertias are still chosen to be in phase 1, Figures 3.10 - 3.15 indicate that the attitude performance about the pitch axis of the nonlinear system is greatly degraded. The simulation results show that the control effect becomes unpredictable. In Figure 3.10, the roll angle from the linear model becomes unbounded while the roll angle from the nonlinear model eventually approaches zero. The pitch angles from both linear and nonlinear models approach large steady-state values. The situation could be easily changed for the nonlinear system to become unstable under the linear control law and system parameter uncertainties. Figure 3.16 shows that the convergence of tracking error of Euler angles can not be achieved in the presence of external disturbances.

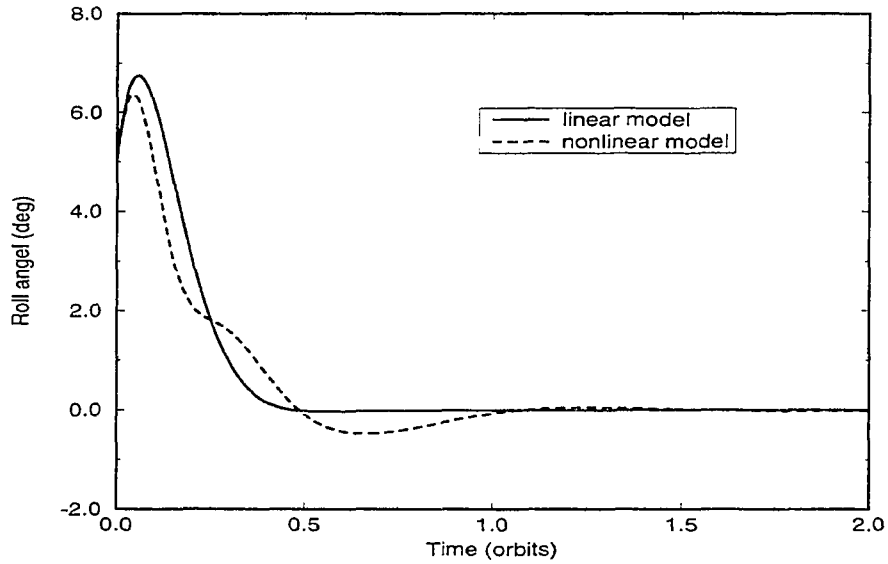

Figure 3.1: Tracking errors of roll angle with LQR controller

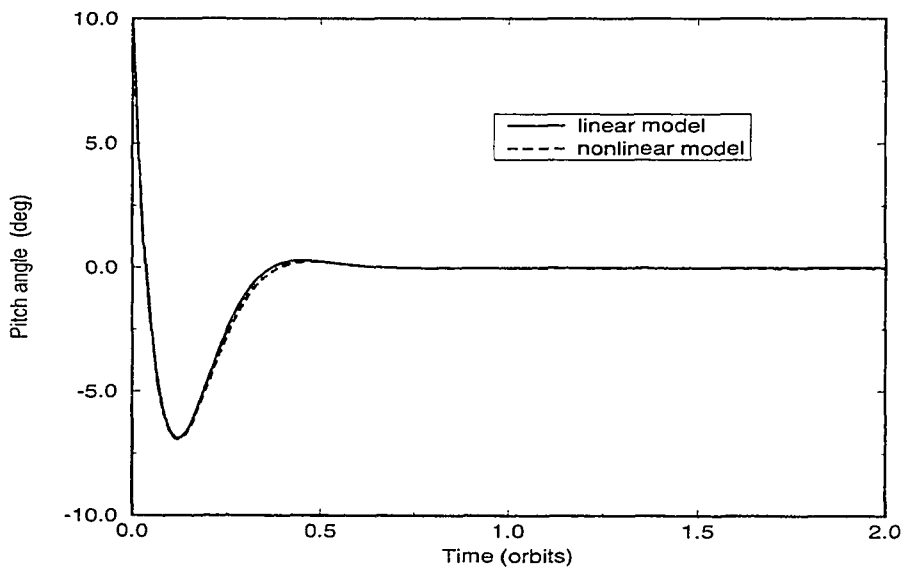

Figure 3.2: Tracking errors of pitch angle with LQR controller

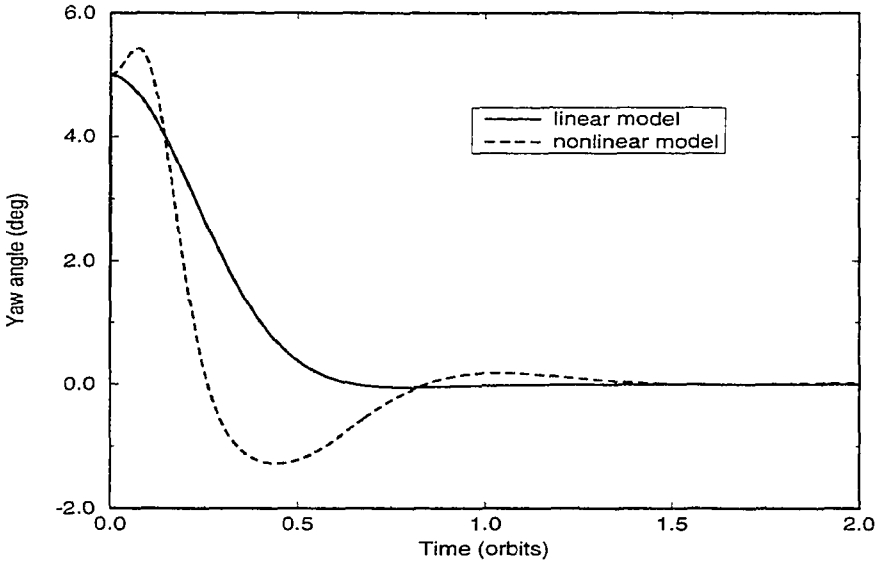

Figure 3.3: Tracking errors of yaw angle with LQR controller

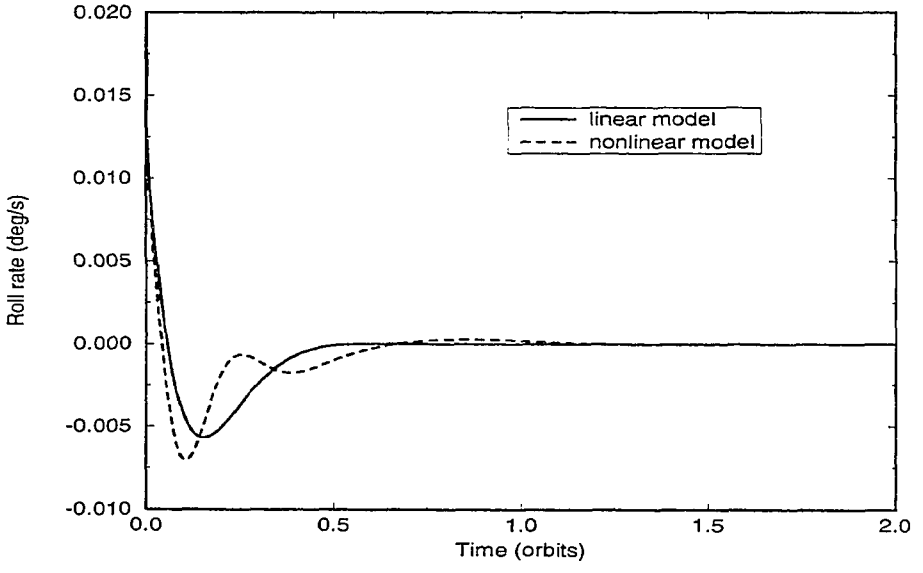

Figure 3.4: Tracking errors of roll rate with LQR controller

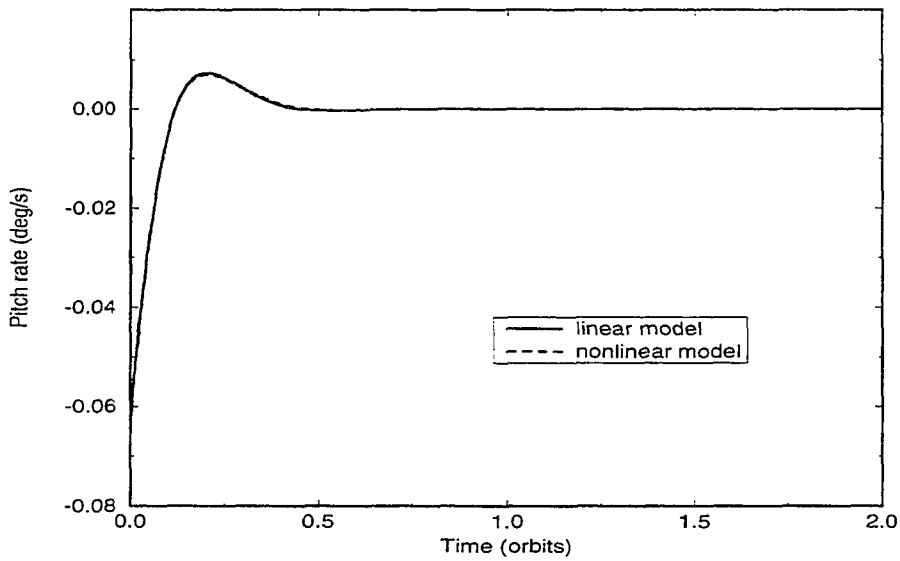

Figure 3.5: Tracking errors of pitch rate with LQR controller

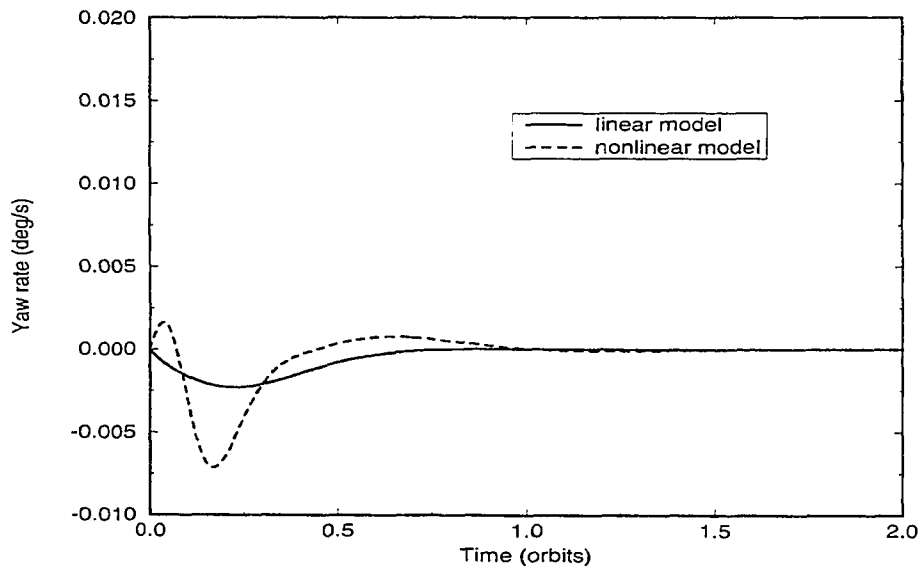

Figure 3.6: Tracking errors of yaw rate with LQR controller

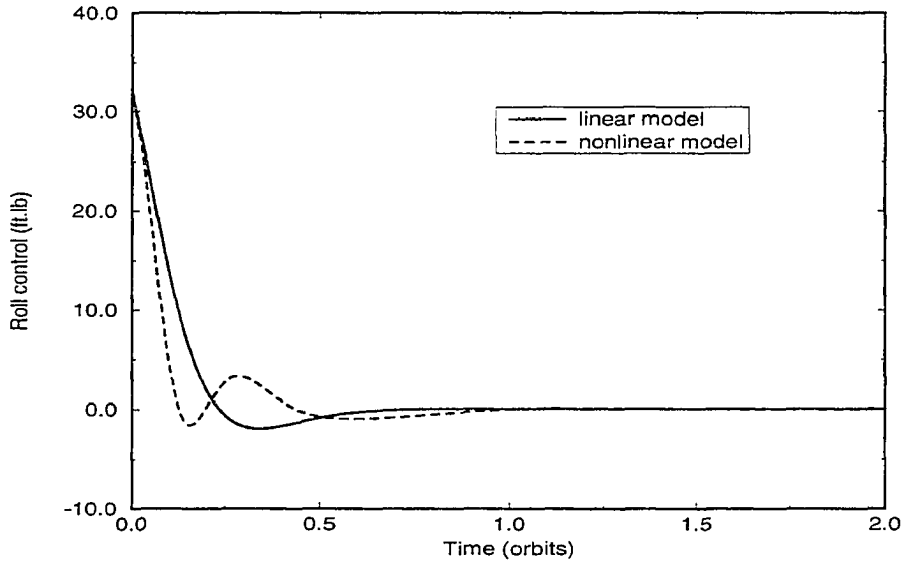

Figure 3.7: Roll control with LQR controller

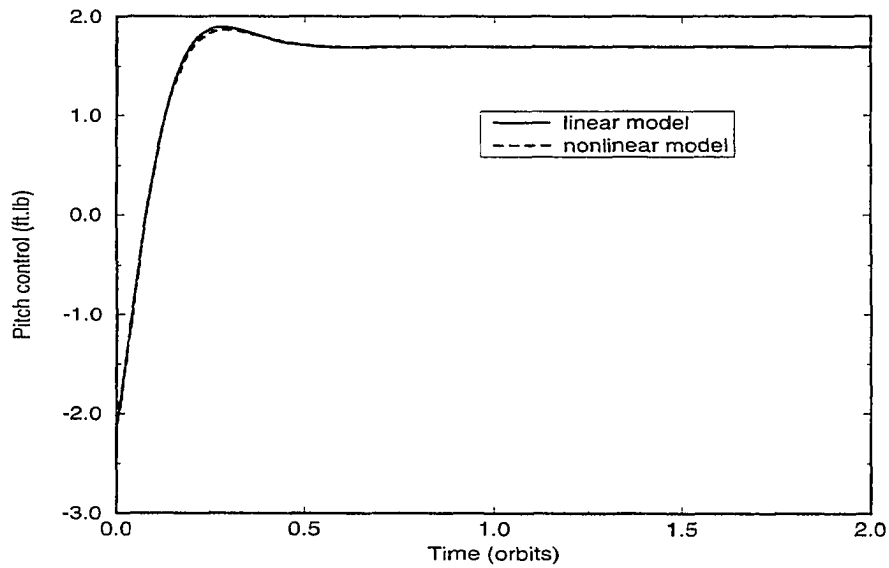

Figure 3.8: Pitch control with LQR controller

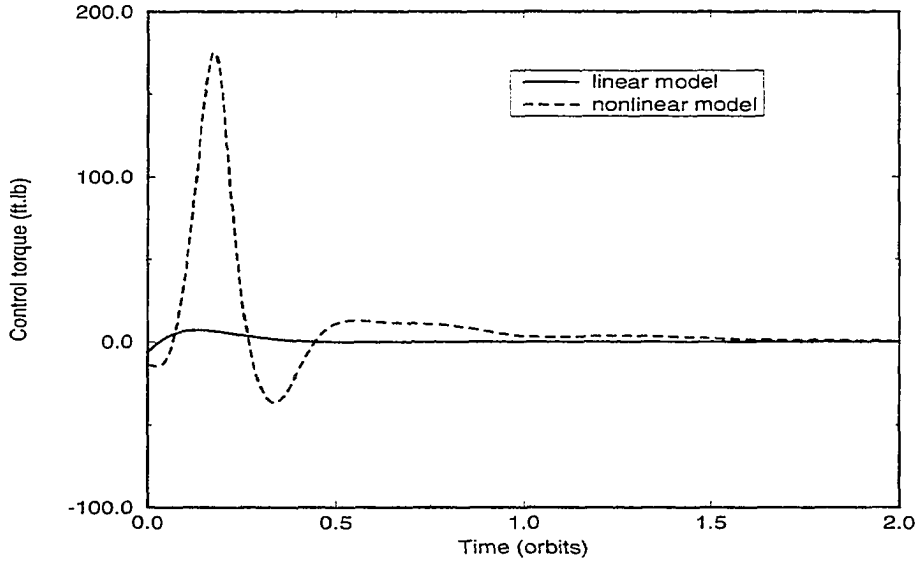

Figure 3.9: Yaw control with LQR controller

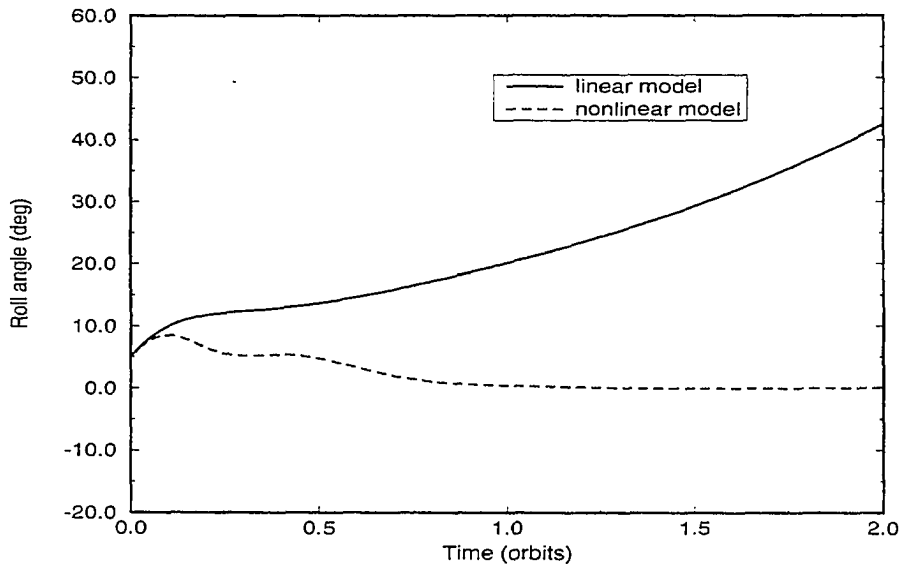

Figure 3.10: Tracking errors of roll angle with configuration change from phase 1 to phase 3 by LQR controller

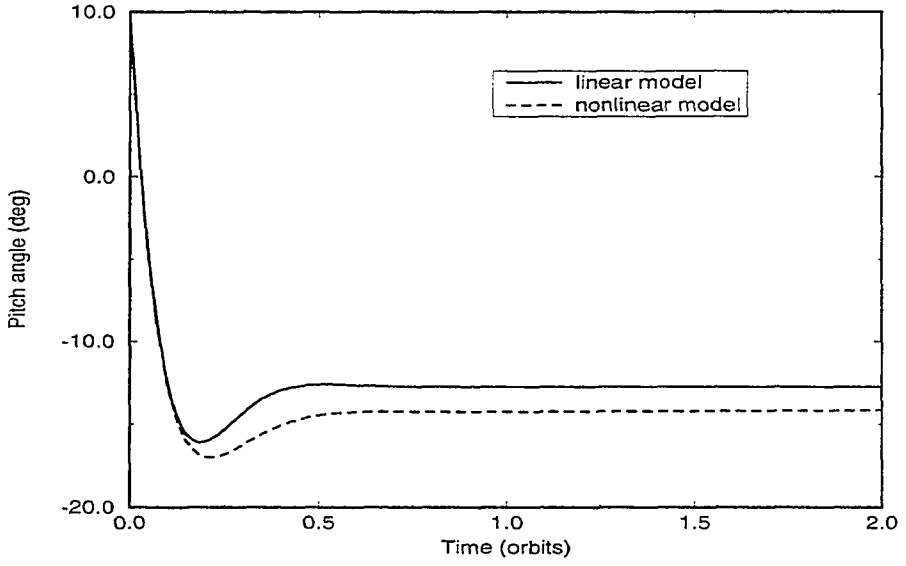

Figure 3.11: Tracking errors of pitch angle with configuration change from phase 1 to phase 3 by LQR controller

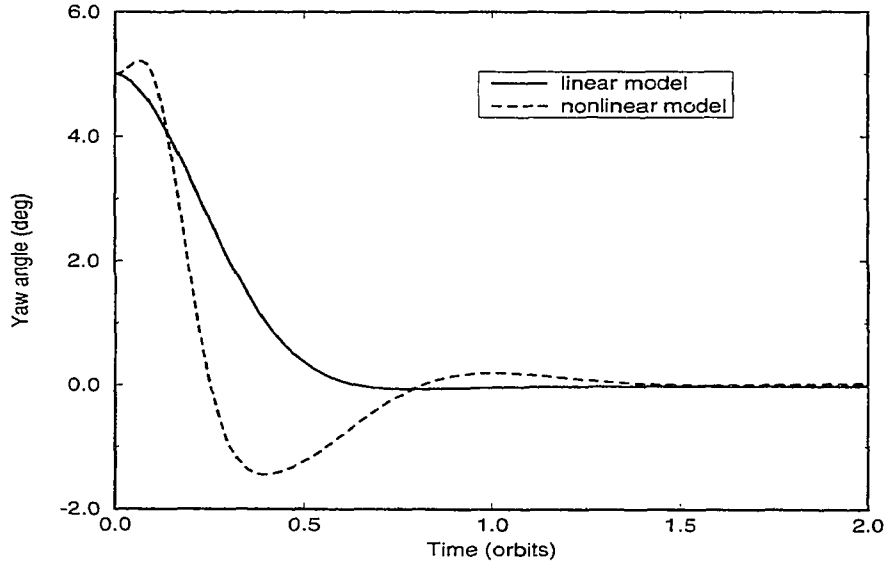

Figure 3.12: Tracking errors of yaw angle with configuration change from phase 1 to phase 3 by LQR controller

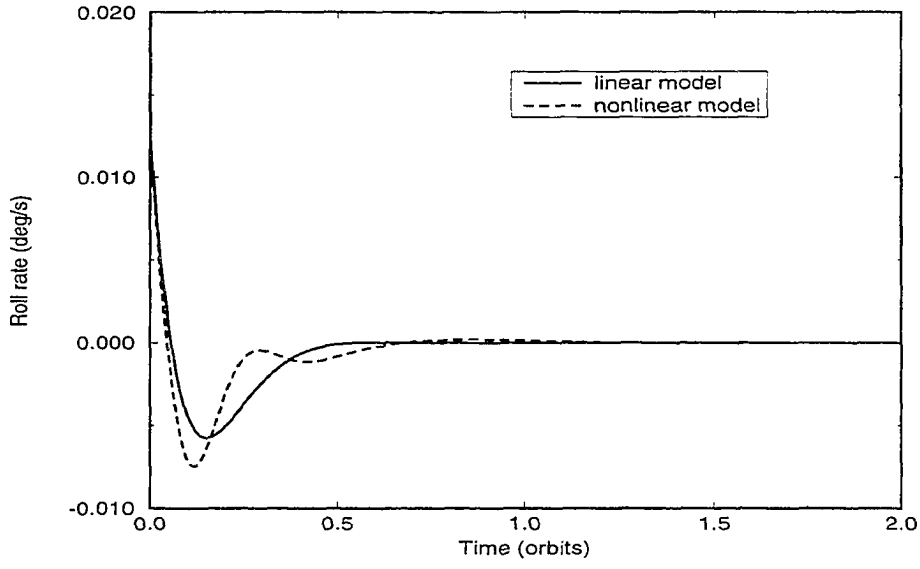

Figure 3.13: Tracking errors of roll rate with configuration change from phase 1 to phase 3 by LQR controller

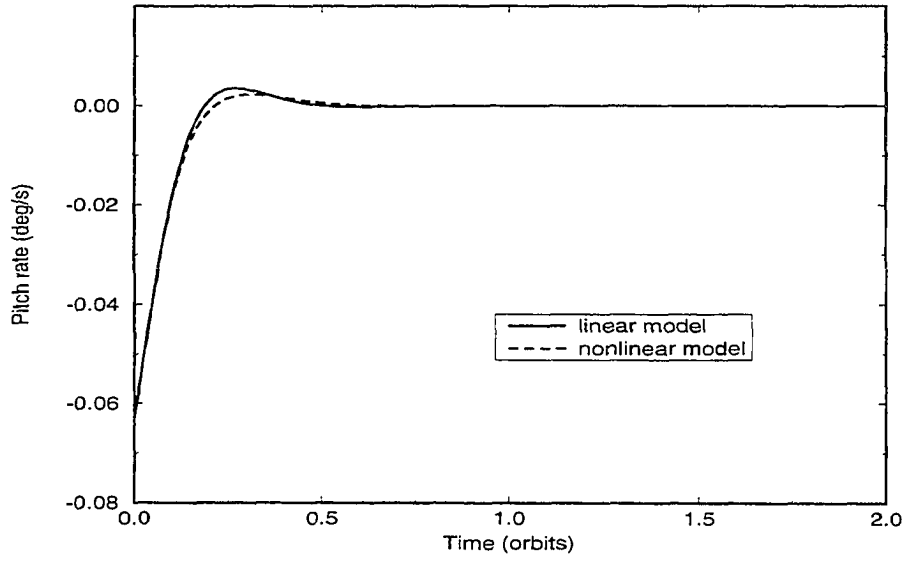

Figure 3.14: Tracking errors of pitch rate with configuration change from phase 1 to phase 3 by LQR controller

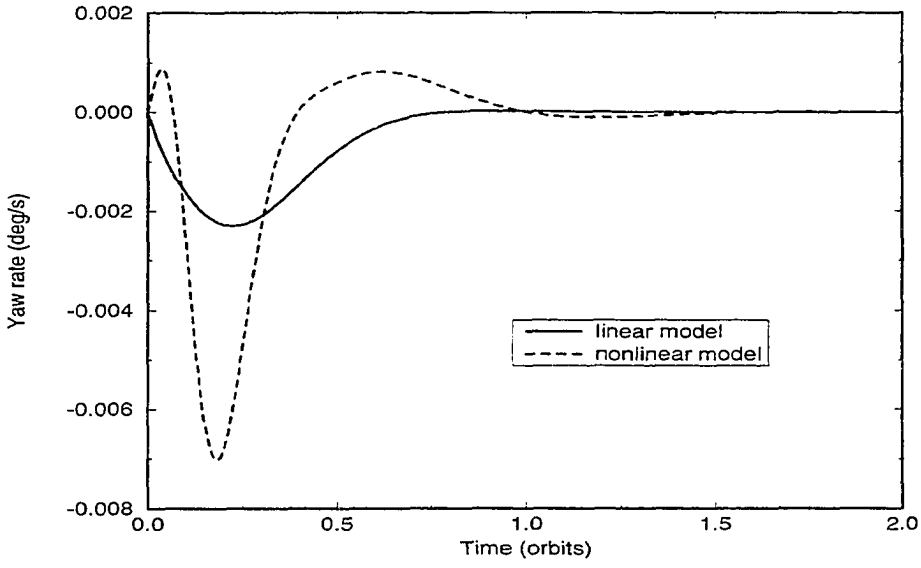

Figure 3.15: Tracking errors of yaw rate with configuration change from phase 1 to phase 3 by LQR controller

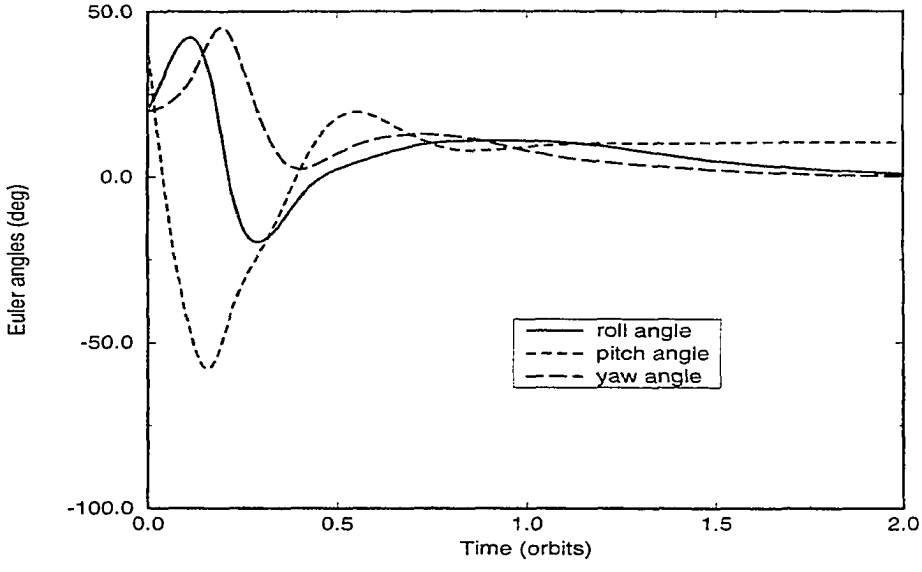

Figure 3.16: Tracking errors of Euler angles for nonlinear model with disturbances by LQR controller

CHAPTER 4. NONLINEAR ADAPTIVE ATTITUDE CONTROL LAWS FOR SPACE STATION

Due to the similar dynamic characteristics of both rigid spacecraft and robot manipulators, this chapter will first discuss two nonlinear adaptive control schemes which were developed based on robot manipulators with both linear parameterization and skew-symmetric property by Slotine and Li [34] and Sponge [36]. Then these controllers are developed considering the periodic disturbance with unknown magnitudes and phase angles. Better transient state responses are achieved by utilizing optimized control parameters. Global convergence of the tracking error is proved in the presence of unknown system parameters and disturbances. Finally, simulation results for several cases are presented.

Adaptive Nonlinear Controller I

Consider the Space Station dynamics in Eqn.(2.17)

$$M(x)\ddot{x} + C(x,\dot{x})\dot{x} + g(x) = \tau \tag{4.1}$$

where $x, \dot{x}, \ddot{x} \in R^n$ are the state variables; $M(x)$ is a mapping: $R^n \rightarrow R^{m\times n}$; $C(x,\dot{x})$: $R^n \rightarrow R^{m\times n}$; $g(x)$: $R^n \rightarrow R^m$; $\tau \in R^m$ is a control vector. Suppose that the moments of inertia of the Space Station are represented by a p-dimensional

constant vector I which appears linearly in the system equations. Then Eqn.(4.1) can be written as

$$M(x)\ddot{x} + C(x,\dot{x})\dot{x} + g(x) = Y(x,\dot{x},\ddot{x})I = \tau \tag{4.2}$$

where Y is an $m \times p$ matrix of known functions of the state variables and their higher derivatives. The skew-symmetric property means that the matrices $M(x)$ and $C(x,\dot{x})$ satisfy the following condition

$$N(x,\dot{x}) = \dot{M}(x) - 2C(x,\dot{x}) \tag{4.3}$$

where N is a skew-symmetric, i.e. $N = -N^T$. With the above two special properties, the controller is designed to obtain system stability with unknown system parameters I. We say that the parameter vector I is "uncertain" if there exists $I_0 \in R^p$ and $\rho \in R_+$, both known, such that

$$\|\tilde{I}\| := \|I - I_0\| \leq \rho \tag{4.4}$$

We say that I is "unknown" if ρ above is unknown. We can always assume that I_0 is known; it is a design quantity. Here, we assume I is unknown.

We define a "nominal" control vector τ_0 as

$$\begin{aligned} \tau_0 &= M_0(x)a + C_0(x,\dot{x})v + g_0(x) - K_D r \\ &= Y(x,\dot{x},v,a)I_0 - K_D r \end{aligned} \tag{4.5}$$

where $M_0(x), C_0(x,\dot{x})$ and $g_0(x)$ are obtained by substituting I with I_0, and the quantities v, a, and r are given by

$$v = \dot{x}_d - \lambda\tilde{x}$$

$$\begin{aligned} a &= \dot{v} \\ r &= \dot{\tilde{x}} + \lambda\tilde{x} \\ \tilde{x} &= x - x_d \end{aligned} \tag{4.6}$$

where x_d is a given twice continuously differentiable reference trajectory and the gain matrices K_D and λ are positive definite (diagonal) matrices. These gain matrices are optimized so that the following performance index is minimized

$$minJ = \int_0^T (x^T Q x + \tau^T R \tau)\, dt \tag{4.7}$$

where Q and R are weighting matrices. The nominal control vector τ_0 in Eqn.(4.5) is defined in terms of fixed parameters given by I_0. These parameters are not changed or updated in time as they would be in an indirect adaptive control strategy. In the case that I_0 is taken to be zero, the nominal control law reduces to a PD type control.

Next we define the control input τ in terms of the nominal vector τ_0 as

$$\tau = \tau_0 + Y(x, \dot{x}, v, a)\eta = Y(x, \dot{x}, v, a)(I_0 + \eta) - K_D r \tag{4.8}$$

where η is an additional control input that will be designed to achieve robustness with respect to the parametric uncertainty represented by $\tilde{I}$ where $\tilde{I}$ is the difference between the estimated and real value. Substituting the control law Eqn.(4.8) into Eqn.(4.2) we obtain after some algebra

$$M(x)\dot{r} + C(x, \dot{x})r + K_D r = Y(x, \dot{x}, v, a)(\tilde{I} + \eta) \tag{4.9}$$

η is chosen according to the sliding rule as

$$\eta = \begin{cases} -\hat{\rho} Y^T r / \|Y^T r\| & \text{if } \|\hat{\rho} Y^T r\| > \varepsilon \\ -\dfrac{\hat{\rho}^2}{\varepsilon} Y^T r & \text{if } \|\hat{\rho} Y^T r\| \leq \varepsilon \end{cases}$$

and $\hat{\rho}$ and ε are chosen according to

$$\dot{\hat{\rho}} = L\|Y^T r\| \tag{4.10}$$

$$\dot{\varepsilon} = -l\varepsilon \tag{4.11}$$

where L, l are some positive numbers. In order to prove the global convergence of tracking error and later results, the following definitions and lemmas are necessary.

Lemma 2.1. (Barbalat's Lemma)[1] If $f : R^+ \to R$ is uniformly continuous for $t \geq 0$, and if the limit of the integral

$$\lim_{t\to\infty} \int_0^t \|f(\tau)\| d\tau$$

exists and is finite, then

$$\lim_{t\to\infty} f(t) = 0$$

Corollary 2.1 [1] If $g \in L_2 \bigcap L_\infty$, and $\dot{g}$ is bounded then

$$\lim_{t\to\infty} g(t) = 0$$

Proof: Let $f(t) = g^2(t)$ and $\dot{g}g$ be uniformly continuous, then $f(t)$ satisfies the condition of lemma 2.1. Therefore the results follows.

Lemma 2.2 [1] Let $f(\bullet)$ be a scalar function. If (1) f is lower bounded, i.e. $\exists c, \forall t \geq 0, f(t) \geq c$; (2) f has a uniformly continuous, non-positive derivative of f, then $\dot{f}(t) \to 0$ as $t \to \infty$.

Then the convergence of the tracking error can be proved.

Proof: We shall prove the result by showing that the function

$$V = \frac{1}{2} r^T M(x) r + \tilde{x}^T \lambda^T K_D \tilde{x} + \frac{1}{2}(\hat{\rho} - \rho)^T L^{-1}(\hat{\rho} - \rho) + \frac{\varepsilon}{l} \tag{4.12}$$

is a Lyapunov function for the closed loop system. The assumption on the inertia matrix $M(x)$ to be positive definite is necessary to guarantee that V is a valid Lyapunov function candidate, a straightforward calculation using the skew-symmetry and the definition of r shows that

$$\dot{V} = -e^T S e + \xi^T (\tilde{I} + \eta) + (\hat{\rho} - \rho)\|\xi\| - \varepsilon \tag{4.13}$$

where $e^T = [\tilde{x}, \dot{\tilde{x}}^T]$, $\xi = Y^T r$, and $S = diag(\lambda^T K_D \lambda)$, K_D and S is positive definite, making the first term in Eqn.(4.13) negative semi-definite. We next consider the remaining terms of Eqn.(4.13).

Case 1): If $\|\xi\| > \varepsilon/\hat{\rho}$, then $\eta = -\hat{\rho}\xi/\|\xi\|$ and we have,

$$\begin{aligned} \xi^T(\tilde{I} + \eta) + (\hat{\rho} - \rho)\|\xi\| - \varepsilon &= \xi^T \tilde{I} - \rho\|\xi\| - \varepsilon \\ &\leq \|\xi\|(\|\tilde{I}\| - \rho) - \varepsilon \\ &\leq 0 \end{aligned}$$

from the Cauchy-Schwartz inequality and assumption on $\|\tilde{I}\|$.

Case 2): If $\|\xi\| \leq \varepsilon/\hat{\rho}$ then $\eta = \hat{\rho}^2/\varepsilon\xi$ and we have

$$\begin{aligned} \xi^T(\tilde{I} + \eta) &+ (\hat{\rho} - \rho)\|\xi\| - \varepsilon \\ &= \xi^T \tilde{I} - \frac{\hat{\rho}^2}{\varepsilon}\|\xi\|^2 - \rho\|\xi\| - \varepsilon \\ &\leq \|\xi\|\|\tilde{I}\| - \rho - \frac{\hat{\rho}^2}{\varepsilon}\|\xi\|^2 + \hat{\rho}\|\xi\| - \varepsilon \\ &\leq 0 \end{aligned}$$

since $\|\tilde{I}\| \leq \rho$ and $\|\xi\| \leq \varepsilon/\hat{\rho}$. Therefore, we have shown that

$$\dot{V} \leq -e^T S e. \tag{4.14}$$

Global convergence now follows from standard arguments. We immediately have from the above that $\tilde{x}$, $\dot{\tilde{x}}$, r and $\hat{\rho}$ are bounded and $\tilde{x}$, $\dot{\tilde{x}}$ and $r \in L_2$. In particular, by Corollary 2.1, this implies that $\tilde{x} \to 0$ as $t \to \infty$. Moreover, it is obvious from the definition of η that $\|\eta\| \leq \hat{\rho}$. Therefore from the equations of motion Eqn.(4.9) we see that $\dot{r}$ is bounded which, in turn, implies that $\dot{\tilde{x}} \to 0$. Note that in Eqn.(4.10), L is a positive number, thus any system noise will cause the upper bound of $\hat{\rho}$ to go to infinity. A more robust scheme for this controller is obtained by simply modifying this updating law as

$$\dot{\hat{\rho}} = -\sigma\hat{\rho} + L\|Y^T r\| \tag{4.15}$$

where σ is some positive number. The increases of $\hat{\rho}$ will be controlled by the first term on the right side of Eqn.(4.15). We also note that while the global convergence of the tracking error can be achieved by using this controller, the parameter vector $\tilde{I}$ is not updated.

Adaptive Nonlinear Controller II

We assume that the desired $x_d, \dot{x}_d$, and $\ddot{x}_d$ are all bounded. Let $\hat{I}$ be the (time-varying) parameter vector estimate, $\tilde{I} = \hat{I} - I_0$ be the parameter estimation error, and $\tilde{x} = x - x_d$ be the tracking error. Consider a Lyapunov-like function

$$V(t) = \frac{1}{2}(r^T M(x) r + \tilde{I}^T \Gamma^{-1} \tilde{I}) \tag{4.16}$$

with the vector r, a measure of the tracking error, defined as

$$r = \dot{\tilde{x}} + \lambda\tilde{x}$$

where Γ is a PD matrix and λ is a strictly positive constant. We define

$$v = \dot{x}_d - \lambda\tilde{x}$$

$$a = \dot{v}$$

$$r = \dot{x} - v$$

Differentiating V(and using the skew-symmetry of the matrix $(\dot{M} - 2C)$ lead to

$$\dot{V} = r^T(\tau - Ma - Cv - g) + \tilde{I}\Gamma^{-1}\dot{\tilde{I}} \tag{4.17}$$

Take the control law to be

$$\tau = M_0 a + C_0 v + g_0 - K_D r \tag{4.18}$$

Similarly to the first controller, K_D and λ are optimized so that the performance index

$$J = \int_0^T (x^T Q x + \tau^T R \tau)\, dt \tag{4.19}$$

is minimized, where Q and R are weighting matrices. Then

$$\dot{V}(t) = r^T(\bar{M}a + \bar{C}v + \bar{g} - K_D r) + \tilde{I}\Gamma^{-1}\dot{\tilde{I}} \tag{4.20}$$

where $\tilde{M} = M_0 - M$, $\tilde{C} = C_0 - C$, $\tilde{g} = g_0 - g$. The linear parameterization of dynamics allows us to define a known matrix $Y(x, \dot{x}, v, a)$ such that

$$\tilde{M}(x)a + \tilde{C}(x, \dot{x})v + \tilde{g}(x) = Y(x, \dot{x}, v, a)\tilde{I} \tag{4.21}$$

Hence

$$\dot{V}(t) = -r^T K_D r + \tilde{I}^T(\Gamma^{-1}\dot{\tilde{I}} + Y^T r) \tag{4.22}$$

Choosing the parameter adaptation law as

$$\dot{\tilde{I}} = -\Gamma Y^T r \tag{4.23}$$

yields

$$\dot{V}(t) = -r^T K_D r \leq 0 \tag{4.24}$$

By Lemma 2.2, this shows that $\dot{V} \to 0$ as $t \to \infty$, which in turn implies that $r \to 0$, thus $\tilde{x} \to 0$ and $\dot{\tilde{x}} \to 0$. Therefore, global stability of the closed-loop system is guaranteed by the above adaptive controllers. We notice again that by Eqn.(4.23), $\dot{\tilde{I}} \to 0$, so $\tilde{I}$ tends to be constant, but not necessarily zero. That is, parameter estimation convergence is not guaranteed. A further discussion on the parameter convergence will be given later.

Controller Design with Unknown Disturbances

Consider a disturbance vector for the Space Station of the form

$$d(t) = \hat{P}\bar{V}(t) \tag{4.25}$$

where

$$\hat{P} = D^T P$$

Here D is a matrix defined in Eqn.(2.14), $\bar{P}$ is a $m \times q$ constant, but unknown matrix, and $\bar{V} \in R^q$ is a vector and the components of which are some known functions of time and are bounded for all $t \geq 0$ of Eqn.(2.20). The system equation in Eqn.(4.1) becomes

$$M(x)\ddot{x} + C(x,\dot{x})\dot{x} + g(x) = \tau + d(t) \tag{4.26}$$

For our controller design, we modify the original controls by adding a term which comprises of the estimated disturbance parameters and tries to cancel the disturbances.

$$\tau = \tau_i - \bar{P}\bar{V} \tag{4.27}$$

where τ_i $i = 1, 2$ are the corresponding expressions as in Eqns.(4.8) and (4.18), $\bar{P}$ is the estimation of the actual P matrix. Let

$$\tilde{P} = \bar{P} - \hat{P}$$

In this case, a Lyapunov function candidate can be chosen as

$$V = V_i + \frac{1}{2} tr(\tilde{P}^T K^{-1} \tilde{P}) \tag{4.28}$$

where $V_i, i = 1, 2$ are equal to the expressions in Eqns.(4.12) and (4.16). $tr()$ indicates the trace of a matrix which is the sum of the all diagonal elements. Then

$$\dot{V} = \dot{V}_i - r^T \tilde{P} \bar{V} + tr(\tilde{P}^T K^{-1} \dot{\tilde{P}}) \tag{4.29}$$

Choose

$$\dot{\tilde{P}} = -Kr\bar{V}^T \tag{4.30}$$

which is equivalent to the parameter update law

$$\dot{\bar{P}} = -Kr\bar{V}^T \tag{4.31}$$

Therefore,

$$\dot{V} = \dot{V}_i \tag{4.32}$$

Since

$$\dot{V}_i \leq 0, \mathrm{i} = 1, 2$$

where $\dot{V}_i, \mathrm{i} = 1, 2$ are expressed in Eqns.(4.14) and (4.24).

$$tr(\tilde{P}^T r\bar{V}^T) = r^T \tilde{P} \bar{V}$$

From the assumption of $\bar{V} \in L_\infty, r \in L_\infty, r \to 0, \Rightarrow \dot{\bar{P}} \to 0$ Therefore, the boundness of the parameter matrix $\bar{P}$ is guaranteed, But the convergence relies on the persistent excitation (PE) property of $\bar{V}\bar{V}^T$. That is, if $\bar{V}\bar{V}^T$ is PE, then $\bar{P} \to P$.

Definition [55] If a vector or matrix Z is said to be persistently exciting if there exist positive constants α_1, α_2 and T_0 such that for all $t \geq 0$

$$\alpha_1 I_q \leq \int_t^{t+T_0} Z^T(\tau) Z(\tau) d\tau \leq \alpha_2 I_q \tag{4.33}$$

Convergence of Parameter Estimations

At this point, we have encountered two issues about convergence of parameter estimation: one is on the system parameters, i.e. the moments of inertia. Another one is on the disturbance parameters which are estimated on-line in order to cancel out their effect. We will discuss these two issues in the following.

Disturbance Parameters

For our problem, the convergence of $\bar{P}$ depends on the PE of $\bar{V}$. Because of the periodic functions of $\bar{V}\bar{V}^T$, if we choose $T_0 = 2\pi$, then

$$\int_t^{t+2\pi} \bar{V}^T \bar{V} d\tau = \int_0^{\frac{2\pi}{n}} \begin{pmatrix} 1 & sin(n\tau) & \cdots & cos(4n\tau) \\ sin(n\tau) & sin^2(n\tau) & \cdots & sin(n\tau)cos(4n\tau) \\ cos(n\tau) & sin(n\tau)cos(n\tau) & \cdots & cos(n\tau)cos(4n\tau) \\ \cdots & \cdots & \cdots\cdots & \\ cos(4n\tau) & sin(n\tau)cos(4n\tau) & \cdots & cos^2(4n\tau) \end{pmatrix}_{9\times 9} d\tau$$

$$= \begin{pmatrix} 2\pi/n & 0 & \cdots & 0 \\ 0 & \pi/n & \cdots & 0 \\ \cdots & \cdots & \cdots & \cdots \\ 0 & 0 & \cdots & \pi/n \end{pmatrix} \tag{4.34}$$

Therefore, if we select $\alpha_1 = 0.5\pi/n$, and $\alpha_2 = 2.5\pi/n$, the Eqn.(4.33) is satisfied and this completed the PE proof for the disturbance parameter estimations. Therefore, the parameter update law in Eqn.(4.30) will lead to $\bar{P} \rightarrow P$.

Principal Moments of Inertias

The adaptation law for the parameters in the second controller is given in Eqn.(4.23)

$$\dot{\hat{I}} = -\Gamma Y^T r \tag{4.35}$$

The convergence of the parameters depends on whether YY^T satisfies the condition in Eqn.(4.33). It is easy to conclude that the maximum number of parameters that can converge is 3 in this case. Thus we will have to restrict the problem to the case where the body axes coincide with the principle axes of the Space Station. In this case, all the products of inertia are zero. For the model which only has principal moments of inertia, the Y becomes a 3×3 square matrix which can be written as

$$YY^T = \begin{pmatrix} y_{11} & y_{12} & y_{13} \\ y_{21} & y_{22} & y_{23} \\ y_{31} & y_{32} & y_{33} \end{pmatrix} \tag{4.36}$$

where

$$y_{11} = \ddot{\theta_1} + \sin\theta_3\ddot{\theta_2} + \dot{\theta_2}\cos(\theta_1)^2\cos\theta_3\dot{\theta_3}\sec(\theta_3)^2 - \dot{\theta_2}\cos(\theta_1)^2\cos\theta_3\sin\theta_3\dot{\theta_3}$$

$$\tan\theta_3 \sec\theta_3 + \dot{\theta_2}\ \sin(\theta_1)^2 \cos\theta_3 \dot{\theta_3}\ \sec(\theta_3)^2 - \dot{\theta_2}\ \sin\theta_1 \cos\theta_3 \sin$$

$$\theta_3 \dot{\theta_1}\ \tan\theta_3 \sec\theta_3 - \dot{\theta_3}\,\dot{\theta_1}\ \sin(\theta_1)^2 \tan\theta_3 + \dot{\theta_3}\ \sin\theta_3 \dot{\theta_1}$$

$$\sin(\theta_1)^2 \sec\theta_3 - \sin\theta_1 \sin\theta_3 \dot{\theta_3}^2 \cos\theta_1 \tan\theta_3 \sec\theta_3 - \dot{\theta_3}\,\dot{\theta_1}$$

$$\cos(\theta_1)^2 \tan\theta_3 + \dot{\theta_3}\ \sin\theta_3 \dot{\theta_1}\ \cos(\theta_1)^2 \sec\theta_3 + \dot{\theta_3}\ \cos\theta_1 \sin\theta_3$$

$$\dot{\theta_1}\ \tan(\theta_3)\sec(\theta_3)$$

$$y_{12} = \sin\theta_3 \ddot{\theta_1} + \sin(\theta_3)^2 \ddot{\theta_2} + \dot{theta_2}\ \cos(\theta_1)^2 \cos\theta_3 \sin\theta_3 \dot{\theta_3}\ \sec(\theta_3)^2$$

$$-\dot{\theta_2}\ \cos(\theta_1)^2 \cos\theta_3 \sin(\theta_3)^2 \dot{\theta_3}\ \tan\theta_3 \sec\theta_3 + \dot{\theta_2}\ \sin(\theta_1)^2 \cos\theta_3 \sin\theta_3$$

$$\dot{\theta_3}\ \sec(\theta_3)^2 - \dot{\theta_2}\ \sin\theta_1 \cos\theta_3 \sin(\theta_3)^2 \dot{\theta_1}\ \tan\theta_3 \sec\theta_3 - \dot{\theta_3}\ \sin\theta_3 \dot{\theta_1}$$

$$\sin(\theta_1)^2 \tan\theta_3 + \dot{\theta_3}\ \sin(\theta_3)^2 \dot{\theta_1}\ \sin(\theta_1)^2 \sec\theta_3 - \sin\theta_1 \sin(\theta_3)^2 \dot{\theta_3}^2$$

$$\cos\theta_1 \tan\theta_3 \sec\theta_3 - \dot{\theta_3}\ \sin\theta_3 \theta_3 \dot{\theta_1}\ \cos(\theta_1)^2 \tan\theta_3 + \dot{\theta_3}\ \sin(\theta_3)^2 \dot{\theta_1}$$

$$\cos(\theta_1)^2 \sec\theta_3 + \dot{\theta_3}\ \cos\theta_1 \sin(\theta_3)^2 \dot{\theta_1}\ \tan\theta_3 \sec\theta_3 + \dot{\theta_3}\ \cos(\theta_1)^2$$

$$\cos\theta_3 \dot{\theta_1} + \dot{\theta_3}\ \cos(\theta_1)^2 \cos\theta_3 \sin\theta_3 \dot{\theta_2} + \dot{\theta_3}\ \sin(\theta_1)^2 \cos\theta_3 \dot{\theta_1}$$

$$+\dot{\theta_3}\ \sin(\theta_1)^2 \cos\theta_3 \sin\theta_3 \dot{\theta_2} + 3n^2 \cos(\theta_3)^2 \cos(\theta_2 + nt) \sin(\theta_2 + nt)$$

$$y_{13} = -\cos\theta_3 (\sin(\theta_1)^2 \dot{\theta_1} + \sin(\theta_1)^2 \sin\theta_3 \dot{\theta_2} + \cos(\theta_1)^2 \dot{\theta_1} + \cos(\theta_1)^2 \sin\theta_3$$

$$(\dot{\theta_2})\dot{\theta_2} - 3n^2 \sin(\theta_2 + nt)^2 \sin\theta_3 \cos\theta_3$$

$$y_{21} = \sin\theta_1 \cos(\theta_3)^2 \dot{\theta_2}^2 \cos\theta_1 + \sin(\theta_1)^2 \cos\theta_3 \dot{\theta_2}\,\dot{\theta_3} - \cos(\theta_1)^2 \dot{\theta_3}\ \cos\theta_3 \dot{\theta_2}$$

$$-\cos\theta_1 \dot{\theta_3}^2 \sin\theta_1 - 3n^2 (\sin\theta_1 \sin(\theta_2 + nt) \sin\theta_3 - \cos\theta_1$$

$$\cos(\theta_2 + nt))(\cos\theta_1 \sin(\theta_2 + nt) \sin\theta_3 + \sin\theta_1 \cos(\theta_2 + nt))$$

$$y_{22} = \cos(\theta_1)^2 \cos(\theta_3)^2 \ddot{\theta_2} + \cos\theta_1 \cos\theta_3 \sin\theta_1 \ddot{\theta_3} - \sin\theta_1 \cos(\theta_3)^2 \dot{\theta_1}\ \cos\theta_1$$

$$\dot{\theta_2} - \dot{\theta_3}\ \sin(\theta_1)^2 \cos(\theta_3)\dot{\theta_1} - \dot{\theta_2}\ \cos(\theta_1)^4 \cos(\theta_3)^3 \dot{\theta_3}\ \tan\theta_3 \sec\theta_3 - \dot{\theta_2}$$

$$\cos(\theta_1)^3 \cos(\theta_3)^2 \sin\theta_1 \dot{\theta_1} - \dot{\theta_2}\ \sin\theta_1 \cos(\theta_3)^3 \cos(\theta_1)^2 \dot{\theta_1}\ \tan\theta_3 \sec\theta_3$$

$$
\begin{aligned}
& -\dot{\theta_2}\ \sin(\theta_1)^3 \cos(\theta_3)^2 \cos\theta_1 \dot{\theta_1} + \dot{\theta_3}\ \cos(\theta_1)^2 \cos(\theta_3)^2 \dot{\theta_1}\ \sin(\theta_1)^2 \sec\theta_3 \\
& - \sin\theta_1 \cos(\theta_1)^3 \cos(\theta_3)^2 \dot{\theta_3}^2 \tan\theta_3 \sec\theta_3 + \dot{\theta_3}\ \cos(\theta_1)^4 \cos(\theta_3)^2 \dot{\theta_1}\ \sec\theta_3 \\
& + \dot{\theta_3}\ \cos(\theta_1)^3 \cos(\theta_3)^2 \dot{\theta_1}\ \tan\theta_3 \sec\theta_3 - \dot{\theta_3}\ \cos(\theta_1)^2 \cos\theta_3 \sin\theta_3 \dot{\theta_2} \\
& - \cos\theta_1 \sin\theta_3 \sin\theta_1 \dot{\theta_3}^2 - 3n^2(\sin(\theta_3)^2 \sin\theta_1 \sin(\theta_2 + nt) - \sin\theta_3 \cos\theta_1 \\
& \cos(\theta_2 + nt) + \sin\theta_1 \cos(\theta_3)^2 \sin(\theta_2 + nt))(\cos\theta_1 \sin(\theta_2 + nt) \sin\theta_3 \\
& + \sin\theta_1 \cos(\theta_2 + nt))
\end{aligned}
$$

$$
\begin{aligned}
y_{23} = \ & \cos\theta_1 \cos\theta_3 \sin\theta_1 \ddot{\theta_2} + \sin(\theta_1)^2 \ddot{\theta_3} + \cos(\theta_1)^2 \dot{\theta_1}\ \cos\theta_3 \dot{\theta_2} + \cos\theta_1 \dot{\theta_1} \\
& \sin\theta_1 \dot{\theta_3} - \dot{\theta_2}\ \sin\theta_1 \cos(\theta_1)^3 \cos(\theta_3)^2 \dot{\theta_3}\ \tan\theta_3 \sec\theta_3 - \dot{\theta_2}\ \cos(\theta_1)^2 \cos\theta_3 \\
& \sin(\theta_1)^2 \dot{\theta_1} - \dot{\theta_2}\ \sin(\theta_1)^2 \cos(\theta_3)^2 \cos\theta_1 \dot{\theta_1}\ \tan\theta_3 \sec\theta_3 - \dot{\theta_2}\ \sin(\theta_1)^4 \cos\theta_3 \\
& \dot{\theta_1} + \cos(\theta_1)^2 \sin\theta_3 \cos\theta_3 \dot{\theta_2}^2 + \dot{\theta_2}\ \cos\theta_1 \sin\theta_3 \sin\theta_1 \dot{\theta_3} + \dot{\theta_3}\ \cos\theta_1 \\
& \cos\theta_3 \sin(\theta_1)^3 \dot{\theta_1}\ \sec\theta_3 - \cos(\theta_1)^2 \cos\theta_3 \sin(\theta_1)^2 \dot{\theta_3}^2 \tan\theta_3 \sec\theta_3 + \dot{\theta_3} \\
& \cos(\theta_1)^3 \cos\theta_3 \sin\theta_1 \dot{\theta_1}\ \sec\theta_3 + \dot{\theta_3}\ \cos(\theta_1)^2 \cos\theta_3 \sin\theta_1 \dot{\theta_1}\ \tan\theta_3 \\
& \sec\theta_3 + 3n^2 \cos\theta_1 \sin(\theta_2 + nt) \cos\theta_3 (\cos\theta_1 \sin(\theta_2 + nt) \sin\theta_3 + \sin\theta_1 \\
& \cos(\theta_2 + nt))
\end{aligned}
$$

$$
\begin{aligned}
y_{31} = \ & -\sin\theta_1 \cos(\theta_3)^2 \dot{\theta_2}^2 \cos\theta_1 + \cos(\theta_1)^2 \dot{\theta_3}\ \cos\theta_3 \dot{\theta_2} - \sin(\theta_1)^2 \cos\theta_3 \dot{\theta_2}\ \dot{\theta_3} \\
& + \cos\theta_1 \dot{\theta_3}^2 \sin\theta_1 + 3n^2(\sin\theta_1 \sin(\theta_2 + nt) \sin\theta_3 - \cos\theta_1 \cos(\theta_2 + nt)) \\
& (\cos\theta_1 \sin(\theta_2 + nt) \sin\theta_3 + \sin\theta_1 \cos(\theta_2 + nt))
\end{aligned}
$$

$$
\begin{aligned}
y_{32} = \ & \sin(\theta_1)^2 \cos(\theta_3)^2 \ddot{\theta_2} - \cos\theta_1 \cos\theta_3 \sin\theta_1 \ddot{\theta_3} + \sin\theta_1 \cos(\theta_3)^2 \dot{\theta_1}\ \cos\theta_1 \dot{\theta_2} \\
& - \cos(\theta_1)^2 \cos\theta_3 \dot{\theta_1}\ \dot{\theta_3} - \dot{\theta_2}\ \cos(\theta_1)^2 \cos(\theta_3)^3 \sin(\theta_1)^2 \dot{\theta_3}\ \tan\theta_3 \sec\theta_3 \\
& + \dot{\theta_2}\ \cos(\theta_1)^3 \cos(\theta_3)^2 \sin\theta_1 \dot{\theta_1} - \dot{\theta_2}\ \sin(\theta_1)^3 \cos(\theta_3)^3 \dot{\theta_1}\ \tan\theta_3 \sec\theta_3 \\
& + \dot{\theta_2}\ \sin(\theta_1)^3 \cos(\theta_3)^2 \cos(\theta_1) \dot{\theta_1} + \dot{\theta_3}\ \sin(\theta_1)^4 \cos(\theta_3)^2 \dot{\theta_1}\ \sec\theta_3 - \sin(\theta_1)^3
\end{aligned}
$$

$$
\begin{aligned}
& \cos(\theta_3)^2\dot{\theta_3}^2\cos\theta_1\tan\theta_3\sec\theta_3+\dot{\theta_3}\cos(\theta_1)^2\cos(\theta_3)^2\dot{\theta_1}\sin(\theta_1)^2\sec\theta_3 \\
& +\dot{\theta_3}\cos\theta_1\sin(\theta_1)^2\cos(\theta_3)^2\dot{\theta_1}\tan\theta_3\sec\theta_3-\dot{\theta_3}\sin\theta_3\sin(\theta_1)^2\cos(\theta_3)\dot{\theta_2} \\
& +\cos\theta_1\sin\theta_3\sin\theta_1\dot{\theta_3}^2+3n^2(\sin(\theta_3)^2\cos\theta_1\sin(\theta_2+nt)+\sin\theta_3 \\
& \sin\theta_1\cos(\theta_2+nt)+\cos\theta_1\cos(\theta_3)^2\sin(\theta_2+nt))\sin(\theta_1\sin(\theta_2+nt) \\
& \sin\theta_3-\cos\theta_1\cos(\theta_2+nt)) \\
y_{33} \;=\; & -\cos\theta_1\cos\theta_3\sin\theta_1\ddot{\theta_2}+\cos(\theta_1)^2\ddot{\theta_3}+\sin(\theta_1)^2\dot{\theta_1}\cos\theta_3\dot{\theta_2}-\cos\theta_1\dot{\theta_1} \\
& \sin\theta_1\dot{\theta_3}+\dot{\theta_2}\sin\theta_1\cos(\theta_1)^3\cos(\theta_3)^2\dot{\theta_3}\tan\theta_3\sec\theta_3-\dot{\theta_2}\cos(\theta_1)^4 \\
& \cos\theta_3\dot{\theta_1}+\dot{\theta_2}\sin(\theta_1)^2\cos(\theta_3)^2\cos\theta_1\dot{\theta_1}\tan\theta_3\sec\theta_3-\dot{\theta_2}\cos(\theta_1)^2 \\
& \cos\theta_3\sin(\theta_1)^2\dot{\theta_1}+\sin\theta_3\sin(\theta_1)^2\cos\theta_3\dot{\theta_2}^2-\dot{\theta_2}\cos\theta_1\sin\theta_3\sin\theta_1\dot{\theta_3} \\
& -\dot{\theta_3}\cos\theta_1\cos\theta_3\sin(\theta_1)^3\dot{\theta_1}\sec\theta_3+\cos(\theta_1)^2\cos\theta_3\sin(\theta_1)^2\dot{\theta_3}^2 \\
& \tan\theta_3\sec\theta_3-\dot{\theta_3}\cos(\theta_1)^3\cos\theta_3\sin\theta_1\dot{\theta_1}\sec\theta_3-\dot{\theta_3}\cos(\theta_1)^2\cos\theta_3 \\
& \sin\theta_1\dot{\theta_1}\tan\theta_3\sec\theta_3+3n^2\sin\theta_1\sin(\theta_2+nt)\cos\theta_3(\sin(\theta_1) \\
& \sin(\theta_2+nt)\sin\theta_3-\cos\theta_1\cos(\theta_2+nt))
\end{aligned}
$$

The convergence of tracking error has been proven, i.e., $\theta \to \theta_d, \dot{\theta} \to \dot{\theta}_d$. and $\ddot{\theta} \to \ddot{\theta}_d$. So, whether or not the PE condition is met depends on the choice of the reference attitude θ_d. It can be shown that the LVLH reference attitude does not satisfy the PE condition. However, if accurate principal moments of inertia are designed to be known, some other reference $\theta_d(t)$ that is close to the LVLH orientation but satisfies the PE condition may be chosen for parameter estimation purpose. once the parameter estimation convergences, the obtained values of the moments of inertia then can be used for the control law to maintain the space station in the LVLH position.

Simulation Results

We'll first implement these adaptive controllers to the complete model with full inertia matrix where the principal axes are not aligned with the body axes and thus the small cross-product terms exist. In order to apply these adaptive laws, we need to use the form of the spacecraft dynamics as specified in Eqn.(2.17).

Case I,

We suppose that the estimated inertias ($slug - ft^2$) are:

$$\begin{aligned} I_{11} &= 46.64e6 \\ I_{12} &= -0.044e6 \\ I_{13} &= 0.93e6 \\ I_{22} &= 2.8e6 \\ I_{23} &= -0.031e6 \\ I_{33} &= 46.48e6 \end{aligned}$$

The spacecraft state is initialized at $\theta = [5^o, 10^o, 5^o] deg$, and $\dot{\theta} = [0.2n, -n, 0] rad/s$, $L = 5000, l = 100$, and the 5×5 matrix $\Gamma = diag(2 \times 10^2)$. The optimized parameters are obtained as follows: For controller I,

$$K_D = \begin{bmatrix} 10^7 & 0 & 0 \\ 0 & 10^6 & 0 \\ 0 & 0 & 5 \times 10^7 \end{bmatrix}$$

$$\Lambda = \begin{bmatrix} 83.2 & 0 & 0 \\ 0 & 98.9 & 0 \\ 0 & 0 & 57.89 \end{bmatrix}$$

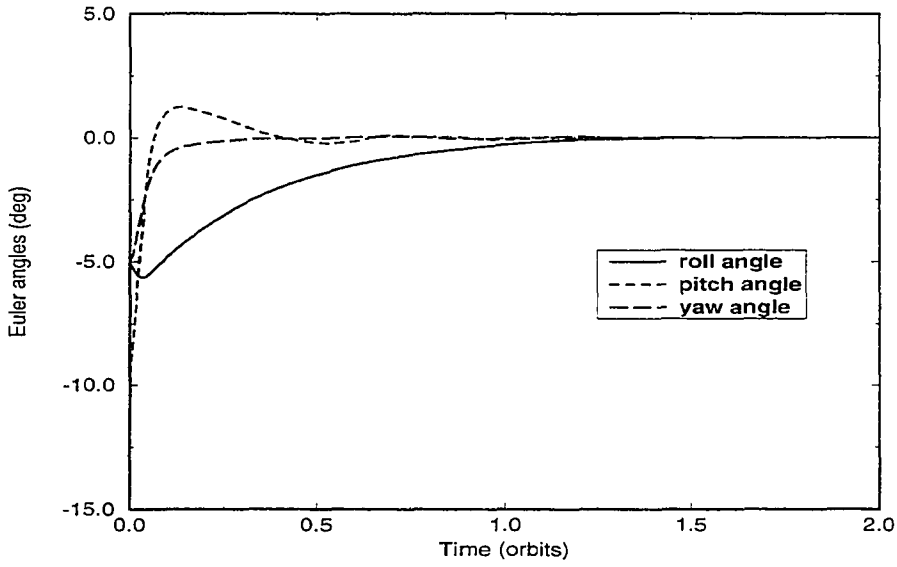

Figure 4.1: Tracking errors of Euler angles with controller I

and for controller II,

$$K_D = \begin{bmatrix} 3 \times 10^7 & 0 & 0 \\ 0 & 3 \times 10^6 & 0 \\ 0 & 0 & 5 \times 10^7 \end{bmatrix}$$

$$\lambda = 38.03$$

The tracking errors of both Euler angle and Euler rate and control torque histories for both adaptive controllers are shown in Figures 4.1 to 4.6.

The simulation results show that the tracking errors of all the states will converge to zero although initial parameter estimation error is 2 times larger than in phase 3. Comparing the results, we notice that both nonlinear schemes perform equally well and the steady state values of control torques are not equal to zero because of the lack of convergence of $\hat{I}$.

Case II:

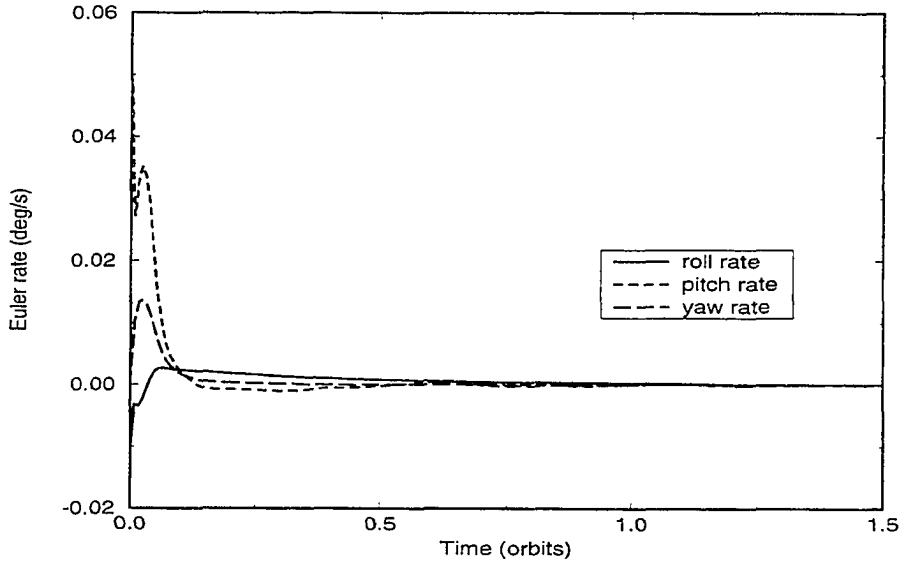

Figure 4.2: Tracking errors of Euler angular rates with controller I

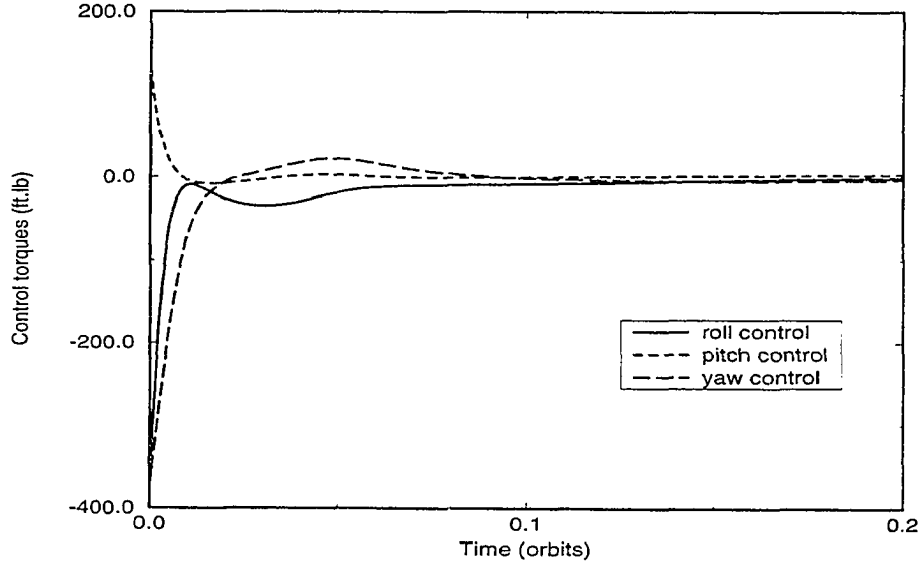

Figure 4.3: Control torque histories with controller I

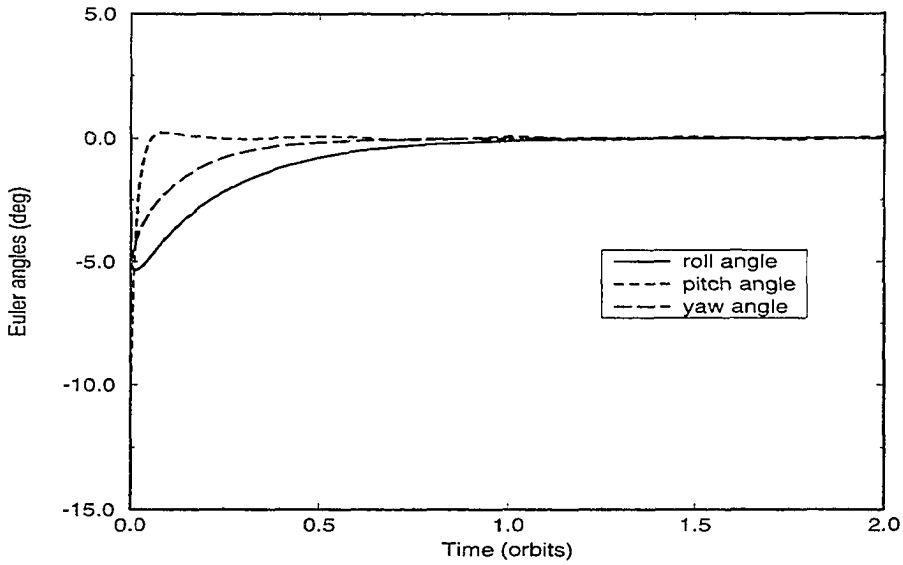

Figure 4.4: Tracking errors of Euler angles with controller II

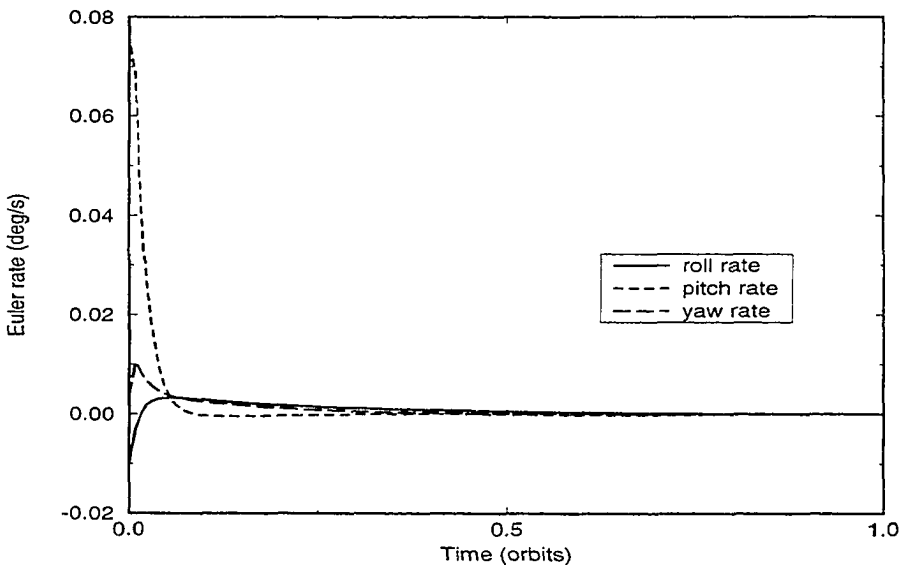

Figure 4.5: Tracking errors of Euler angular rates with controller II

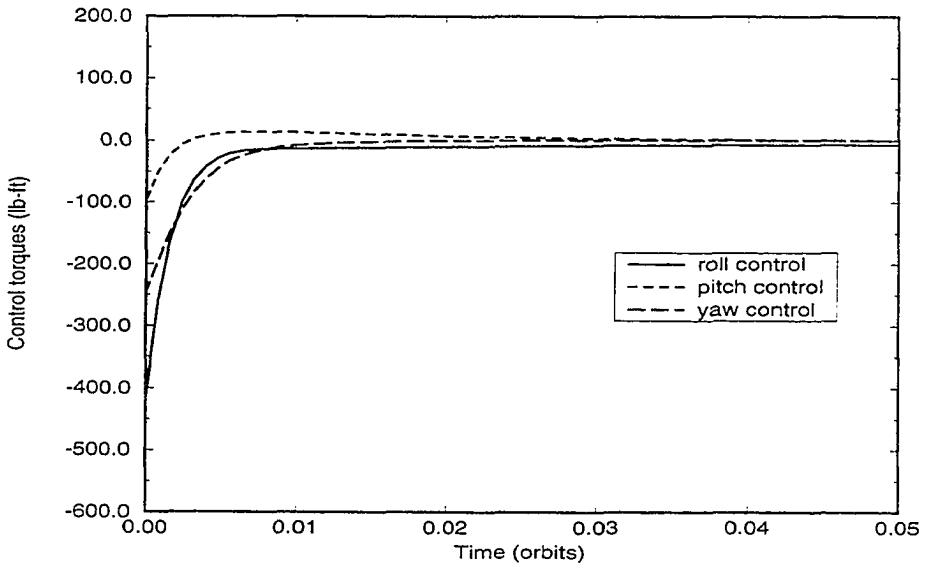

Figure 4.6: Control torque histories with controller II

Consider the existence of disturbances shown in Table 2.2. The estimated disturbance parameters are initialized as:

$$\bar{P}(0) = \begin{bmatrix} 0.0 & 2.0 & 1.5 & 0.5 & 1.0 \\ 15.0 & 1.5 & 4.0 & 0.6 & 1.0 \\ 0.0 & 0.0 & 1.0 & 0.0 & 1.0 \end{bmatrix}$$

The comparison of system performances with and without applying the modified controllers are shown in Figure 4.7 to Figure 4.12. It is evident that the disturbances degrade system behavior more in pitch axis than in roll/yaw motion. The simulation results also show that both proposed control schemes are able to stabilize the Space Station to the desired orientation, but the second controller has faster response speed.

Case III:

Now, assume the body-axes are the same as the principal axes. Convergence of moments of inertia is shown in Figure 4.13 when the desired trajectories are chosen

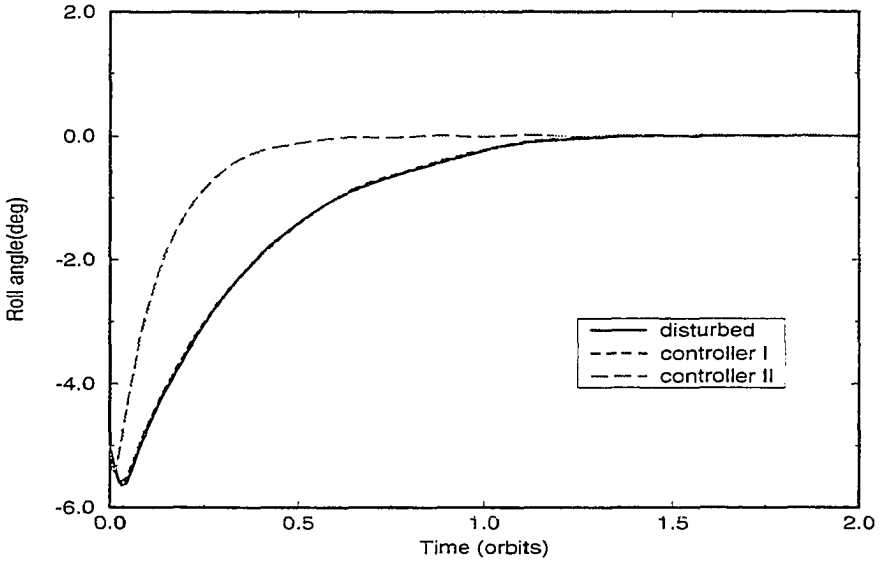

Figure 4.7: Tracking errors of roll angles with the disturbances.

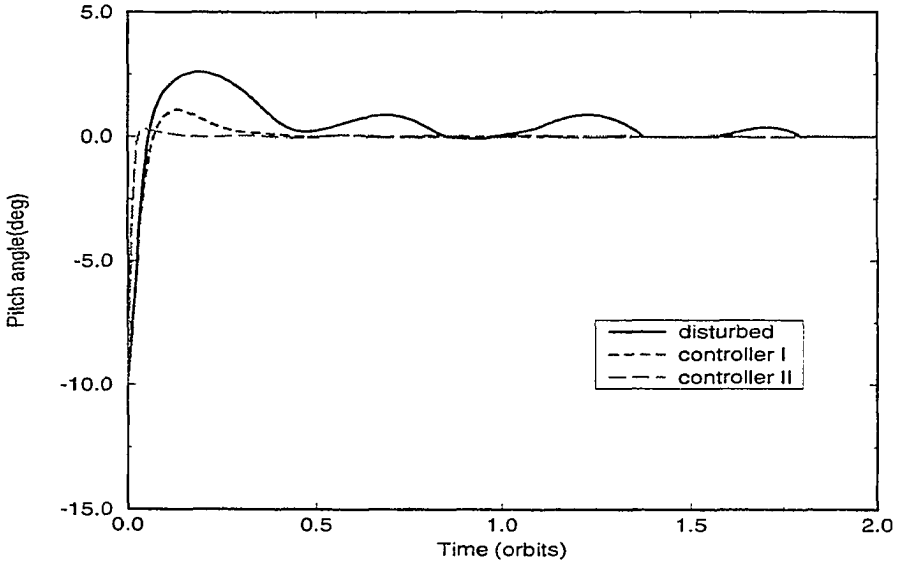

Figure 4.8: Tracking errors of pitch angles with the disturbances.

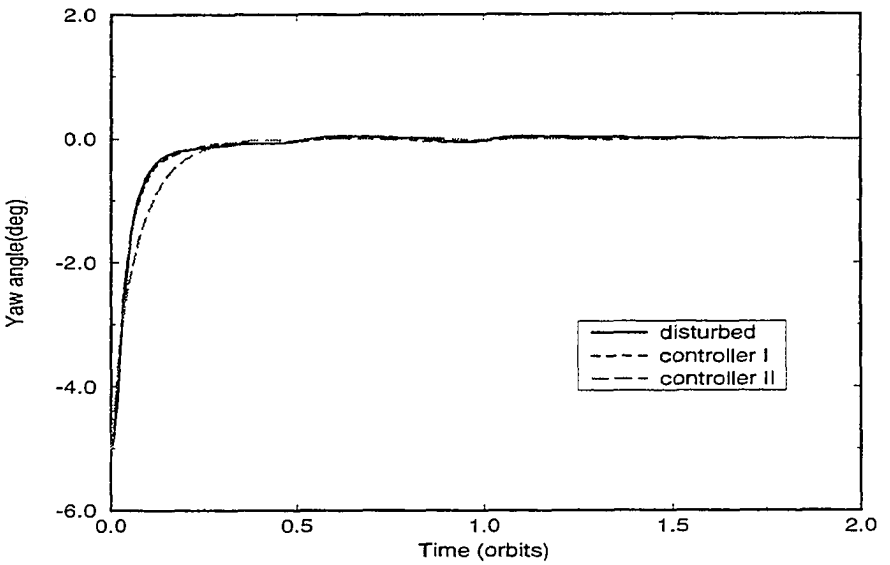

Figure 4.9: Tracking errors of yaw angles with the disturbances.

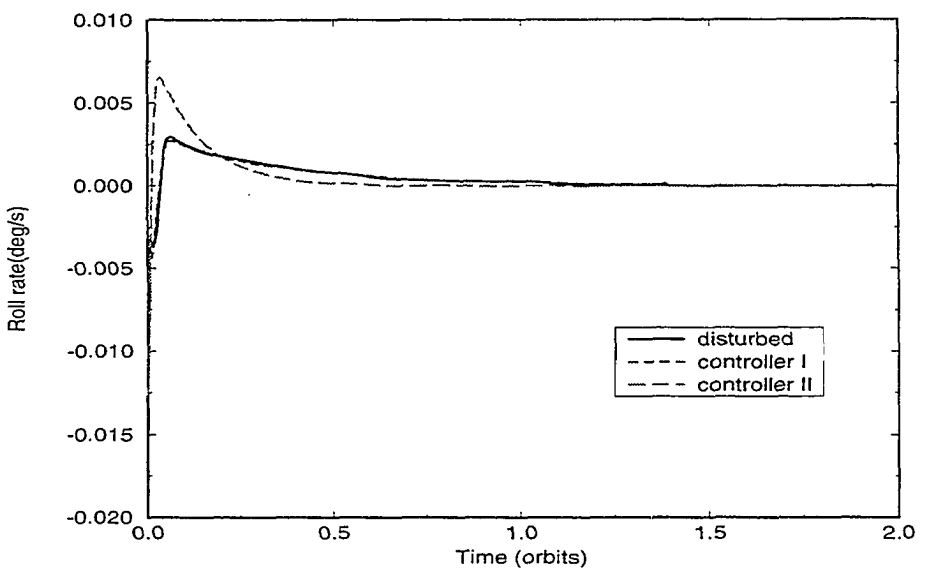

Figure 4.10: Tracking errors of roll rates with the disturbances.

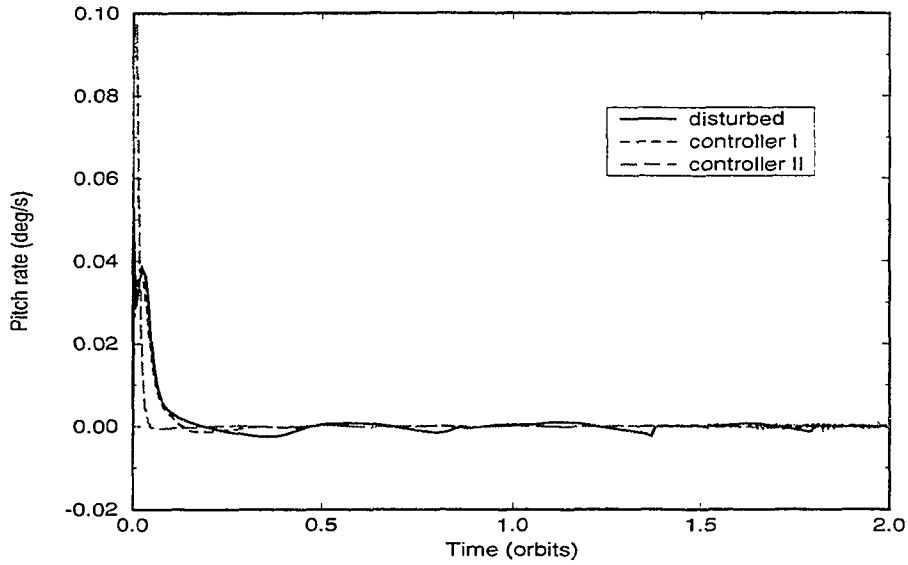

Figure 4.11: Tracking errors of pitch rates with the disturbances.

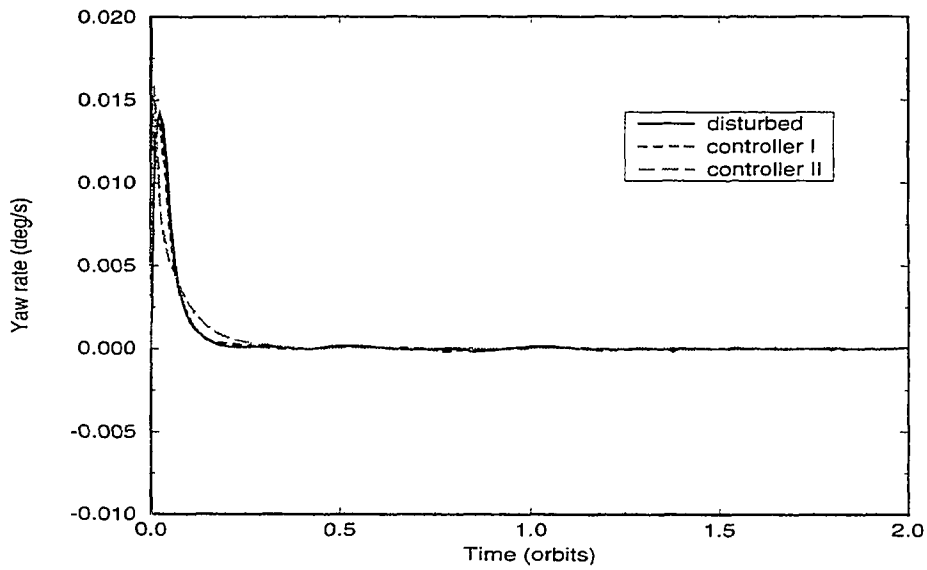

Figure 4.12: Tracking errors of yaw rates with the disturbances.

to be persistent exciting:

$$\begin{aligned} \theta_{1d} &= 0.001\sin(2.5nt) \\ \theta_{2d} &= 0.005\sin(3nt) \\ \theta_{3d} &= 0.005\sin(3.5nt + \frac{\pi}{4}) \end{aligned} \tag{4.37}$$

The initial estimation errors are chosen to be:

$$\tilde{I}_{11}(0) = 23.0e6$$

$$\tilde{I}_{22}(0) = 1.4e6$$

$$\tilde{I}_{33}(0) = 23.0e6$$

Figure 4.13 shows that all parameter errors converge to zero after about 0.4 orbital period.

Case IV:

To test the robustness of these controllers at the existence of the unmodeled dynamics such as the orbital rate is time-varying instead of a constant value. We choose

$$n = n_0(1 + 0.5\sin(n_0 * t)) \tag{4.38}$$

where n_0 is the originally chosen constant orbital rate.

This may correspond to a situation where the orbit of the Space Station is not exactly circular, but slightly elliptic. The system performances are shown from Figure 4.14 to Figure 4.17 for both controller I and II. The results show that smoother tracking histories

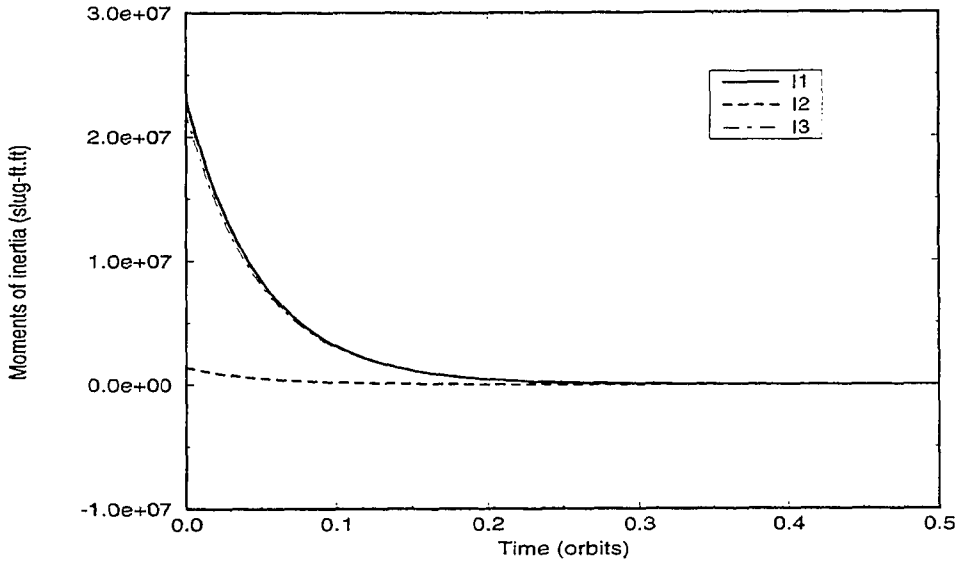

Figure 4.13: Convergence of the estimated errors of the moments of inertia with controller II.

of Euler angles can be achieved with controller I while better tracking results for the angular rates are obtained by controller II.

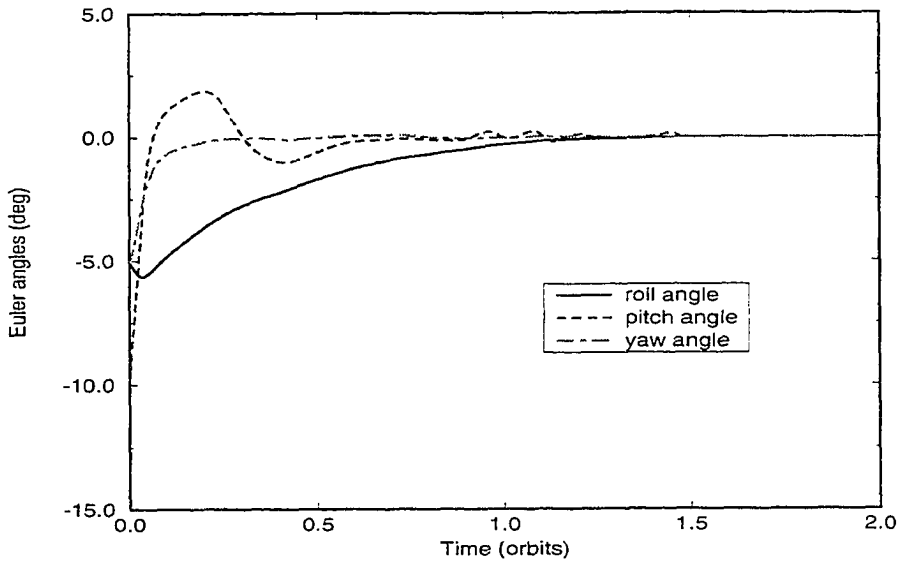

Figure 4.14: Tracking errors of Euler angles at the existence of unmodeled dynamics with controller I.

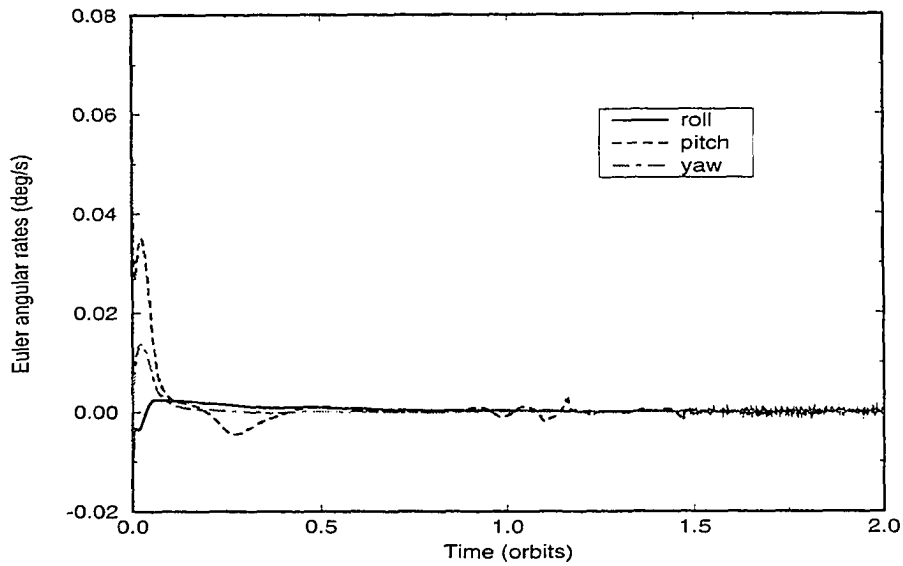

Figure 4.15: Tracking errors of angular rates at the existence of unmodeled dynamics with controller I.

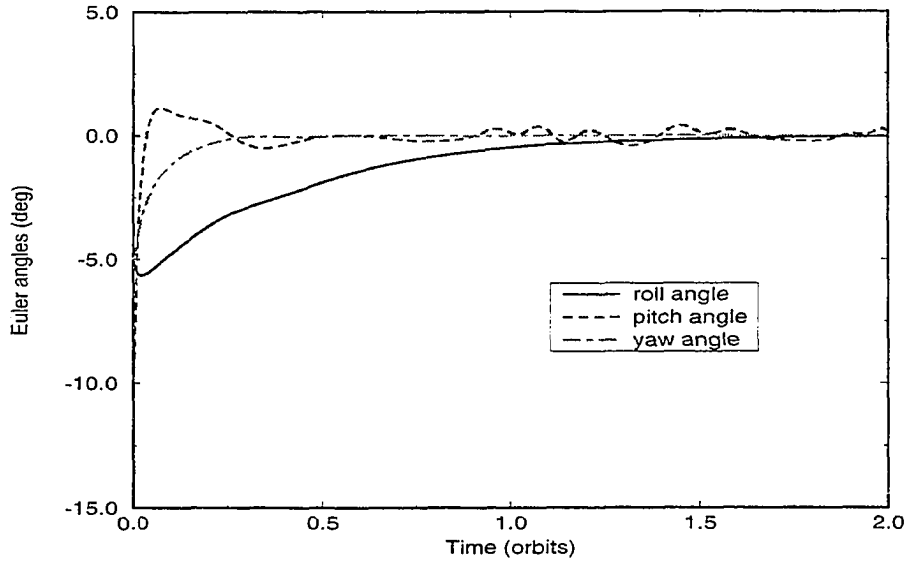

Figure 4.16: Tracking errors of Euler angles at the existence of unmodeled dynamics with controller II.

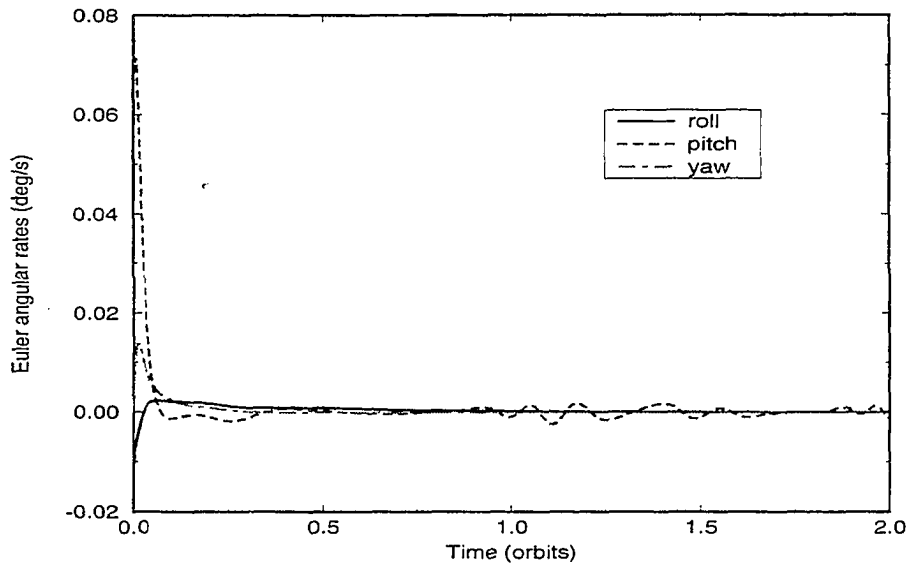

Figure 4.17: Tracking errors of angular rates at the existence of unmodeled dynamics with controller II.

CHAPTER 5. DIRECT ADAPTIVE CONTROL VIA RADIAL BASIS FUNCTION

Although the Space Station can be controlled in the presence of disturbances by the direct adaptive control methods discussed in Chapter 4, the required control is large for large initial errors and disturbances. For more general disturbances which can not be linearly parameterized as in Chapter 2, the methods in Chapter 4 are not applicable. In this chapter, a radial basis function neural network is discussed as an approximator to nonlinear functions. Then a forward regression algorithm based on an orthogonal decomposition of the regression matrix is employed to select a suitable set of radial basis function centers from a large number of possible candidates, and this provides effective online learning for compensating for plant error resulting from the disturbances. A direct adaptive control law via the RBF (radial basis function) network in combination with the nonlinear controllers in Chapter 4 is presented.

The Radial Basis Function Network

A radial basis function network can be designed as a special two-layer feedforward network which is linear in the parameters by fixing the hidden layer. The structure of the RBF network with n inputs and m output is shown in Figure 5.1. This network implements a mapping $f_r : R^n \rightarrow R^m$ according to

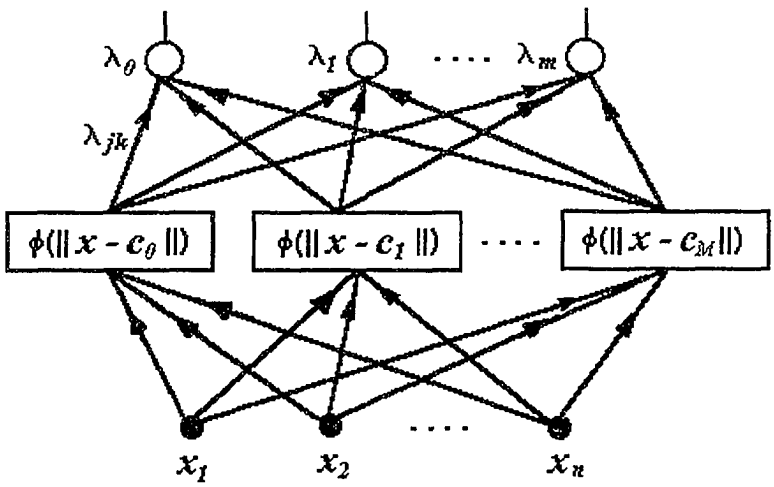

Figure 5.1: A radial basis function network.

$$fr(x) = \Lambda_o + \sum_{j=1}^{M} \Lambda_j \phi(\|x - c_j\|) \tag{5.1}$$

Where $x \in R^n; \phi(\bullet)$ is a function from R^+ to R; $\| \bullet \|$ denotes the Euclidean norm; M is the number of the RBF centroid: $\Lambda_j \in R^m, j = 0, \cdots,$ M are the weight vectors; and $c_j \in R^n, j = 1, \cdots,$ M are the radial basis function centers. Let

$$\Lambda_j = [\lambda_{1j} \cdots \lambda mj]^T, \; j = 0, 1, \cdots, M \tag{5.2}$$

Therefore Eqn.(5.1) can be written in the decomposition form

$$f_{ri}(x) = \lambda_{io} + \sum_{j=1}^{M} \lambda_{ij} \phi(\|x - c_j\|), \; i = 1, \cdots, m \tag{5.3}$$

In fact, a multi-output case can be separated by a group of single-output network implemented by Eqn.(5.3). Given the functional form $\phi(\bullet)$ and the center c_j, the values of the weight matrix λ_{ij} for $i = 1, \cdots, m$ and $j = 0, 1, \cdots, M$ are updated

to compensate for plant disturbances. Park and Sandberg [48] have shown that the RBF network is capable of universal approximation for activation functions of the form

$$\phi(\frac{\|x - c_j\|}{\sigma}) \tag{5.4}$$

where σ is a smoothing factor or width, for each kernel node j. Typically used RBFs activation functions researched by Powell [49] and Schagen [50] are given in the following Table 5.1.

Table 5.1: Activation functions for RBF network

$\phi(r)$	RBF Classification
r	linear
r^3	cubic
$r^2 log(r)$	thin plate spline
$(r^2 + c^2)^{\frac{1}{2}}$	multiquadratics
$(r^2 + c^2)^{-\frac{1}{2}}$	inverse multiquadratics
$e^{-(\frac{r}{c})^2}$	multivariate Gaussian

The multivariate Guassian activation function is used in this study. Generally, for a single output with (M+1) kernel nodes which is linear in the parameter model, the decomposition form can be represented in the following

$$\begin{bmatrix} y(1) \\ y(2) \\ \vdots \\ y(N) \end{bmatrix} = \begin{bmatrix} 1 & \phi(\|x_1 - c_1\|) & \cdots & \phi(\|x_1 - c_M\|) \\ 1 & \phi(\|x_2 - c_1\|) & \cdots & \phi(\|x_2 - c_M\|) \\ \vdots & \vdots & \ddots & \vdots \\ 1 & \phi(\|x_N - c_1\|) & \cdots & \phi(\|x_N - c_M\|) \end{bmatrix} \begin{bmatrix} \lambda_0 \\ \lambda_1 \\ \vdots \\ \lambda_M \end{bmatrix} + \begin{bmatrix} \varepsilon(1) \\ \varepsilon(2) \\ \vdots \\ \varepsilon(N) \end{bmatrix} \tag{5.5}$$

N is define as the number of the candidate data set and

$$y(i) = f_{r1}(x(i))$$

$$i = 1, \cdots, N$$

$$y = [y(1)\, y(2) \cdots y(N)]^T$$

$$E = [\varepsilon(1)\, \varepsilon(2) \cdots \varepsilon(N)]^T$$

$$\Upsilon = \begin{bmatrix} 1 & \phi(\|x_1 - c_1\|) & \cdots & \phi(\|x_1 - c_M\|) \\ 1 & \phi(\|x_2 - c_1\|) & \cdots & \phi(\|x_2 - c_M\|) \\ \vdots & \vdots & \ddots & \vdots \\ 1 & \phi(\|x_N - c_1\|) & \cdots & \phi(\|x_N - c_M\|) \end{bmatrix} = [v_0\, v_1 \cdots v_M] \tag{5.6}$$

$$\Xi = \begin{bmatrix} \lambda_0 \\ \lambda_1 \\ \vdots \\ \lambda_M \end{bmatrix}$$

$$v_j = [v_j(1)\, v_j(2) \cdots, v_j(N)],\ j = 0, \cdots, M$$

Where y(t) is the desired output, the λ_i are the parameter; the $v_i(t)$ are known as the regressors; and the $\varepsilon(t)$ is the zero residual errors which are assumed uncorrelated with λ_i; N is the number of total available candidate data; and M is the number of selected centroids. The selection of centroids c_j and σ for RBF network is critical in determining the network performance. Usually, we randomly select the centroids from the data set and use the "P nearest-neighbor" method given by Moody and Darken [51] for σ. Next, we introduce the orthogonal least square learning algorithm for finding c_j.

Orthogonal Least Square Learning Algorithm

Consider the linear-in-the-parameter model written in the form

$$y = \Upsilon \Xi + E \tag{5.7}$$

For the special case of a square matrix of RBFs containing no bias terms, which is the case where the selected centroids are equal to input data set. Micchelli [52] proved that the matrix is always nonsingular if the input data points are all unique. The reason we do not simply solve the Eqn.(5.7) by inverting the RBF matrix is that all available data can not be guaranteed to be unique and those data are generally uncorrelated. The RBF matrix can become very ill-conditioned for most of the cases. The singular value method has to be employed to solve this problem. In order to know how each regression contributes to the output variance. The OLS method is employed to transform the set of v_j into a set of orthogonal basis vectors, and thus make it possible to calculate the individual contribution to the desired output from each basis vector. The RBF matrix can then be decomposed into orthogonal form

$$\Upsilon = WA \tag{5.8}$$

The Υ matrix is known as the regression matrix defined in Eqn.(5.6). The space spanned by the set of Υ is same as the space spanned by the set of orthogonal

vectors w_j. The A matrix is a (M+1)×(M+1) unitary upper triangular matrix

$$A = \begin{bmatrix} 1 & a_{12} & a_{13} & \cdots & a_{1,M+1} \\ & 1 & a_{23} & \cdots & a_{2,M+1} \\ & & \ddots & \ddots & \vdots \\ & & & \ddots & a_{M,M+1} \\ & & & 0 & 1 \end{bmatrix} \tag{5.9}$$

and W is a N × (M+1) orthogonal matrix, subject to

$$W^T W = D \tag{5.10}$$

$$D = diag(d_1 \cdots d_{M+1}) \tag{5.11}$$

$$d_j = < w_j, w_j >, j = 1, \cdots, M+1 \tag{5.12}$$

$$W = [w_1 \, w_2 \cdots w_{M+1}] \tag{5.13}$$

where $< \bullet >$ denotes the inner product. The Eqn.(5.7) can then be rewritten as

$$y = Wg + E \tag{5.14}$$

$$g = A\Xi \tag{5.15}$$

The least-square solution for Eqn.(5.15) is

$$\hat{g} = (W^T W)^{-1} W^T y \tag{5.16}$$

By using the classical or modified Gram-Schmidit methods, we can solve for the LS estimate of $\hat{\Xi}$ from Eqns. (5.16). Since there is always a large number of data $x(t)$ for the input of RBF network, and the adequate modeling only needs N_c ($\ll$M) significant regressors, OLS is a more effective method than LS in such cases. Here,

we do not try to seek OLS solution for Eqn.(5.14), but use it for the selection of the centroid for the RBF network.

The orthogonal decomposition of Υ can be obtained by calculating matrix A one column at a time and orthogonal Υ as follow: at the kth stage, make the kth column be orthogonal to each of the $(k-1)^{th}$ already orthogonalized columns and repeat the operation for all i=1, $\cdots$, M+1. This procedure can be represented as

$$\left.\begin{aligned} w_1 &= v_1 \\ \alpha_{ik} &= w_i^T d_k/(w_i^T w_i),\ 1 \le i < k \\ w_k &= v_k - \sum_{i=1}^{k-1} \alpha_{ik} w_i \end{aligned}\right\} \text{k=2, } \cdots\text{, M+1} \tag{5.17}$$

In order to find how the regressors and the residual error term will contribute to the desired output variance, we calculate the dot product of y vector and divided by N, then we obtain

$$N^{-1} y^T y = N^{-1} \sum_{i=1}^{M+1} g_i^2 w_i w_i + N^{-1} E^T E \tag{5.18}$$

The $g_j^2 w_i^T w_i/N$ is the increment to the desired output variance introduced by w_i. The contribution of a particular regressor to the output variance can be defined as a error ratio term

$$\eta_j = \frac{g_j^2 w_i^T w_i}{y^T y},\ \ 1 \le i \le M+1 \tag{5.19}$$

The larger the error ratio means the more significant the regressor contributes to the desired output variance, This provides us a very simple and effective methods to calculate the centroids of the RBF network. The computational procedure can be summarized by Chen, Cowan, and Grant [43] as follows

- At the first step, for 1 $\le$ i $\le$ M+1 compute

$$\left.\begin{aligned} w_1^{(i)} &= v_1 \\ g_1^{(i)} &= (w_1^{(i)})^T y/((w_1^{(i)})^T w_1^{(i)}) \\ \eta_1^{(i)} &= (g_1^{(i)})^2 (w_1^{(i)})^T w_1^{(i)}/(y^T y) \end{aligned}\right\}$$

Find

$$\eta_1^{(i_1)} = max[\eta_1^{(i)},\ 1 \le i \le M+1]$$

and select

$$w_1 = w_1^{(i_1)} = v_{i_1}$$

- At the kth step where k $\geq$ 2, for 1 $\leq$ i $\leq$ M+1, i $\neq i_1, \cdots,$ i $\neq i_{k-1}$, computer

$$\left.\begin{aligned} \alpha_{ik}^{i} &= w_j^T v_i/(w_j^T w_j), 1 \le j < k \\ w_k^{(i)} &= v_i - \sum_{j=1}^{k-1} \alpha_{ik}^{(i)} w_j \\ g_k^{(i)} &= (w_k^{(i)})^T y/(w_k^{(i)})^T w_k^{(i)} \\ \eta_k^{(i)} &= (g_k^{(i)})^2 (w_k^{(i)})^T w_k^{(i)}/(y^T y) \end{aligned}\right\}$$

Find

$$\eta_1^{(i_1)} = max[\eta_1^{(i)},\ 1 \le i \le M+1,\ i \ne i_1, \cdots, i \ne i_{k-1}]$$

and select

$$w_k = w_k^{i_k} = v_{i_k} - \sum_{j=1}^{k-1} \alpha_{jk} w_j$$

where $\alpha_{jk} = \alpha_{jk}^{i_k}$, 1 $\leq$ j < k.

- The procedure is terminated at the N_cth step when

$$1 - \sum_{j=1}^{N_c} \eta_j < \rho$$

where $0 < \rho < 1$ is a chosen tolerance. This gives rise to a subset model containing N_C significant regressors.

where ρ is a very important factor which represents the accuracy and the complexity of the RBF network. The more accurate realization of the network will be achieved at the expenses of selecting the more complex network. Thus, this term is chosen by compromising the accuracy and the complexity for better network performances.

Application to Space Station Control

Consider the nonlinear dynamic equation of the Space Station in Eqn.(4.1) with disturbances of the form

$$M(x)\ddot{x} + C(x,\dot{x})\dot{x} + g(x) = \tau + d \tag{5.20}$$

where d is the disturbance vector which is assumed to be unknown and bounded. In order to implement a stable system control in the presence of the disturbances, a means to cancel out the effect of the disturbances on the system is required. A radial basis function neural network is used to produce an approximation to d when implemented. Initial training of the RBF is conducted prior to the flight from a mathematical model. Such model based on training is refered to as off-line training.

If d is known and the realization of d is perfect, then we can achieve the same global stable system performance by using (Eqn.(5.20) - d). Unfortunately, the information about d is often not known. Therefore, the adaptive control architecture is chosen as:

$$\tau_i(t) = \tau_{nl_i}(t) + \tau_{ad_i}(t)$$

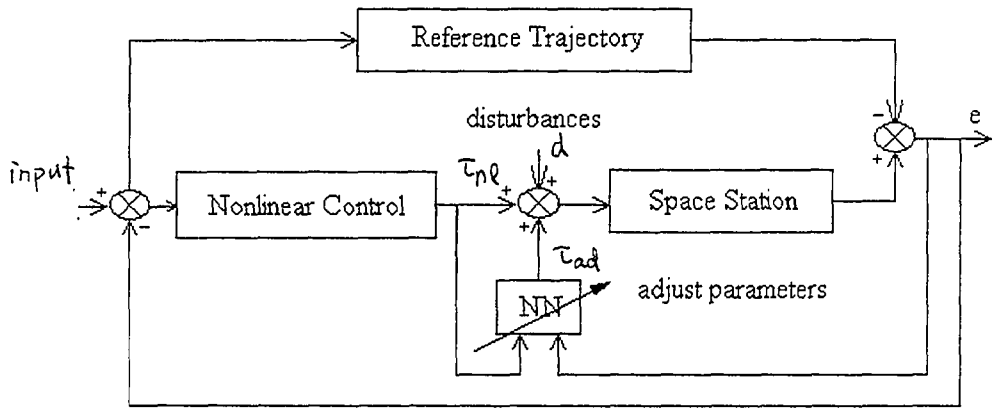

Figure 5.2: Direct adaptive control via the RBF network.

$$i = 1, 2, 3 \tag{5.21}$$

where τ_{nl_i} is a nonlinear control term which is derived from Chapter 4 and τ_{ad_i} is the adaptive control term generated by the RBF. The τ_{nl_i} is used to shape the system response and the τ_{ad_i} is to compensate the effect of the unknown disturbances during operation. The schematic structure of this controller is shown in Figure 5.2. The adaptive control signals are represented as follows:

$$\begin{aligned} \tau_{ad_1} &= \sum_{j=1}^{N_{c_1}} \omega_{1j} f_{1j}(x, \tau_{nl}) \\ \tau_{ad_2} &= \sum_{j=1}^{N_{c_2}} \omega_{2j} f_{2j}(x, \tau_{nl}) \\ \tau_{ad_3} &= \sum_{j=1}^{N_{c_3}} \omega_{3j} f_{3j}(x, \tau_{nl}) \end{aligned} \tag{5.22}$$

where $N_{c_1}, N_{c_2}, N_{c_3}$ are the corresponding numbers of centers for the networks.

and ω_{ij}, i=1,2,3, is to be updated on-line. Note that the adaptive control τ_{ad_i} in Eqn.(5.22) is linearly parameterized. This feature makes it possible to derive a stable on-line adaptation rule. The proof is similar to the one in Section 4.3, which is omitted here.

This adaptation rule was designed as follows:

$$\dot{\omega}_i = \begin{cases} -\gamma_i r_i^T f_i \text{ when } \|r_i\|_2 > r_{0i} \\ 0 \text{ when } \|r_i\| \leq r_{0i} \end{cases} \tag{5.23}$$

where $\gamma_i > 0$ is the adaptation gain (or learning rate). In the adaptation rule of Eqn.(5.23) the parameters are adjusted only when the norm of the state error vector lies outside a "dead zone", whose size is defined by r_{0i} For easy comparison purpose, we selected the same configuration of the Space Station model as Chapter 4. The training data was generated using the second nonlinear adaptive controller in the presence of the disturbance in Table 2.2 which encompasses 2 time orbits of simulated spacecraft operation. This resulted in 350 input-output combinations provided by the simulation.

We implemented the neural networks using the initial conditions other than those used to generate the training data. For a tolerance of 0.001, the design process resulted in 3,4,4 kernel nodes for the three networks. The RBF centers of this solution is shown in Table 5.2 to Table 5.4.

Simulation Result

To demonstrate the performance of the method of adaptive control for a Space Station, the model with non-principal axes in Eqn.(2.17) stated in Chapter 2 is used. Figure 5.3 and Figure 5.4 show that full state tracking can be achieved by using RBF

Table 5.2: RBF centers of the Network I

	i		
	1	2	3
c_{1i}	5.0026E+0	1.2750E+1	8.6190E−1
c_{2i}	3.0000E−4	-1.0000E−4	-4.0000E−4
c_{3i}	5.0019E+0	1.0768E+0	1.4900E+0
c_{4i}	-9.0000E−4	-3.0000E−4	-7.0000E−4
c_{5i}	5.0024E+0	1.0730E+0	6.6390E−1
c_{6i}	2.0000E−4	-1.0000E+0	-3.0000E−4
c_{7i}	-5.31295E+1	4.6110E−1	-2.2640E−1
c_{8i}	-4.09007E+1	-8.8988E+0	-9.6562E+0
c_{9i}	-4.31944E+1	6.8550E−1	-9.0600E−1

controller and Figure 5.5 indicates that the requirement of maximum control torques is much less than using the previous nonlinear controllers alone. The wellness of the trained networks is shown in Figure 5.6 and Figure 5.8. It is obvious that the best result is in pitch axis and yaw axis is trained better than roll axis. When additional untrained disturbances are added to the system, Figure 5.9 and Figure 5.10 show that these networks are actually extrapolating. i.e. this method is still valid for untrained disturbances. It should be pointed out that while the demonstration of the RBF based controller is done with the disturbances used in the previous chapters. This approach is applicable to more general disturbances. In particular, the disturbances do not have to be in the form of Eqn.(2.18).

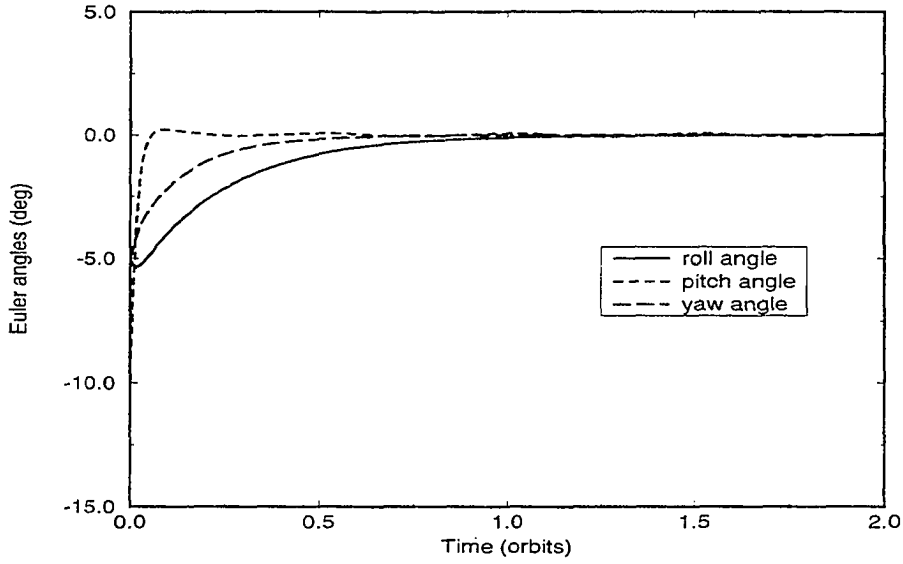

Figure 5.3: Tracking errors of Euler angles with neural network control with disturbances.

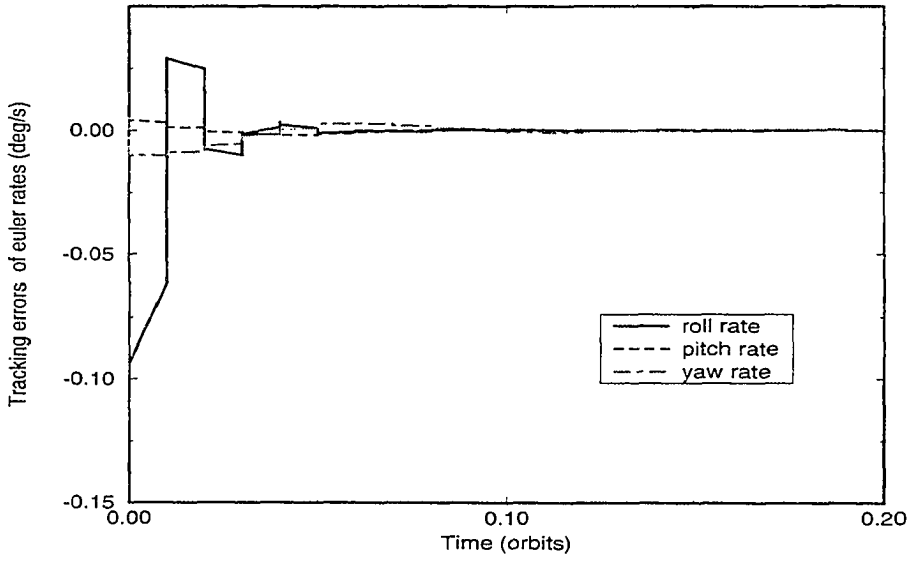

Figure 5.4: Tracking errors of Euler rates with neural network control with disturbances.

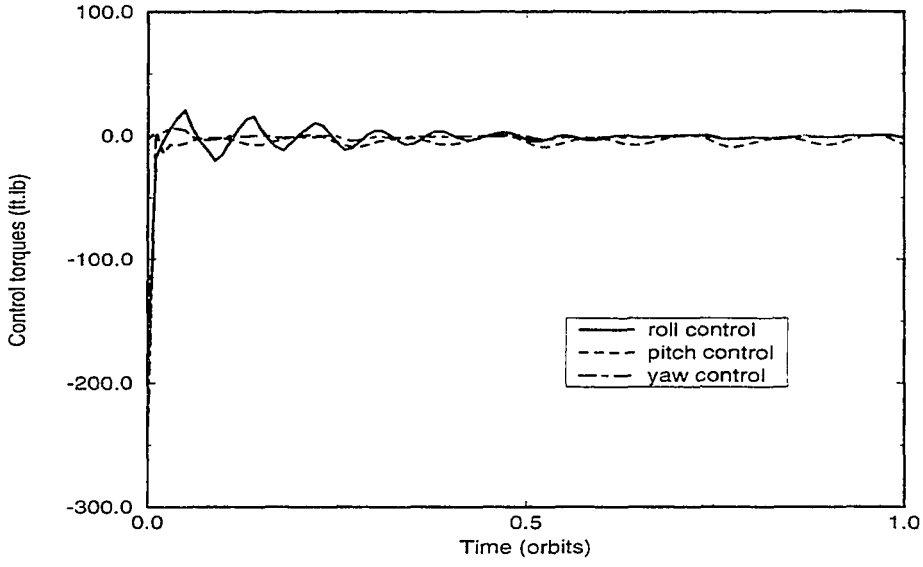

Figure 5.5: Control histories with neural network control.

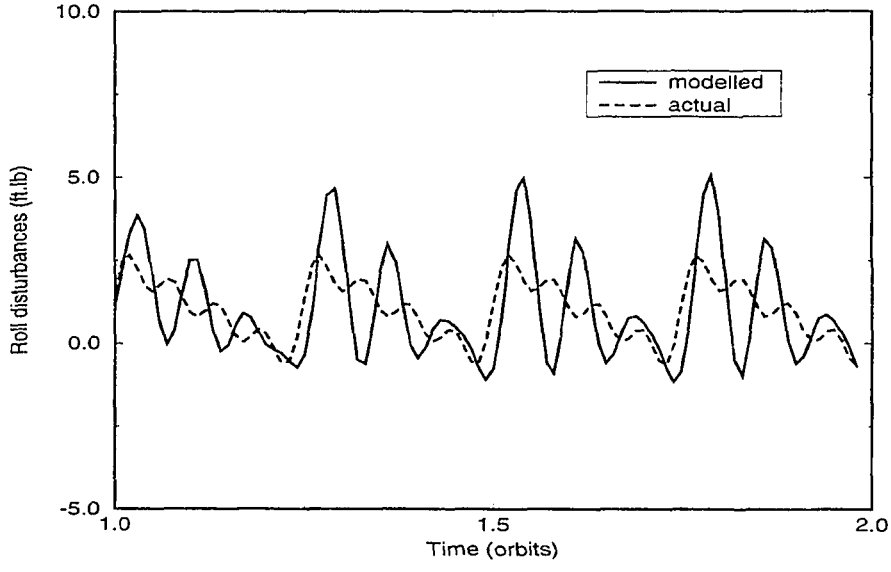

Figure 5.6: Roll comparison of neural model output and actual disturbance.

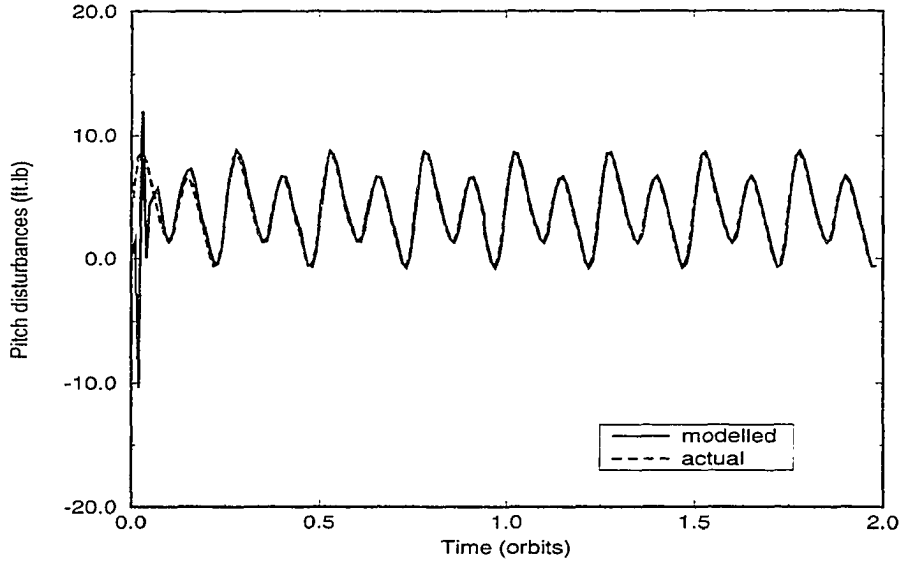

Figure 5.7: Pitch comparison of neural model output and actual disturbance.

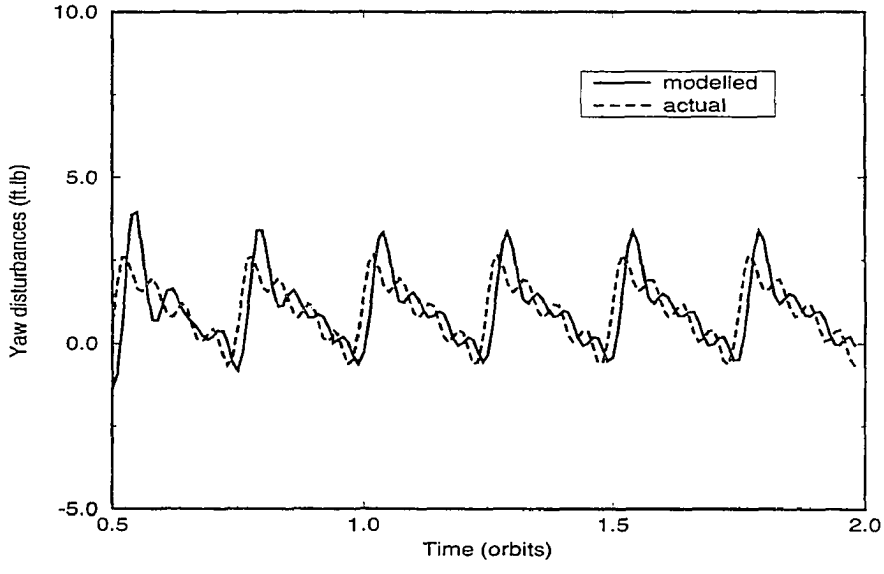

Figure 5.8: Yaw comparison of neural model output and actual disturbance.

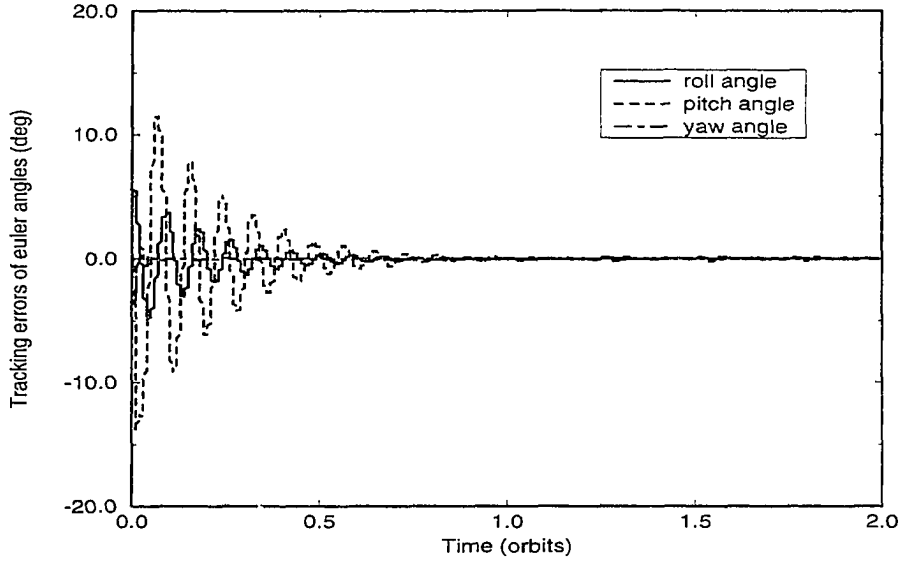

Figure 5.9: Tracking errors of Euler angles with untrained disturbance.

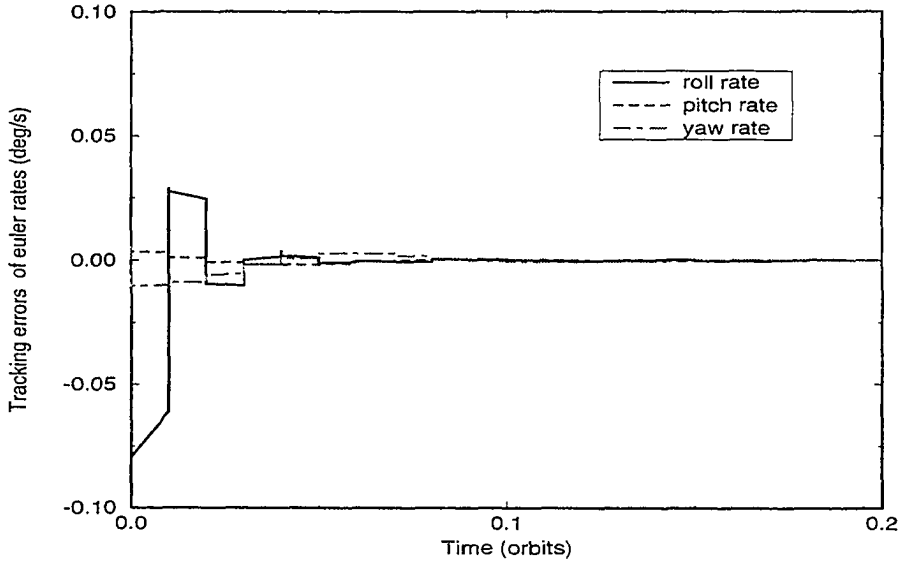

Figure 5.10: Tracking errors of Euler rates with untrained disturbance.

Table 5.3: RBF centers of the Network II

	i			
	1	2	3	4
c_{1i}	1.2060E−1	1.2850E−1	4.6110E−1	-2.0000E−4
c_{2i}	1.0000E−4	-1.0000E−4	-8.8988E+0	7.7700E−2
c_{3i}	2.0490E+0	2.1189E+0	6.8550E−1	-1.0000E−4
c_{4i}	-9.0000E−4	1.2750E−1	1.1930E−1	5.2565E−1
c_{5i}	1.1410E−1	-1.0000E−4	-1.0000E−4	-9.0989E+0
c_{6i}	1.0000E−4	1.0768E+0	1.0597E+0	7.2150E−1
c_{7i}	-2.8779E+0	-3.0000E−4	8.0500E−2	7.4100E−2
c_{8i}	-1.80412E+1	1.0730E−1	-1.0000E−4	-1.0000E−4
c_{9i}	-2.80930E+0	1.0000E−4	1.0657E+0	1.0594E+0

Table 5.4: RBF centers of the Network III

	i			
	1	2	3	4
c_{1i}	5.0026E+0	4.9883E+0	5.1290E−1	-7.0000E−4
c_{2i}	3.0000E−4	-1.6000E−3	-9.0269E+0	6.6390E−1
c_{3i}	5.0019E+0	3.6394E+0	7.0580E−1	-3.0000E−4
c_{4i}	-9.0000E−4	8.1800E−2	7.5400E−2	-2.2640E−1
c_{5i}	5.0024E+0	-1.0000E−4	-1.0000E−4	-9.6562E+0
c_{6i}	2.0000E−4	1.0688E+0	1.0589E+0	-9.0600E−1
c_{7i}	-5.31295E+1	-2.0000E−4	8.6190E−1	8.3040E−1
c_{8i}	-4.09007E+1	7.9000E−2	-4.0000E−4	-4.0000E−4
c_{9i}	-4.31944E+1	1.0000E−4	1.4900E+0	1.4265E+0

CHAPTER 6. ATTITUDE CONTROL AND CMG MANAGEMENT

In the previous chapters, control momentum gyros (CMGs) management was not considered in our attitude control studies. Since the CMGs are one of the several commonly employed attitude control actuating devices during nominal operation, several controllers for space station attitude control and CMG management have been developed. A nonlinear approach based on the feedback linearization method has been applied to Space Station by Bishop, et al. [9] to develop linear control law for the transformed Space Station system so that both attitude control problem and CMG management are able to be treated simultaneously. In this chapter, we will first review this standard approach. Then an adaptive controller based on an approximate feedback linearization model is presented to cope with constant disturbances.

Exact Feedback Linearization Techniques

The system equations in the SISO case are simplified to

$$\begin{aligned} \dot{x} &= f(x) + g(x)u \\ y(x) &= h(x) \end{aligned} \tag{6.1}$$

where $x \in \Re^n$, $u, y \in \Re$, f and g are smooth vector fields on $\Re^n$. (i.e. $f(x) \in T_x\Re^n \in \Re^n$, $x \in \Re^n$), and $h : \Re^n \rightarrow \Re$ is a smooth function. Differentiating the

plant output y with respect to time we get

$$\dot{y} = L_f h(x) + L_g h(x) u \tag{6.2}$$

where $L_f h(x)$ is the Lie derivative of the function h along the vector field f i.e. $L_f h(x) = \frac{\partial h(x)}{\partial x} f(x)$. If $L_g h(x) = 0$ then $\dot{y}$ does not depend directly on the input and we differentiate again to get

$$\ddot{y} = L_f^2 h(x) + L_g L_f h(x) u \tag{6.3}$$

where $L_f^2 h(x) = L_f((L_f h)(x))$ and $L_g L_f = L_g((L_f h)(x))$. If the second derivative is still not directly dependent on the input, we can keep differentiating in this way until some derivative of y depends directly on the input. This process leads to the following definition of strong relative degree.

Definition 6.1 The system in Eqn.(6.1) is said to have strong relative degree γ if $L_g h(x) = L_g L_f h(x) = L_g L_f^{\gamma-2} h(x) = 0$ for all x and $L_g L_f^{\gamma-1} h(x)$ is bounded away from zero for all x.

If a system has a strong relative degree γ the $\gamma \leq n$. Also, by differentiating the output as above one can verify that the first $\gamma - 1$ time derivatives of y do not directly depend on the input and the γ-order derivative is given by

$$y^{(\gamma)} = L_f^{\gamma} h(x) + L_g L_f^{\gamma-1} h(x) u \tag{6.4}$$

If the plant (6.1) has strong relative degree γ then static state feedback of the form

$$u = \frac{1}{L_g L_f^{\gamma-1} h(x)} (v - L_f^{\gamma} h(x)) \tag{6.5}$$

yields the equation

$$y^{(\gamma)} = v \tag{6.6}$$

Define new state variable $z_1 = y$, $z_2 = \dot{y}$, $\cdots$, $z_n = y^{(n-1)}$. In the new state variables, the system is linear and complete controllable

$$\dot{z} = \begin{bmatrix} 0 & 1 & \cdots & 0 \\ 0 & 0 & \ddots & 1 \\ 0 & 0 & \cdots & 0 \end{bmatrix} z + \begin{bmatrix} 0 \\ \vdots \\ 1 \end{bmatrix} v \tag{6.7}$$

This is referred as exact feedback linearization because no truncated Taylor series are used.

The extension of this linearizing technique to multi-input and multi-output plant is easy to obtain. For a MIMO nonlinear system with m-input, m-output of the form:

$$\begin{aligned} \dot{x} &= f(x) + g_1(x)u_1 + \cdots + g_m(x)u_m \\ y_1 &= h_1(x) \\ &\vdots \\ y_m &= h_m(x) \end{aligned} \tag{6.8}$$

Where $x \in \Re^n$, $u, y \in \Re^m$, and f, g^i, h_j are assumed to be smooth. Now, differentiate the y_j with respect to time to get

$$\dot{y}_j = L_f h_j(x) + \sum_{i=1}^{m} (L_{gi} h_j) u_i, j = 1, \cdots, m \tag{6.9}$$

Note that if each of $L_{gi}h_j(x) = 0$, then the input does not appear in Eqn.(6.9). Define γ_j to be the smallest integer such that at least one of the inputs appears in the $y_j^{\gamma_j}$. Therefore,

$$y_j^{\gamma_j} = L_f^{\gamma_j} h_j + \sum_{i=1}^{m} L_{gi}(L_f^{\gamma_j - 1} h_j) u_i \tag{6.10}$$

with at least one of the $L_{gi}(L_f^{\gamma_j-1} \neq 0\ \forall x$. Define the $m \times m$ matrix $A(x)$ as

$$A(x) = \begin{bmatrix} L_{g1}(L_f^{\gamma_1-1}h_1) & \cdots & L_{gm}(L_f^{\gamma_1-1}h_1) \\ \vdots & & \vdots \\ L_{g1}(L_f^{\gamma m-1}h_m) & \cdots & L_{gm}(L_f^{\gamma m-1}h_m) \end{bmatrix} \tag{6.11}$$

Then the Eqn.(6.9) can be written as

$$\begin{bmatrix} y_1^{\gamma 1} \\ \vdots \\ y_m^{\gamma m} \end{bmatrix} = \begin{bmatrix} L_f^{\gamma 1}h_1 \\ \vdots \\ L_f^{\gamma m}h_m \end{bmatrix} + A(x) \begin{bmatrix} u_1 \\ \vdots \\ u_m \end{bmatrix} \tag{6.12}$$

If $A(x) \in \Re^{m \times m}$ is bounded away from singularity, the state feedback control law

$$u = A^{-1}(x)(-\begin{bmatrix} L_f^{\gamma 1}h_1 \\ \vdots \\ L_f^{\gamma m}h_m \end{bmatrix} + v) \tag{6.13}$$

yields the closed loop decoupled linear equation

$$\begin{bmatrix} y_1^{(\gamma_1)} \\ \vdots \\ y_m^{(\gamma m)} \end{bmatrix} = \begin{bmatrix} v_1 \\ \vdots \\ v_m \end{bmatrix} \tag{6.14}$$

Once the linear system has been achieved, further control approaches such as pole placement, linear quadratic regulator etc. can be easily applied. Even if the matrix $A(x)$ is singular, linearization may still be achieved using dynamic state feedback. The development may be followed by using integrator before some of the inputs. Details can be seen in [53].

Control Design

The complete nonlinear dynamic equations with principal axes for a Space Station utilized in the control design are:

Attitude Dynamics:

$$\dot{\theta} = D(\theta)\omega + \bar{n} \tag{6.15}$$

where

$$D(\theta) = \begin{bmatrix} 1 & -\cos\theta_1 \tan\theta_3 & \sin\theta_1 \tan\theta_3 \\ 0 & \cos\theta_1 \sec\theta_3 & -\sin\theta_1 \sec\theta_3 \\ 0 & \sin\theta_1 & \cos\theta_1 \end{bmatrix}$$

Rotational Dynamics:

$$\dot{\omega} = I^{-1}(-\omega \times I\omega + 3n^2 c \times Ic - u + d) \tag{6.16}$$

where

$$c = \begin{pmatrix} -\sin\theta_2 \cos\theta_3 \\ \cos\theta_1 \sin\theta_2 \sin\theta_3 + \sin\theta_1 \cos\theta_2 \\ -\sin\theta_1 \sin\theta_2 \sin\theta_3 + \cos\theta_1 \cos\theta_2 \end{pmatrix}$$

$$I = \begin{bmatrix} I_1 & 0 & 0 \\ 0 & I_2 & 0 \\ 0 & 0 & I_3 \end{bmatrix}$$

and d is the disturbance torque.

CMG Momentum:

$$\dot{h} = -\omega \times h + u \tag{6.17}$$

where h_1, h_2 and h_3 are the body axis components of the CMG momentum. For the control law design in this section, d will be assumed to be zero. In order to design a

controller such that CMG momentum can be minimized while maintaining the body orientation of the Space Station near LVLH orientation, we choose nine state variables $x = (\theta_1, \theta_2, \theta_3, \omega_1, \omega_2, \omega_3, h_1, h_2, h_3)$, and three control torque inputs acting on CMGs $u = (u_1, u_2, u_3)$. It is essential to properly select three output functions such that the sum of the relative degrees for those three output functions is nine to meet the conditions for exact feedback linearization. In this studies, the same outputs are taken as in the work by [17]. The three chosen output functions are: LVLH yaw and pitch axis components of the total momentum (sum of momentum of the Space Station and CMGs) H_3 and H_2 which have relative degree of 4 and 3; respectively, the third one is yaw angle which has relative degree 2. The transformation from body frame to LVLH frame can be achieved through the following T matrix:

$$\begin{bmatrix} \cos\theta_3 \cos\theta_2 & -\cos\theta_1 \sin\theta_3 \cos\theta_2 + \sin\theta_1 \sin\theta_2 & \sin\theta_1 \sin\theta_3 \cos\theta_2 + \cos\theta_1 \sin\theta_2 \\ \sin\theta_3 & \cos\theta_1 \cos\theta_3 & -\sin\theta_1 \cos\theta_3 \\ -\cos\theta_3 sin\theta_2 & \cos\theta_1 \sin\theta_3 \sin\theta_2 + \sin\theta_1 \cos\theta_2 & -\sin\theta_1 \sin\theta_3 \sin\theta_2 + \cos\theta_1 \cos\theta_2 \end{bmatrix} \tag{6.18}$$

The components and its first and second time derivatives of matrix T are defined as following:

$$\begin{aligned} T_{11} &= \cos\theta_3 \cos\theta_2 \\ T_{12} &= -\cos\theta_1 \sin\theta_3 \cos\theta_2 + \sin\theta_1 \sin\theta_2 \\ T_{13} &= \sin\theta_1 \sin\theta_3 \cos\theta_2 + \cos\theta_1 \sin\theta_2 \\ T_{21} &= \sin\theta_3 \\ T_{22} &= \cos\theta_1 \cos\theta_3 \end{aligned}$$

$$
\begin{aligned}
T_{23} &= -\sin\theta_1 \cos\theta_3 \\
T_{31} &= -\cos\theta_3 \sin\theta_2 \\
T_{32} &= \cos\theta_1 \sin\theta_3 \sin\theta_2 + \sin\theta_1 \cos\theta_2 \\
T_{33} &= -\sin\theta_1 \sin\theta_3 \sin\theta_2 + \cos\theta_1 \cos\theta_2
\end{aligned} \tag{6.19}
$$

$$
\begin{aligned}
\dot{T}_{11} &= -T_{13}\omega_2 + T_{12}\omega_3 + T_{13}n \\
\dot{T}_{12} &= T_{13}\omega_1 - T_{11}\omega_3 + T_{32}n \\
\dot{T}_{13} &= -T_{12}\omega_1 + T_{11}\omega_2 + T_{33}n \\
\dot{T}_{21} &= -T_{23}\omega_2 + T_{22}\omega_3 \\
\dot{T}_{22} &= T_{23}\omega_1 - T_{21}\omega_3 \\
\dot{T}_{23} &= -T_{22}\omega_1 + T_{21}\omega_2 \\
\dot{T}_{31} &= -T_{33}\omega_2 + T_{32}\omega_3 - T_{11}n \\
\dot{T}_{32} &= T_{33}\omega_1 - T_{31}\omega_3 - T_{12}n \\
\dot{T}_{33} &= -T32\omega_1 + T_{31}\omega_2 - T_{13}n
\end{aligned} \tag{6.20}
$$

$$
\begin{aligned}
\ddot{T}_{11} &= -\dot{T}_{13}\omega_2 - T_{13}\dot{\omega}_2 + \dot{T}_{12}\omega_3 + T_{13}\dot{\omega}_3 + \dot{T}_{31}n \\
\ddot{T}_{12} &= \dot{T}_{13}\omega_1 + T_{13}\dot{\omega}_1 - \dot{T}_{11}\omega_3 - \dot{\omega}_3 + \dot{T}_{32}n \\
\ddot{T}_{13} &= -\dot{T}_{12}\omega_1 + T_{12}\dot{\omega}_1 + \dot{T}_{11}\omega_2 + T_{11}\dot{\omega}_2 + \dot{T}_{33}n \\
\ddot{T}_{21} &= -\dot{T}_{23}\omega_2 - T_{23}\dot{\omega}_2 + \dot{T}_{22}\omega_3 + T_{22}\dot{\omega}_3 \\
\ddot{T}_{22} &= \dot{T}_{23}\omega_1 + T_{23}\dot{\omega}_1 - \dot{T}_{21}\omega_3 - T_{21}\dot{\omega}_3 \\
\ddot{T}_{23} &= -\dot{T}_{22}\omega_1 - T_{22}\dot{\omega}_1 + \dot{T}_{21}\omega_2 + T_{21}\dot{\omega}_2 \\
\ddot{T}_{31} &= -\dot{T}_{33}\omega_2 - T_{33}\dot{\omega}_2 + \dot{T}_{32}\omega_3 + T_{32}\dot{\omega}_3 - \dot{T}_{11}n \\
\ddot{T}_{32} &= \dot{T}_{33}\omega_1 + T_{33}\dot{\omega}_1 - \dot{T}_{31}\omega_3 - T_{31}\dot{\omega}_3 + \dot{T}_{11}n
\end{aligned}
$$

$$\ddot{T}_{33} = -\dot{T}_{32}\omega_1 - T_{32}\dot{\omega}_1 - \dot{T}_{31}\omega_3 - T_{31}\dot{\omega}_3 - \dot{T}_{13}n \tag{6.21}$$

Hence, the H_1, H_2 and H_3 can be calculated by

$$\begin{aligned} H_1 &= T_{11}(h_1 + I_1\omega_1) + T_{12}(h_2 + I_2\omega_2) + T_{13}(h_3 + I_3\omega_3) \\ H_2 &= T_{21}(h_1 + I_1\omega_1) + T_{22}(h_2 + I_2\omega_2) + T_{23}(h_3 + I_3\omega_3) \\ H_3 &= T_{31}(h_1 + I_1\omega_1) + T_{32}(h_2 + I_2\omega_2) + T_{33}(h_3 + I_3\omega_3) \end{aligned} \tag{6.22}$$

The chosen linearizing transformation is $z = \Phi(x)$. Therefore, the local coordinate transformation for the Space Station can be represented by the following new variables:

$$\begin{aligned} z_{11} &= H_3 \\ z_{12} &= -nH_1 \\ z_{13} &= -n^2H_3 + 3n^3(T_{21}T_{31}I_1 + T_{22}T_{32}I_2 + T_{23}T_{33}I_3) \\ z_{14} &= n^3H_1 - 3n^4(T_{11}T_{21}I_1 + T_{12}T_{22}I_2 + T_{13}T_{23}I_3) \\ &\quad +3n^3(T_{23}T_{32} + T_{22}T_{33})(I_2 - I_3)\omega_1 \\ &\quad +3n^3(T_{23}T_{31} + T_{21}T_{33})(I_3 - I_1)\omega_2 \\ &\quad +3n^3(T_{22}T_{31} + T_{21}T_{32})(I_1 - I_2)\omega_3 \\ z_{21} &= H_2 \\ z_{22} &= 3n^2(T_{11}T_{31}I_1 + T_{12}T_{32}I_2 + T_{13}T_{33}I_3) \\ z_{23} &= -3n^3(T_{11}^2 - T_{31}^2)I_1 - 3n^3(T_{12}^2 - T_{32}^2)I_2 - 3n^3(T_{13}^2 - T_{33}^2)I_3 \\ &\quad +3n^2(T_{13}T_{32} + T_{12}T_{33})(I_2 - I_3)\omega_1 \\ &\quad +3n^2(T_{13}T_{31} + T_{11}T_{33})(I_3 - I_1)\omega_2 \\ &\quad +3n^2(T_{12}T_{31} + T_{11}T_{32}(I_1 - I_2)\omega_3 \end{aligned}$$

$$\begin{aligned} z_{31} &= \theta_3 \\ z_{32} &= \omega_3 \cos\theta_1 + \omega_2 \sin\theta_1 \end{aligned} \tag{6.23}$$

In this analysis, the control matrix $A(x)$ now becomes

$$-3n^3 \begin{bmatrix} \Delta_1(T_{23}T_{32} + T_{22}T_{33}) & \Delta_2(T_{23}T_{31} + T_{21}T_{33}) & \Delta_3(T_{22}T_{31} + T_{21}T_{32}) \\ \Delta_1(T_{13}T_{32} + T_{12}T_{33}) & \Delta_2(T_{13}T_{31} + T_{11}T_{33}) & \Delta_3(T_{12}T_{31} + T_{11}T_{32}) \\ 0 & \frac{\sin\theta_1}{3n^3 I_2} & \frac{\cos\theta_1}{3n^3 I_3} \end{bmatrix} \tag{6.24}$$

where

$$\Delta_1 = \frac{I_2 - I_3}{I_1},\ \Delta_2 = \frac{I_3 - I_1}{I_2},\ \Delta_3 = \frac{I_1 - I_2}{I_3}$$

The control matrix evaluated at TEA x_0 (i.e. $\theta = [0,0,0]$, $\omega = [0,-n,0]$, $h = [0,0,0]$)

$$A(x_0) = \begin{bmatrix} 3n^3(\frac{I_2 - I_3}{I_1}) & 0 & 0 \\ 0 & 3n^3(\frac{I_3 - I_1}{I_2}) & 0 \\ 0 & 0 & \frac{1}{I_3} \end{bmatrix} \tag{6.25}$$

As long as $I_1 \neq I_2$, and $I_2 \neq I_3$, $A(x_0)$ is not singular and controls can be calculated through Eqn.(6.13). The new control vector v is chosen to be linear feedback of the form

$$\begin{aligned} v_1 &= -k_1(z_{11} - z_{11_d}) - k_2(z_{12} - z_{12_d}) - k_3(z_{13} - z_{13_d}) - k_4(z_{14} - z_{14_d}) + \dot{z}_{14_d} \\ v_2 &= -k_5(z_{21} - z_{21_d}) - k_6(z_{22} - z_{22_d}) - k_7(z_{23} - z_{23_d}) + \dot{z}_{23_d} \\ v_3 &= -k_8(z_{31} - z_{31_d}) - k_9(z_{32} - z_{32_d}) + \dot{z}_{32_d} \end{aligned} \tag{6.26}$$

where z_{ij_d} is the desired reference trajectory so that the characteristic equation for the linear decoupled system is

$$\lambda(x) = (s^4 + k_1 s^3 + k_2 s^2 + k_3 s + k_4)(s^3 + k_5 s^2 + k_6 s + k_7)(s^2 + k_8 s + k_9) \tag{6.27}$$

Simulation Results

The Space Station is initialized at $\theta = [5^o, 10^o, 5^o] deg$, $\omega = [0.2n, -n, 0] rad/s$, h=0, with $n = 0.0011 rad/sec$. The closed loop poles are chosen to be $[-5.5 \pm 2.32i]$, $[-4.386 \pm 0.57i]$, $[-2.75 \pm 1.3i]$,-0.2597, $[-2.7 \pm 0.7i]$. The simulation results are shown from Figure 6.1 and Figure 6.3. The simulation results indicate the good performance can be achieved for the Space Station in a disturbance free environment if we properly choose the closed-loop poles. But in some situations, aerodynamic disturbances, drag in particular can not be ignored. For a Space Station in a circular orbit, the aerodynamic drag torque may be approximated by a constant vector. With small disturbances, the system stability may still be maintained by using the same feedback linearization controller, but the system performance will be greatly degraded. The cumulative CMGs momentum is high which can be seen in Figure 6.4 and Figure 6.5. This is the case where constant disturbance torques $[1, 4, 1]$ lb-ft are applied in the three body axes. When the disturbances get larger, the system will become unstable. Figure 6.6 shows the variation of the Euler angles when the disturbances are [2, 16, 2] lb-ft. Notice that the pitch angle diverged in less than $\frac{4}{5}$ orbital period (i.e. about 4600 sec.).

Approximate Feedback Linearization Control with Unknown Constant Disturbances

In the face of the constant disturbances, the simulation in the preceding section has shown the necessity of further compensation. The modifications of the exact feedback linearization for Space Station attitude control and CMGs momentum management with the unknown disturbances can be performed by the new transformation

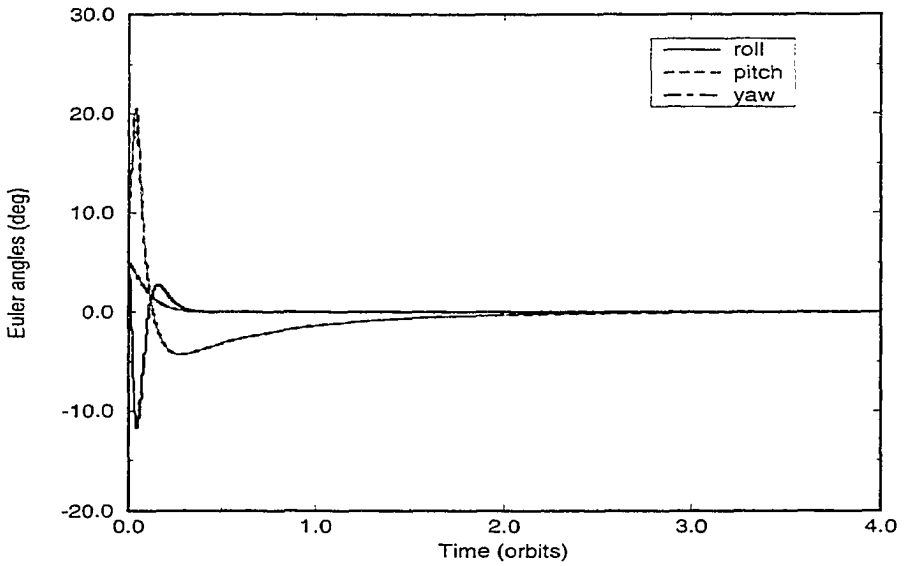

Figure 6.1: Euler angles with feedback linearization control.

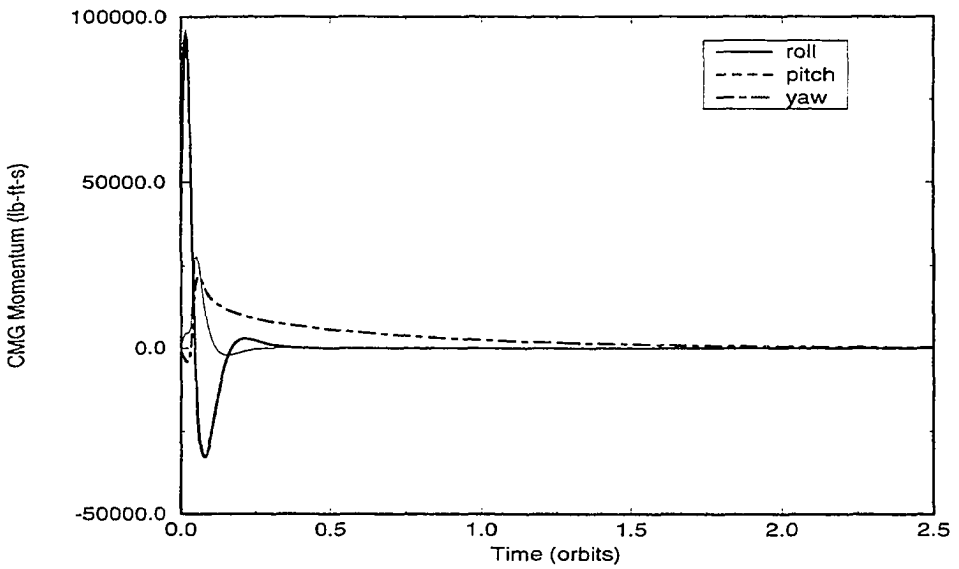

Figure 6.2: CMGs momentum with feedback linearization control.

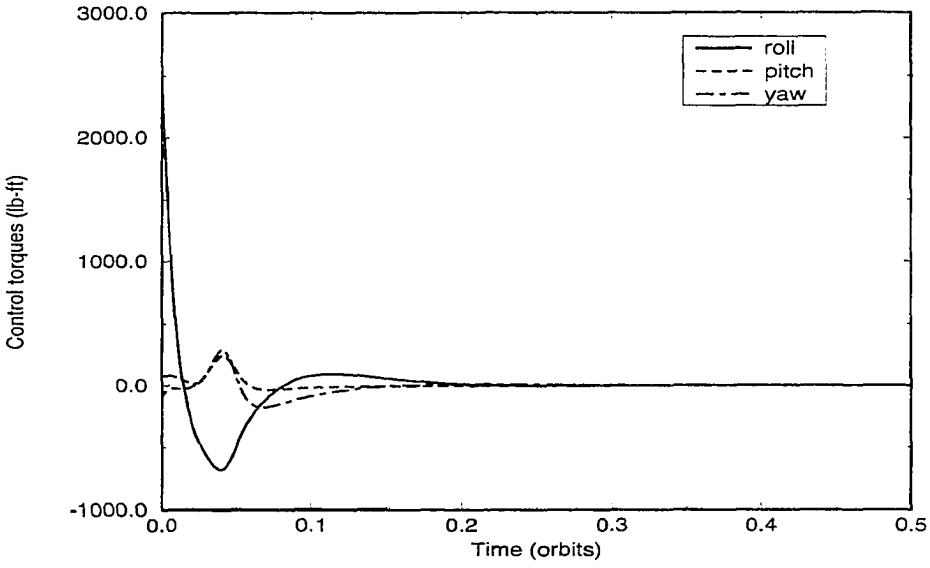

Figure 6.3: Histories of control torques with feedback linearization control.

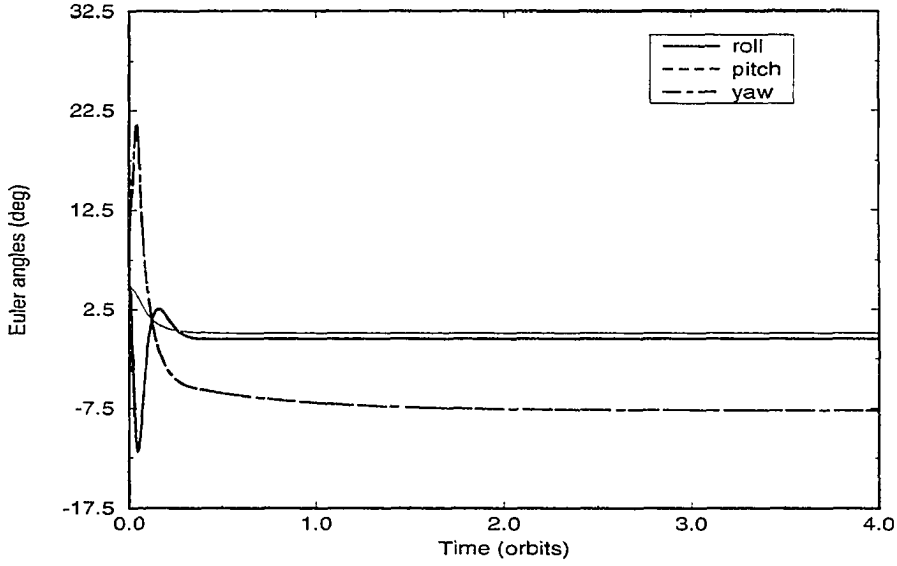

Figure 6.4: Euler angles with small constant disturbances by feedback linearization control.

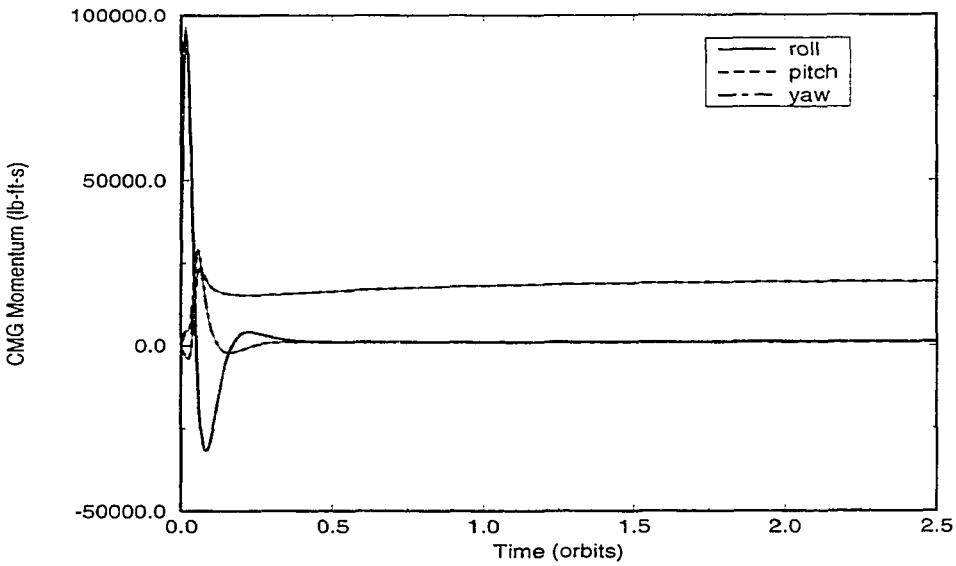

Figure 6.5: CMGs momentum with small constant disturbances by feedback linearization control.

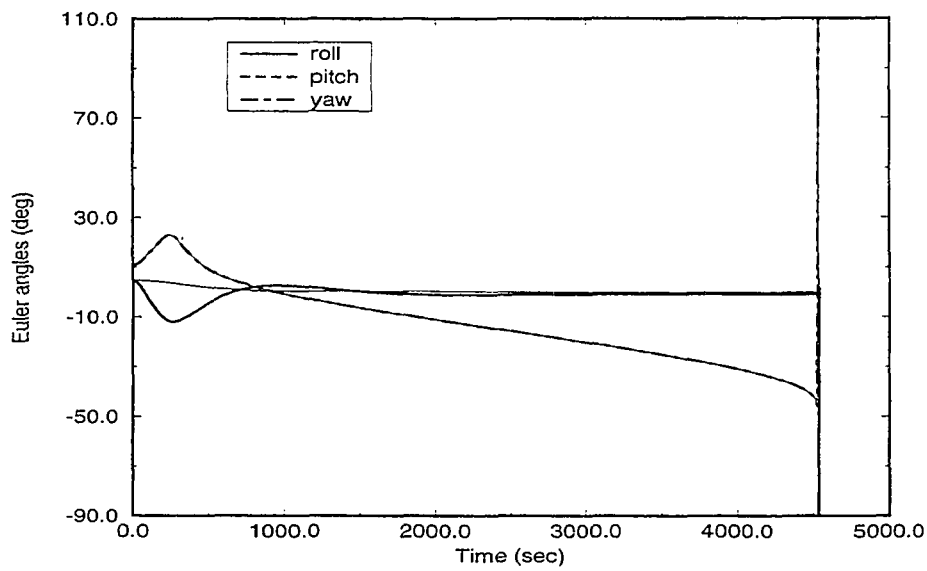

Figure 6.6: Euler angles with large constant disturbances by feedback linearization control.

$\hat{z} = \hat{\Phi}(x, \hat{d})$ which are

$$\begin{aligned}
\hat{z}_{11} &= z_{11} \\
\hat{z}_{12} &= z_{12} + \hat{d}_1 T_{31} + \hat{d}_2 T_{32} + \hat{d}_3 T_{33} \\
\hat{z}_{13} &= z_{13} - n(\hat{d}_1 T_{11} + \hat{d}_2 T_{12} + \hat{d}_3 T_{13}) \\
&\quad + \hat{d}_1 \dot{T}_{31} + \hat{d}_2 \dot{T}_{32} + \hat{d}_3 \dot{T}_{33} \\
\hat{z}_{14} &= z_{14} - n^2(\hat{d}_1 T_{31} + \hat{d}_2 T_{32} + \hat{d}_3 T_{33}) \\
&\quad - n(\hat{d}_1 \dot{T}_{11} + \hat{d}_2 \dot{T}_{12} + \hat{d}_3 \dot{T}_{13}) \\
&\quad + \hat{d}_1 \ddot{T}_{31} + \hat{d}_2 \ddot{T}_{32} + \hat{d}_3 \ddot{T}_{33} \\
\hat{z}_{21} &= z_{21} \\
\hat{z}_{22} &= z_{22} + (\hat{d}_1 T_{21} + \hat{d}_2 T_{22} + \hat{d}_3 T_{23}) \\
\hat{z}_{23} &= z_{23} + (\hat{d}_1 \dot{T}_{21} + \hat{d}_2 \dot{T}_{22} + \hat{d}_3 \dot{T}_{23}) \\
\hat{z}_{31} &= z_{31} \\
\hat{z}_{32} &= z_{32}
\end{aligned} \tag{6.28}$$

where z_{ij} is the new variable for the original transformation and $\hat{d}_1$, $\hat{d}_2$ and $\hat{d}_3$ are the estimations of the unknown, but constant disturbances d_1, d_2, and d_3 acting on the three body axes of the Space Station. Due to the effects of the disturbances, the condition of relative degree of 4 for H_3 is no longer satisfied. Instead of $\gamma_1 = 4$, the control torque appears in the term $\dot{\hat{z}}_{13}$ so that the relative degree reduces to 3 as shown in the following.

$$\begin{aligned}
\dot{\hat{z}}_{13} &= z_{14} - n^2(\hat{d}_1 T_{31} + \hat{d}_2 T_{32} + \hat{d}_3 T_{33}) - n(\hat{d}_1 \dot{T}_{11} + \hat{d}_2 \dot{T}_{12} + \hat{d}_3 \dot{T}_{13}) \\
&\quad \hat{d}_1(-\dot{T}_{33}\omega_2 + \dot{T}_{32}\omega_3 - \dot{T}_{11} n - T_{33}(\frac{(I_3 - I_1)}{I_2}(\omega_1 \omega_3 - 3n^2 T_{31} T_{33})))
\end{aligned}$$

$$
\begin{aligned}
&+T_{32}(\frac{(I_1-I_2)}{I_3}(\omega_1\omega_2-3n^2T_{31}T_{32}))) + \hat{d}_2(\dot{T}_{33}\omega_1+\dot{T}_{31}\omega_3+\dot{T}_{12}n \\
&+T_{33}(\frac{(I_2-I_3)}{I_1}(\omega_2\omega_3-3n^2T_{32}T_{33})-T_{31}(\frac{(I_1-I_2)}{I_3}(\omega_1\omega_2-3n^2T_{31}T_{32}))) \\
&\hat{d}_3(-\dot{T}_{32}\omega_2+\dot{T}_{31}\omega_3-\dot{T}_{13}n-T_{32}(\frac{(I_2-I_3)}{I_1}(\omega_2\omega_3-3n^2T_{32}T_{33}) \\
&+T_{31}(\frac{(I_1-I_2)}{I_3}(\omega_1\omega_2-3n^2T_{31}T_{32}))) + (-\hat{d}_2T_{33}/I_1+\hat{d}_2T_{32}/I_1)u_1 \\
&+(-\hat{d}_1T_{33}/I_2+\hat{d}_3T_{32}/I_2)u_2+(\hat{d}_2T_{31}/I_3-\hat{d}_3T_{31}/I_3)u_3 \\
= \;& f_{13}(x)+g_1'(x,\hat{d})u_1+g_2'(x,\hat{d})u_2+g_3'(x,\hat{d})u_3 \qquad (6.29)
\end{aligned}
$$

Therefore, the exact feedback linearization is not applicable to this problem. Since the magnitudes of the coefficients of the control terms are found to be small compared with other terms 5 order of magnitude smaller at the beginning, we opt to use the approximate feedback linearization technique by simply neglecting the terms which include controls in $\hat{z}_{13}$. i.e. $g_1'(x,\hat{d})u_1$, $g_2'(x,\hat{d})u_2$ and $g_3'(x,\hat{d})u_3$.

For detailed theoretical background, see Hauser [19]. In this way, the lost relative degree is "recovered". We rewrite the transformed state equations in the form:

$$
\begin{aligned}
\dot{\hat{z}} &= \frac{\partial\hat{z}}{\partial x}\dot{x}+\frac{\partial\hat{z}}{\partial\hat{d}}\dot{\hat{d}} \\
&= \frac{\partial\hat{z}}{\partial x}(f(x)+G(x)u+W\hat{d}+W\tilde{d})+\frac{\partial\hat{z}}{\partial\hat{d}}\dot{\hat{d}} \\
&= Z_x(f(x)+G(x)u+W\hat{d})+Z_xW\tilde{d}+Z_d\dot{d} \qquad (6.30)
\end{aligned}
$$

where

$$
W=\begin{bmatrix}
0 & 0 & 0 & 1/I_1 & 0 & 0 & 0 & 0 & 0 \\
0 & 0 & 0 & 0 & 1/I_2 & 0 & 0 & 0 & 0 \\
0 & 0 & 0 & 0 & 0 & 1/I_3 & 0 & 0 & 0
\end{bmatrix}^T
$$

$Z_x=\frac{\partial\hat{z}}{\partial x}$, and $Z_d=-\frac{\partial\hat{z}}{\partial\hat{d}}$, $\tilde{d}=d-\hat{d}$. $Z_x\in\Re^{9\times9}$, $Z_d\in\Re^{9\times3}$. The approximate

linear control law is then

$$u(x,\hat{d}) = \hat{A}(x,\hat{d})^{-1}(-\begin{bmatrix} L_f^4 H_3(x,\hat{d}) \\ L_f^3 H_2(x,\hat{d}) \\ L_f^2 \theta_3(x,\hat{d}) \end{bmatrix} + v) \tag{6.31}$$

where

$$\hat{A}(x,\hat{d}) = A(x)$$
$$- \begin{bmatrix} (-\hat{d}_2 T_{33} + \hat{d}_3 T_{32})/I_1 & (\hat{d}_1 T_{33} - T_{31}\hat{d}_3)/I_2 & (-T_{32}\hat{d}_1 + T_{31}\hat{d}_2)/I_3 \\ (\hat{d}_2 T_{23} - \hat{d}_3 T_{22})/I_1 & -(\hat{d}_1 T_{23} - \hat{d}_3 T_{21})/I_2 & (\hat{d}_1 T_{22} - \hat{d}_2 T_{21})/I_3 \\ 0 & \frac{\sin\theta_1}{I_2} & \frac{\cos\theta_1}{I_3} \end{bmatrix} \tag{6.32}$$

Let Z_{ij_d} be the desired trajectory and denote the tracking error as in the Space Station system e_C whose components are $\hat{z}_{ij} - \hat{z}_{ij_d}$. If we choose our nominal control

$$v = \begin{bmatrix} -k_1(\hat{z}_{11} - \hat{z}_{11_d}) - k_2(\hat{z}_{12} - \hat{z}_{12_d}) - k_3(\hat{z}_{13} - \hat{z}_{13_d}) - k_4(\hat{z}_{14} - \hat{z}_{14_d})) + \dot{\hat{z}}_{14_d} \\ -k_5(\hat{z}_{21} - \hat{z}_{21_d}) - k_6(\hat{z}_{22} - \hat{z}_{22_d}) - k_7(\hat{z}_{23} - \hat{z}_{23_d}) + \dot{\hat{z}}_{23_d} \\ -k_8(\hat{z}_{31} - \hat{z}_{31_d}) - k_9(\hat{z}_{32} - \hat{z}_{32_d})) + \dot{\hat{z}}_{32_d} \end{bmatrix} \tag{6.33}$$

The closed-loop decoupled system can be obtained and written as

$$\dot{e}_C = A_C e_C + Z_x \tilde{d} + Z_d \dot{\tilde{d}} \tag{6.34}$$

where

$$A_c = \begin{bmatrix} 0 & 1 & 0 & 0 & 0 & 0 & 0 & 0 & 0 \\ 0 & 0 & 1 & 0 & 0 & 0 & 0 & 0 & 0 \\ 0 & 0 & 0 & 1 & 0 & 0 & 0 & 0 & 0 \\ -k_1 & -K_2 & -K_3 & -k_4 & 0 & 0 & 0 & 0 & 0 \\ 0 & 0 & 0 & 0 & 0 & 1 & 0 & 0 & 0 \\ 0 & 0 & 0 & 0 & 0 & 0 & 1 & 0 & 0 \\ 0 & 0 & 0 & 0 & -k_5 & -k_6 & -K_7 & 0 & 0 \\ 0 & 0 & 0 & 0 & 0 & 0 & 0 & 0 & 1 \\ 0 & 0 & 0 & 0 & 0 & 0 & 0 & -k_8 & -k_9 \end{bmatrix}$$

Since in general, it is difficult to know the exact value of the disturbances $d = [d_1, d_2, d_3]^T$, estimation must be made for satisfactory performance. An adaptation law for the disturbances is assumed to be

$$\dot{\tilde{d}} = L_c e_c \tag{6.35}$$

In order to design this adaptation law such that the tracking error will go to zero asymptotically, we consider a Lyapunov function candidate

$$V = e_c^T P_c^{-1} e_c + \tilde{d}^T P_d^{-1} \tilde{d} \tag{6.36}$$

where P_c is a positive matrix and P_d is a constant positive matrix. The time derivative of V along the closed-loop trajectory is

$$\begin{aligned} \dot{V} &= \dot{e}_c^T P_c^{-1} e_c - e_c^T P_c^{-1} \dot{P}_c P_c^{-1} e_c + e_c^T P_c \dot{e}_c + 2\tilde{d}^T P_d^{-1} L_c e_c \\ &= e_c^T P_c^{-1} (A_c P_c + P_c A_c^T + Z_d L_c P_c + P_c L_c^T Z_d^T - \dot{P}_c) P_c^{-1} e_c \\ &\quad + 2\tilde{d}(P_d^{-1} L_c + Z_x^T P_c^{-1}) e_c \end{aligned} \tag{6.37}$$

To cancel the cross-product term, we choose

$$L_c = -P_d Z_x^T P_c^{-1} \tag{6.38}$$

Let $Y = -Z_d P_d Z_x^T$, and choose

$$Q = (\alpha + 1) I_n + Y Y^T \tag{6.39}$$

$$\dot{P}_c = A_c P_c + P_c A_c^T + Q \tag{6.40}$$

Substitute Eqns.(6.33), (6.36) and (6.38) into Eqn.(6.35) so that

$$\begin{aligned} \dot{V} &= e_c^T P_c^1 (A_c P_c + P_c A_c^T - Y - Y^T - \dot{P}_c) P_c^{-1} e_c \\ &= -e_c^T P_c^1 (\alpha I_n + (I_n + Y)(I_n + Y^T)) P_c^{-1} e_c < 0 \ for \ \forall e_c \neq 0 \end{aligned} \tag{6.41}$$

where α is a positive constant. Therefore, the asymptotic error-tracking can be achieved by Eqn.(6.29), (6.38) and together with the adaptation law

$$\dot{\tilde{d}} = -P_d Z_x^T P_c^{-1} e_c \tag{6.42}$$

Simulation Results

For comparison purpose, we use the same initial conditions and control law parameters for the Space Station, and the disturbances are also the same as in previous section. To investigate the improvements by using this adaptive controller, we choose the desired trajectory

$$\begin{aligned} \hat{Z}_{11_d} &= 0 \\ \hat{Z}_{21_d} &= -I_2 * n \\ \hat{Z}_{31_d} &= 0 \end{aligned} \tag{6.43}$$

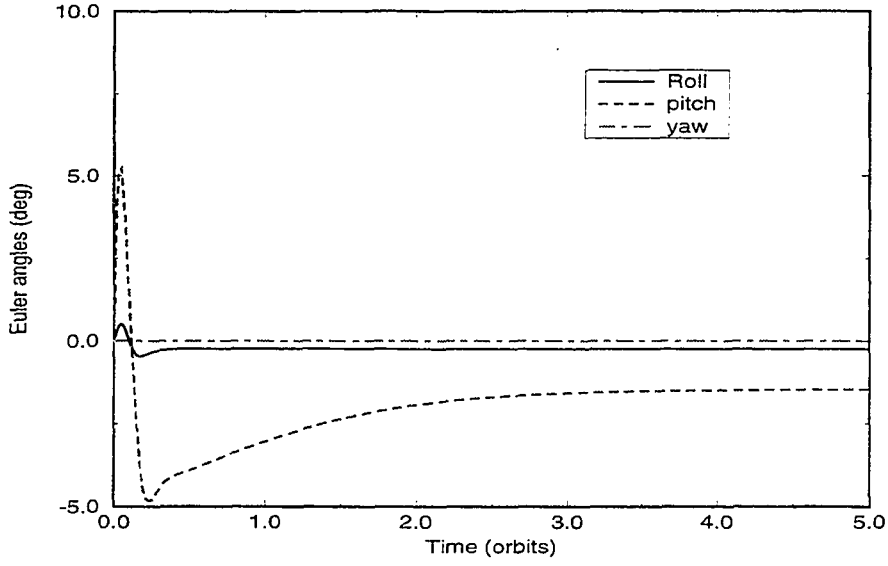

Figure 6.7: Euler angles with small constant disturbances by adaptive controller.

which, when $d = 0$, correspond to the LVLH position. Two simulations are carried out; one is for the smaller disturbance ($d_1 = 1$, $d_2 = 4$, $d_3 = 1$) lb-ft; the other is for the larger disturbance ($d_1 = 2.d_2 = 16$,$d_3 = 2$) lb-ft. Figure 6.7 and Figure 6.8 display the simulation results for Case 1. The improvement of the performance is obvious compared with the case without the modification (Figs. 6.4 and 6.5). Both Euler angles and CMGs momentum are stabilized to smaller values. More importantly, this adaptive control is able to stabilize the system with large disturbances while the exact feedback linearization can not. This can be seen in Figure 6.9 and Figure 6.10 compared to Figure 6.6. It should be pointed out that in this case, convergence of parameter estimation is not guaranteed. So $\hat{d}$ can converge to values different than d, and the converged value closely depends on the magnitude of disturbances.

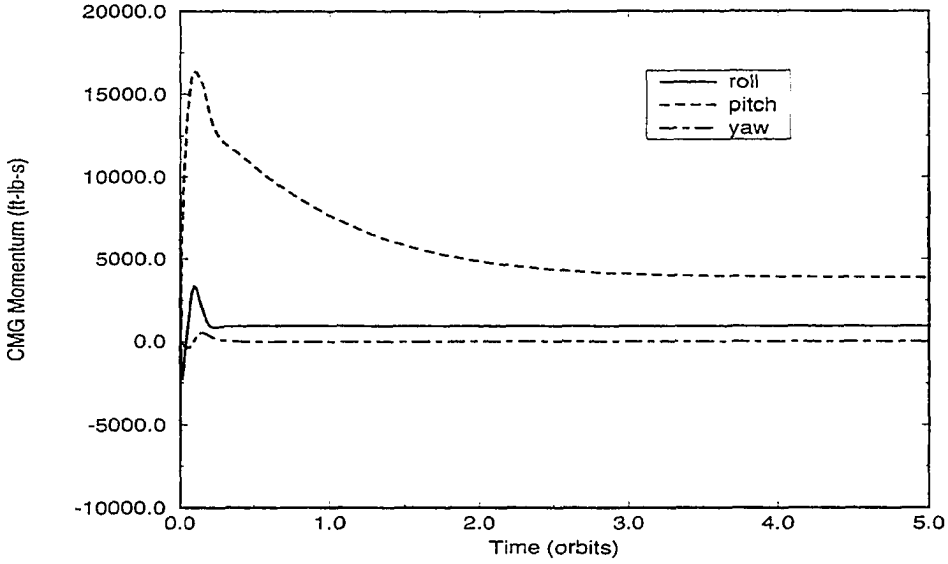

Figure 6.8: CMGs momentum with small constant disturbances by adaptive controller.

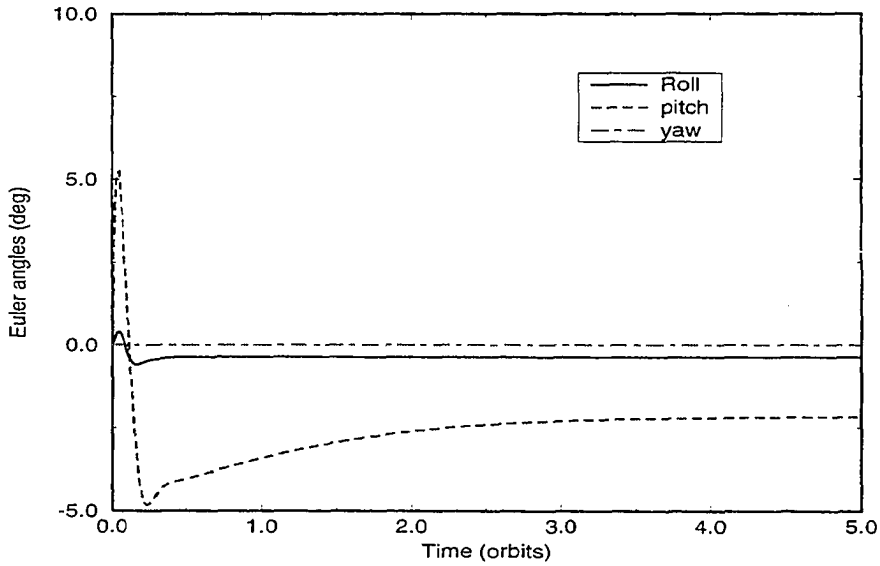

Figure 6.9: Euler angles with large disturbances by adaptive controller.

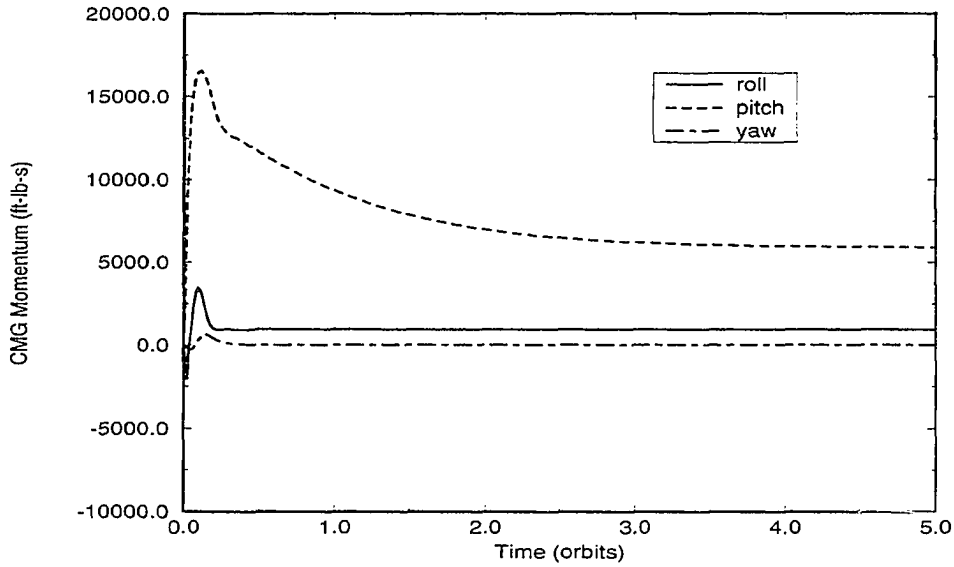

Figure 6.10: CMGs momentum with large disturbances by adaptive controller.

CHAPTER 7. CONCLUSIONS

A linear controller was first examined ed for the nonlinear Space Station dynamics. As expected, it worked well for small overall perturbations and small system parameter uncertainties. The performance degraded as the perturbations increase. Thus, it is necessary to study nonlinear control approaches.

Two nonlinear adaptive controllers which were originally designed for robot manipulators were first developed to solve the robustness problem which arises from the parameter uncertainties for the system inertias and the unknown disturbances. The spacecraft was assumed to be a rigid body so that the requirements for the linear parameterization and skew-symmetric properties were satisfied in this problem. The first controller was a nonlinear adaptive controller which needs some prior information about the parameters but requires less effort to tune the parameters. A sliding rule associated with the adaptive laws for the parameters was required for this controller to achieve global stability of the uncertain systems. The other was an adaptive nonlinear controller which extracted information from the tracking errors and their higher derivatives to actuate the parameter update. Asymptotic convergence of both adaptive controllers were proved.

Since the disturbance torques are modeled as a constant term plus some periodic functions with unknown magnitudes and phase angles, the above two adaptive

controllers were modified by introducing a term involving the estimated parameters and the known sinusoid vector. Its purpose was to compensate for the effects of the disturbances. The convergence of the disturbance parameters was proved by showing that the disturbance vector was persistently excited. A number of simulations were carried out to evaluate the performance of the adaptive controllers. Both controllers were shown to have equally good tracking performances with the uncertain parameters in terms of the convergence rate and smooth state response. But the second controller has better convergence rate than the first one. For the second adaptive controller, the convergence of the parameters was tested with the cross-products of inertia neglected. Both nonlinear adaptive controllers were found to be robust with the unmodeled dynamics.

A neural network control design via radial basis function (RBF) was investigated. This RBF neural network control method was used in conjunction with a baseline control which can be any of the above two adaptive controllers to shape the system response. It acted as an open-loop control to predict the disturbances and to cancel their effects. The disturbances were not necessarily periodic functions as long as some prior information about the structure of the disturbance was provided. It has been shown that the orthogonal forward regression procedure provides a powerful method for fitting radial basis function models to spacecraft attitude control problem. Although the numbers of the centers were found to be very few for our three networks, their fitting abilities were remarkable. Simulation results also showed that the required control torques were relatively smaller than just using the nonlinear adaptive controllers. Its ability of extrapolation for the untrained disturbances are also tested.

When control momentum gyros (CMGs) are used for attitude control, both the magnitude of the CMG momentum and the Space Station attitude need to be regulated. While in a disturbance-free environment, the exact feedback linearization method has been successful in this regard, the system performance degrades and eventually instability will occur as the disturbances appear and increase in size. An approximate feedback linearization approach was employed to simultaneous attitude control and control momentum gyro (CMGs) management for the Space Station problem with unknown constant disturbances. By designing a direct adaptive tracking controller based on the approximate feedback linearized system, we were able to stabilize the system and control the state variables to a reasonable small range.

Future work is still needed in comprehensive investigation of the control of the transient state responses to reduce the maximum required control effort. The structure flexibility will be another concern for more realistic studies of the adaptive controllers for the spacecraft attitude control. Finally, time-varying disturbances may need to be studied in the attitude control and CMGs management problem.

REFERENCES

[1] Chen, C. T., *Linear System Theory and Design*, New York, Holt, Rinehart and Winston, 1981.

[2] Warren, W., and Wie, B., "Periodic-Disturbance Accommodating Control of the Space Station for Asymtotic Momentum Management," *Journal of Guidance, Navigation and Control,* Vol 13, No.6, 1990, pp.984-992.

[3] Chu, P., Wie, B., Cretz, B.,and Plescia, C., "Space station Attitude Control: Modeling and Design," *AIAA Paper 88-4133* Aug., 1988

[4] Wie, B., Byun, K. W., and Warren, V. W., "New Approach to Attitude/Momentum Control for the Space Station," *Int. J. of Guidance, Navigation and Control,* Vol 12, No.5, 1989, pp.714-721.

[5] Wie, B., and Plescia, C. T.. "Attitude Stabilization of Flexible Spacecraft During Stationkeeping Manuever," *Journal of Guidance, Control, and Dynamics,* Vol.7, July-Aug. 1985, pp.430-436.

[6] Wie, B., Lehner, J. A., and Plescia, C. T., "Roll/Yaw Control of a flexible Spacecraft Using Skewed Bias Momentum Wheels," *Journal of Guidance, Control, and Dynamics,* Vol.8, July-Aug. 1986, pp.447-453.

[7] Wie, B., and Bryson, A. E., "On Multivariable Control Robustness Examples: A Classical Approach," *Journal of Guidance, Control, and Dynamics,* Vol.10, Jan.-Feb. 1987, pp.118-120.

[8] Wie, B., and Byun, K. W., "A New Concept of Generalized Structural Filtering for Active Vibration Control Synthesis," *AIAA Paper 87-2456*

[9] Bishop R. H., Paynter S. J., and Sunkel, J. W., "Adaptive Control of Space Station During Nominal Operations with CMGs," *Proc. of the 30th Conference on Decision and Control,* Brighton, England, December 1991.

[10] Balas, G., Pachard, A., and Harduvel, J., "Applications of μ-Synthesis Techniques to Momentum Management and Attitude Control of the Space Station," *AIAA Guidance, Navigation and Control Conference,* Paper no. AIAA-91-2662-CP, Jan. 1991.

[11] Byun, K. W., Wie, B., Geller, D., and Sunkel, J., "Robust H^∞ Control Design for the Space Station with Structured Parameter Uncertainty," *AIAA Guidance, Navigation and Control Conference,* Aug. 20-22, 1990/Portland Oregon.

[12] Wie, B., Byun, K. W., and Sunkel, J., "Robust Control Synthesis for Uncertain Dynamical Syatems," *AIAA Paper No. 89-3516*

[13] Doyle, J., Glover, K., Khargonokar, B., and Francis, B., "State-space Solutions to Standard H_2 and H_∞ Control Problems," *IEEE Transactions on Automatic Control,* Vol.AC-34, No.8. 1988,

[14] Harduvel, J., "Continous Momentum Management of Earth-Oriented Spacecraft," *AIAA Guidance, Navigation and Control Conference,* Aug. 20-22, 1990/Portland Oregon.

[15] Morton, B., "New Application of μ to Real Parameter Variation Problems," *Proceedings of the IEEE Conference on Decision and Control,* 1985.

[16] Rhee, I., and Speyer, J., "A Game Theoretic Controller for a Linear Time-Invariant System with Parameter Uncertainty and its Application to the Space Station," *AIAA Guidance, Navigation and Control Conference,* Aug. 20-22, 1990/Portland Oregon.

[17] Sheen, J. J. , *Adaptive nonlinear control spacecraft*, The University of Texas at Austin, Ph.D Dissertation, 1993.

[18] Krener, A., "On the Equivalence of Control Syatems and the Linearization of Nonlinear Syatems," *SIAM J. Control* 11(4):670-676, Nov. 1973.

[19] Hauser, J., Sastry, S., and Kokotovic, P, "Nonlinear Control Via Approximate Input-Output Linearization: the Ball and Beam Example," *IEEE Transactions on Automatic Control,* Vol 37, No.3, March 1992, pp.392-398.

[20] Nam, K., and Arapostathis, A., "A Model Reference Adaptive Control Scheme for Pure-Feedback Nonlinear System,s" *IEEE Transactions on Automatic Control,* Vol 33, No.9, 1988, pp.803-811.

[21] Pomet, J., and Praly, L., "Adpative Nonlinear Regulatioon: Estimation from the Lyapunov Equation," *IEEE Transactioons on Automatic Control,* Vol 37, No.6, 1992, pp.729-740.

[22] Kanellakopoulos, I., and Kokotovic, P. V., "Systematic Design of Adaptive Controllers for Feedback Linearizable Systems," *IEEE Transaction on Automatic Control,* Vol 36, No.11, 1991, pp.1241-1991.

[23] Taylor D. G., Kokotovic, P. V., Marino, R., and Kanellakopoulos, I., "Adaptive Regulation of Nonlinear Systems with Unmodeled Dynamics," *IEEE Transactioons on Automatic Control,* Vol 34, No.4, 1989, pp.405-412.

[24] Hunt, R., Su, L. R., and Meyer G., "Global Transformations of Nonlinear Systems," *IEEE Transaction on Automatic Control,* Vol. AC-28, pp24-31, 1983.

[25] Hunt, R., Su. L. R., and Meyer, G., "Design for Multi-Input Nonlinear Systems," *in Differential Geometric Control Theory,* R.W.Brockett, R.S.Williams, and H. Sussmann (Eds.), Brikhauser, Boston, 1983, pp.268-298.

[26] Hunt, R., and Su, L. R., "Linear Equivalents of Nonlinear Time-Varying Systems," *Int. Symposium on Math. Theory of Networks and Systems,* Santa Monica, 1981, pp.119-123.

[27] Isidori, A., *Nonlinear Control Systems,* Berlin, Springer-Verlag ,1989.

[28] Sastry, S. S., Isidori, A., "Adaptive Control of Linearizable Systems," *IEEE Transactioons on Automatic Control,* Vol 34, No.11, 1989, pp.1123-1131.

[29] Dwyer, T., "Exact Nonlinear Control of Large Angle Rotational Manuvers," *IEEE Transaction on Automatic Control,* Vol. AC-29, Sept. 1984, pp.769-774.

[30] Dwyer, T.. "Exact Nonlinear Control of Spacecraft Slewing Manuver with Internal Momentum Transfer," *AIAA Journal of Guidance, Control and Dynamics,* Vol.9, No.2, 1986, pp.240-247.

[31] Dzielski, J., Bergmann, E., and Paradiso, J., "A Computational Algorithm for Spacecraft Control and Momentum Management," *Proceedings of 1990 American Control Conference,* San Diego, California, pp.1320-1325.

[32] Singh, S. N., and Bossari, T. C., "Feedback Linearization and Nonlinear Ultimate Boundness Control of the Space Station using CMG," *AIAA GNCC Conference Proceedings,* Vol.1, No.90-3354-CP, 1990, pp.369-376.

[33] Singh, S. N., and Bossari, T. C., "Invertibility of Map, Zero Dynamics and Nonlinear Control of Space Station," *AIAA GNCC Conference Proceedings,* Vol.1, No.91-2663-CP, 1991, pp.576-584.

[34] Slotine J. E., and Li, W., "Composite Adaptive Control of Robot Manipulators," *Automatica,* Vol 25, No.4, 1989, pp.509-519.

[35] Slotine, J. E., and Li, W., "Applied Nonlinear Control," Englewood Cliffs, New Jersy 07632.

[36] Spong, W. M., "Adaptive Control of Robot Manipulators: Design and Robustness," *Proc. of the 4th IFAC workshop,* San Francisco, California, June, 1983. pp.2826-2830.

[37] Chen, D., and Paden, B., "Adaptive Linearization of Hybrid Step Motors: Stability Anaysis," *IEEE Transactions on Automatic Control,* Vol.38, No.6, 1993, pp.874-887.

[38] Narendra, K. S., and Parthasarathy, K., "Identification and Control of Dynamical Systems Using Neural Networks," *IEEE Transactions on Neural Networks*, Vol.1, No.1, 1990, pp.4-27.

[39] Mills, P. M., Zomaya, A. Y., and Tade, M. O., "Adaptive Model-Based Control Using Neural Networks," *Int. J. Control*, Vol 60, No.6, 1994, pp.1163-1192.

[40] Sanner, R.M., and Slotine, J.J.E., "Gaussian Networks for Direct Adaptive Control," *IEEE Transactions on Neural Networks*, Vol.3, No.6, 1992, pp.837-863.

[41] Gomi, H., and Kawato, M., "Neural Network Control for Close-Loop System Using Feedback-Error-Learning," *Neural Networks*, Vol.6, 1993, pp.933-946.

[42] Calise, A. J., Kim, B. S. Leitner, J. and Prasad, J.V.R., "Helicopter Adaptive Flight Control Using Neural Networks," *Proc. of the 33rd Conference on Decision and Control*, Lake Buena Vista, FL, December, 1994. pp.3336-3341.

[43] Chen, S., Cowa, C.F.N., and Grant, P.M., "Orthogonal Least Squares Learning Algorithm for Radial Basis Function Netwroks," *IEEE Transactions on Neural Network*, Vól 2. No.2 March, 1991.

[44] Chen, S., Billing, S.A., Cowan, C.F.N., and Grant, P.M., "Nonlinear Systems Identification Using Radial Basis Functions," *Int. J. Systems Science*, Vol.21. No.12, 1990, pp.2513-2539.

[45] Clancy, D. J., Özguner, M., and Graham, R. E., "Optimal Space Station Solar Array Gimbal Angle Determination Via Radial Basis Function Neural Network," *NASA Technical Memorandum 106482*, Feb, 1994.

[46] Troudet, T., and Grag, S., and Merrill, W. C., "Neural Network Application to Aircraft Control System Design," *Proceedings of the AIAA on Guidance, Navigation and Control Conference,* New Orleans, Aug. 1991, pp.993-1009.

[47] Baker, W. L., and Farrel, J. A., "Learning Augumented Flight Control for High Performance Aircraft," *Proceedings of the AIAA on Guidance, Navigation and Control Conference,* Aug. 1991, pp.347-358.

[48] Park, J., and Sandberg I.W., "Universal Approximation Using Radial Basis Function Netwroks," *Neural Computation,* 3:246-257, 1991.

[49] Powell, M., "Radial Basis Function for Multivariable Interpolation: A review" *Proceedinds of the IMA Conference on Algorithms for the Approximation of Functions and Data,* Royal Military College of Scieence, Shrivenhan, July 1985.

[50] Schagen, I.P., "Seqential Exploration of Unknown Multidimensional Functions as an Aid to Optimization," *IMA Journal of Numerical Analysis,* 4:337-247, 1984.

[51] Moody, J., and Darken, C.J., "Fast Laerning in Networks of Locally-Tuned Processing Units," *Neural Computation,* 1:281-294, 1989.

[52] Micchelli, C.A. "Interpolation of Scattered Data: Distance Matrices and Conditionally Positive Definite Functions," *Constructive Approximation,* 2:11-22, 1986.

[53] Descusse J., and Moong C. H., "Decoupling with Dynamic Compensation for Strongly Invertible Affine Nonlinear Systems," *Int. J. Control,* No.42, 1985, pp.1387-1398.

[54] Hughs, P. C., *Spacecraft Attitude Dynamics*, New York, John Wiley and Sons, 1986.

[55] Narendra, K. S., *Stable Adaptive Systems*, N.J. Prentice Hall, Englewood Cliffs, c1989.

APPENDIX A. SEQUENTIAL ORTHOGONAL ROTATIONS

Consider the sequence of the orientations of a rigid body with body fixed axes e_1, e_2 and e_3 associated with unit vectors $\hat{e}_1, \hat{e}_2$, and $\hat{e}_3$ relative to a LVLH axes E_1, E_2, and E_3 associated with unit vector $\hat{E}_1, \hat{E}_2$, and $\hat{E}_3$ is 2-3-1 which represents the Euler angle sequence pitch, yaw, and roll(θ_2, θ_3, and θ_1).

Let the rotation of a unit vector $\hat{e}_\alpha$ through an angle ϕ relative to LVLH unit vector $\hat{E}_\beta$ which is shown in Figure A.1. where α, β subscripts take the values of 1,2,3.

The components of $\hat{E}_1$ along $\hat{e}_1$ directions are given by

$$\begin{aligned} \hat{e}_1 &= \hat{E}_1 \\ \hat{e}_2 &= \hat{E}_2 \cos\phi + \hat{E}_3 \sin\phi \\ \hat{e}_3 &= -\hat{E}_2 \sin\phi + \hat{E}_3 \cos\phi \end{aligned} \tag{A.1}$$

or in matrix form as

$$\begin{pmatrix} \hat{e}_1 \\ \hat{e}_2 \\ \hat{e}_3 \end{pmatrix} = \begin{pmatrix} 1 & 0 & 0 \\ 0 & \cos\phi & \sin\phi \\ 0 & -\sin\phi & \cos\phi \end{pmatrix} \begin{pmatrix} \hat{E}_1 \\ \hat{E}_2 \\ \hat{E}_3 \end{pmatrix} = R(\phi) \begin{pmatrix} \hat{E}_1 \\ \hat{E}_2 \\ \hat{E}_3 \end{pmatrix} \tag{A.2}$$

where $R(\phi)$ is called the rotational matrix which represents the rotation of $\hat{e}_\alpha$ about $\hat{E}_\beta$. Therefore, the orientation from body frame to LVLH frame can be expressed in

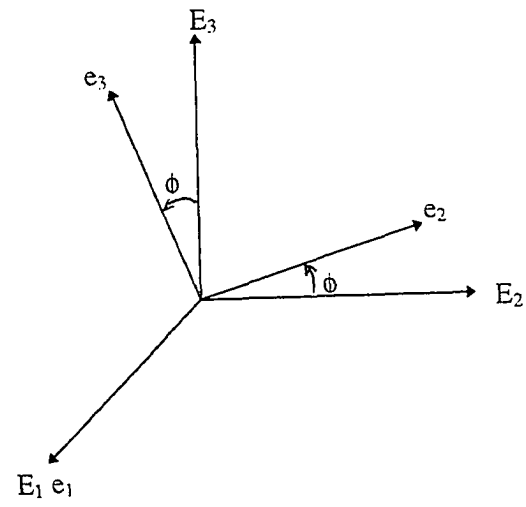

Figure A.1: Sequential orthogonal rotations

terms of the orthogonal rotation matrices as follows:

$$\begin{pmatrix} \hat{e}_1' \\ \hat{e}_2' \\ \hat{e}_3' \end{pmatrix} = R(\theta_2) \begin{pmatrix} \hat{E}_1 \\ \hat{E}_2 \\ \hat{E}_3 \end{pmatrix} \tag{A.3}$$

$$\begin{pmatrix} \hat{e}_1'' \\ \hat{e}_2'' \\ \hat{e}_3'' \end{pmatrix} = R(\theta_3) \begin{pmatrix} \hat{e}_1' \\ \hat{e}_2' \\ \hat{e}_3' \end{pmatrix} \tag{A.4}$$

$$\begin{pmatrix} \hat{e}_1 \\ \hat{e}_2 \\ \hat{e}_3 \end{pmatrix} = R(\theta_1) \begin{pmatrix} \hat{e}_1'' \\ \hat{e}_2'' \\ \hat{e}_3'' \end{pmatrix} \tag{A.5}$$

$$\begin{pmatrix} \hat{e}_1 \\ \hat{e}_2 \\ \hat{e}_3 \end{pmatrix} = R(\theta_1)R(\theta_3)R(\theta_2) \begin{pmatrix} \hat{E}_1 \\ \hat{E}_2 \\ \hat{E}_3 \end{pmatrix} \tag{A.6}$$

where

$$R(\theta_2) = \begin{pmatrix} \cos\theta_2 & -\sin\theta_2 & 0 \\ 0 & 1 & 0 \\ \sin\theta_2 & 0 & \cos\theta_2 \end{pmatrix}$$

$$R(\theta_3) = \begin{pmatrix} \cos\theta_3 & \sin\theta_3 & 0 \\ -\sin\theta_3 & \cos\theta_3 & 0 \\ 0 & 0 & 1 \end{pmatrix}$$

$$R(\theta_1) = \begin{pmatrix} 1 & 0 & 0 \\ 0 & \cos\theta_1 & \sin\theta_1 \\ 0 & -\sin\theta_1 & \cos\theta_1 \end{pmatrix}$$

The combined matrix for 2-3-1 sequence of rotation is the product of the orthogonal rotation matrices. It is

$$R_{231} = R(\theta_1)R(\theta_3)R(\theta_2) =$$

$$\begin{pmatrix} \cos\theta_3\cos\theta_2 & -\cos\theta_1\sin\theta_3\cos\theta_2 + \sin\theta_1\sin\theta_2 & \sin\theta_1\sin\theta_3\cos\theta_2 + \cos\theta_1\sin\theta_2 \\ \sin\theta_3 & \cos\theta_1\cos\theta_3 & -\sin\theta_1\cos\theta_3 \\ -\cos\theta_3\sin\theta_2 & \cos\theta_1\sin\theta_3\sin\theta_2 + \sin\theta_1\cos\theta_2 & -\sin\theta_1\sin\theta_3\sin\theta_2 + \sin\theta_1\cos\theta_2 \end{pmatrix} \tag{A.7}$$

where R_{231} indicates the rotation matrix of body axes through Euler angles to the

LVLH axes. The inverse relationship in Eqn.(A.6) is of the form

$$\begin{pmatrix} \hat{E}_1 \\ \hat{E}_2 \\ \hat{E}_3 \end{pmatrix} = R_{231}^{-1} \begin{pmatrix} \hat{e}_1 \\ \hat{e}_2 \\ \hat{e}_3 \end{pmatrix} \tag{A.8}$$

Because of the orthogonality, the inverse matrix is equivalent to its transpose; that is

$$R_{231}^{-1} = R_{231}^{'} \tag{A.9}$$

The rotation from LVLH frame to body frame can simply be obtained through matrix $R_{231}^{'}$.